Electronic Supplementary Material (ESI) for Dalton Transactions.

Supplementary Information

1. General experimental section

All reactions were carried out under a nitrogen atmosphere using standard Schlenk line techniques or nitrogen-filled glove box. Petroleum ether (bp 40-60 °C) and other solvents were distilled under nitrogen atmosphere according to the standard procedures. All ketones, $[Ni(COD)_2]$ and other chemicals were obtained from commercial sources, stored in a glovebox and used as received. Ph_2PH[1], $[NiCl_2(DME)]$[2], **1a-c**[3] and **L1H2**[4] were prepared according to the reported procedures. All ^1H NMR (400 or 500 MHz), $^{13}C\{^1H\}$ (100 MHz or 125.75 MHz) and $^{31}P\{^1H\}$ (202.45 MHz) spectra were recorded at 298 K. ^1H NMR chemical shifts are referenced with respect to the chemical shift of the residual proton present in the deuterated solvent. $^{13}C\{^1H\}$ NMR spectra were referenced with respect to the chemical shift of the carbon atom of $CDCl_3$. H_3PO_4 (85%) was used as an external standard for $^{31}P\{^1H\}$ NMR measurements. Chemical shifts are in parts per million (ppm) and coupling constants are in Hz. ATR spectra were recorded using Perkin-Elmer Spectrum Rx. High resolution mass spectra (ESI+/–) were obtained using Agilent AdvanceBio 6545XT LC/Q-TOF system. Electronic absorption spectra (800–200 nm) were recorded on a Shimadzu (Model UV-2450) spectrophotometer at room temperature. Elemental analyses were carried out using a Perkin-Elmer 2400 CHN analyzer. Thermoscientific Trace 1310 GC chromatograph was used for monitoring products formation.

Table S1. Transfer hydrogenation with added solvents.[a]

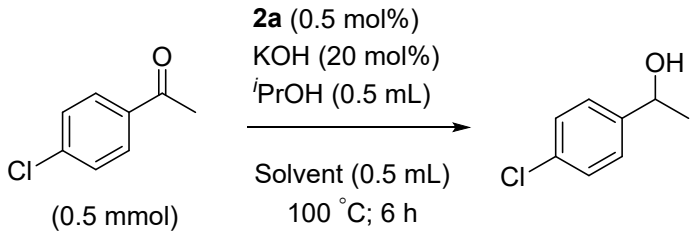

Entry	Solvent (0.5 mL)	Conversion(%)[b]	Yield(%)[c]
1	THF	92	83
2	1,4-dioxane	90	81
3	benzene	94	81
4	toluene	91	80
5	DMSO	71	65
6	acetonitrile	90	24
7	DCM	0	0
8	MeOH	5	1
9	EtOH	0	0

[a] Reaction conditions: ketone (0.5 mmol), ^{i}PrOH (0.5 mL), KOH (20 mol%), N_2 or Ar atmosphere; [b] estimated by GC; [c] isolated yield.

Table S2. Transfer hydrogenation using different hydrogen donors.[a]

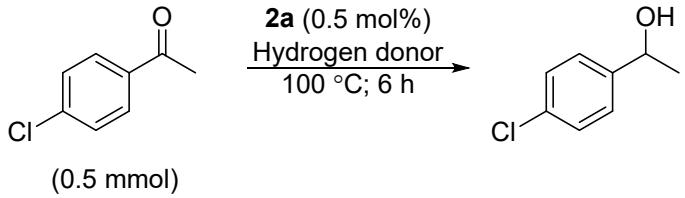

Entry	Hydrogen Donor	Solvent	Conversion (%)[b]	Yield (%)[c]
1	^{i}PrOH (1 mL)	-	98	91
2	EtOH (1 mL)	-	0	0
3	MeOH (1 mL)	-	0	0
4	HCOOH/Et_3N (5:2 mole ratio)	-	0	0
5	$HCOONH_4$ (4 equiv)	THF (1 mL)	0	0

[a] Reaction conditions: **2a** (0.5 mol%), ketone (0.5 mmol), KOH (20 mol%), 100 °C, 6 h, N_2 or Ar atmosphere; KOH not used for entry 4 and 5; [b] estimated by GC; [c] isolated yield;

Table S3. Transfer hydrogenation with different bases.[a]

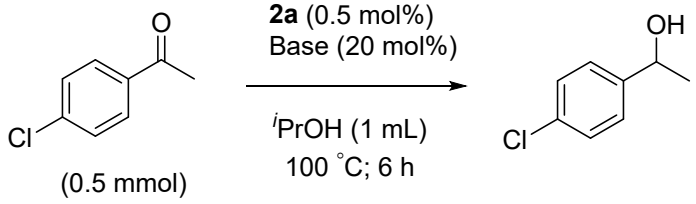

Entry	Base	Conversion (%)[b]	Yield (%)[c]
1	KOH	98	91
2	KO^{t}Bu	92	87
3	NaOH	99	92
4	K_3PO_4	38	34
5	Cs_2CO_3	40	35
6	K_2CO_3	NR	0
7	Na_2CO_3	NR	0
8	Et_3N	20	16

[a] Reaction conditions: ketone (0.5 mmol), ^{i}PrOH (1 mL), base (20 mol%), N_2 or Ar atmosphere; [b] estimated by GC; [c] isolated yield.

Typical procedure for Ni(0) NMR tube reactions

Inside the glove box, a NMR tube was charged with ligand **L1H2** (0.015 g, 0.021 mmol) and $Ni(COD)_2$ (0.006 g, 0.021 mmol). A sealed capillary tube filled with D_2O was inserted and then 0.5 mL of toluene was added. The NMR tube was sealed by using paraffin and then it was taken out of the glove box for recording ^{31}P NMR spectrum.

2. NMR, ATR, HRMS and UV-vis data

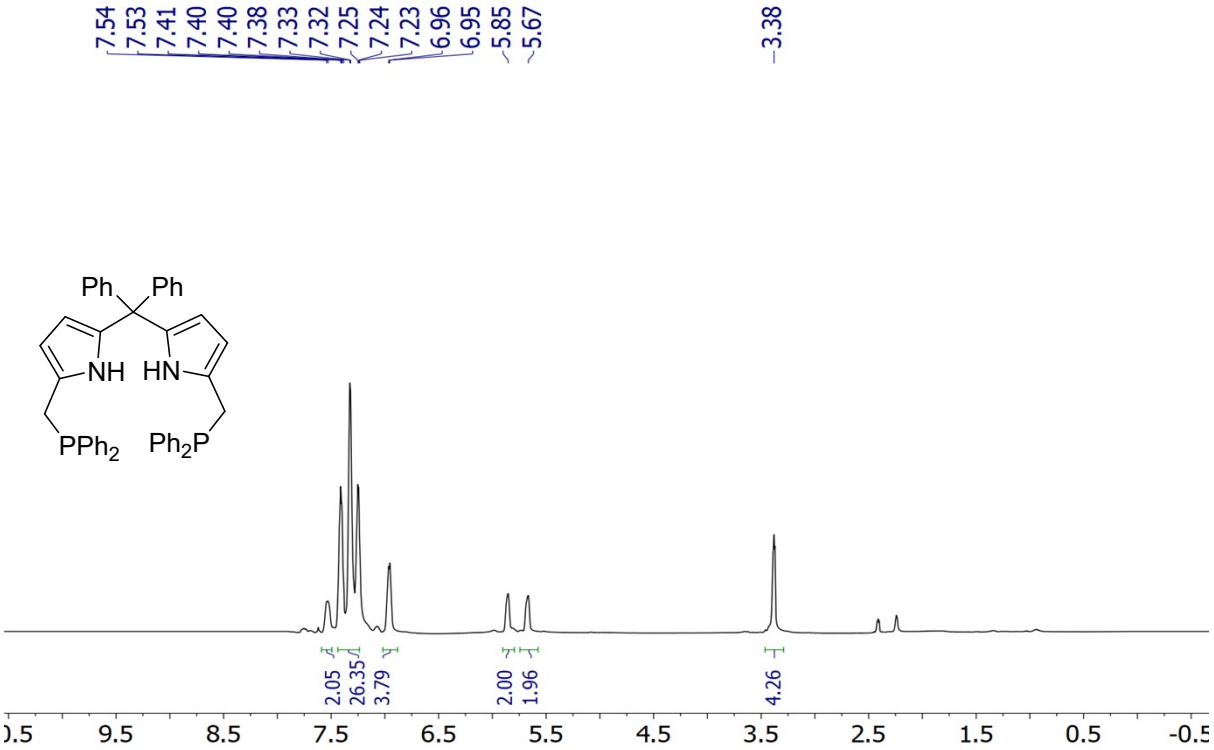

Figure S1. ^{1}H NMR ($CDCl_3$, 400 MHz) spectrum of 1,9-bis(diphenylphosphinomethyl)diphenyldipyrrolylmethane, **L1H2.**

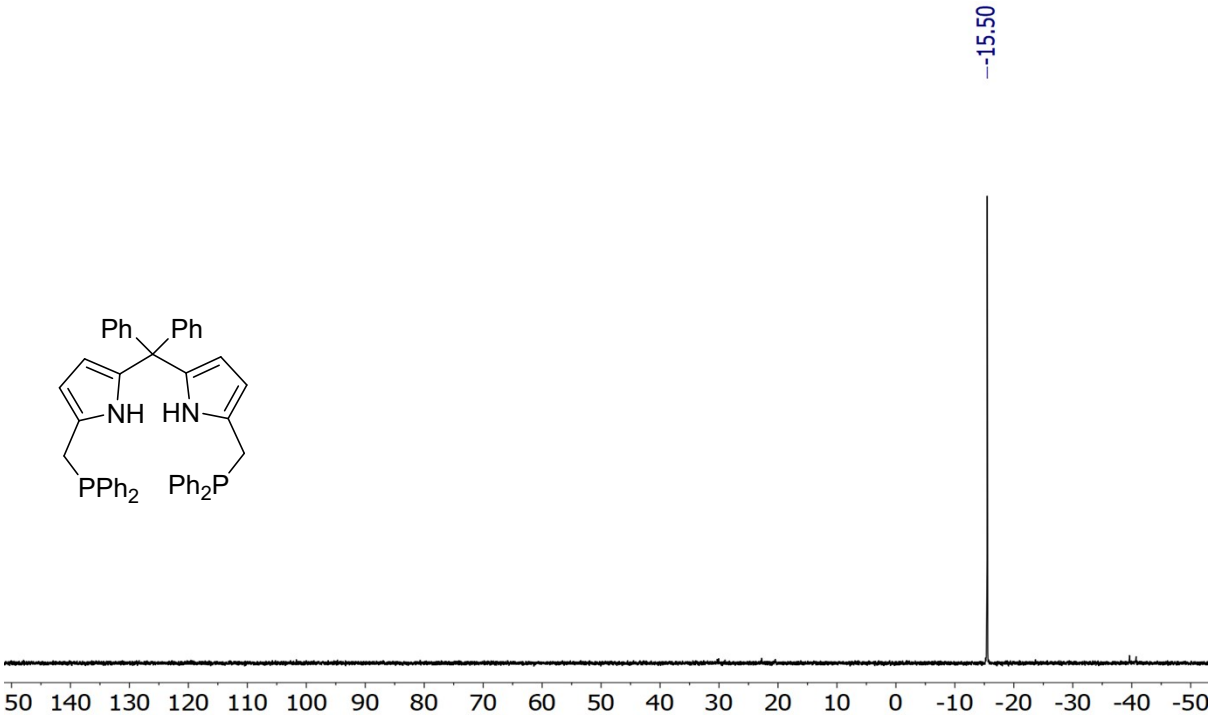

Figure S2. $^{31}P\{^{1}H\}$ NMR ($CDCl_3$, 202.45 MHz) spectrum of 1,9-bis(diphenylphosphinomethyl)diphenyldipyrrolylmethane, **L1H2.**

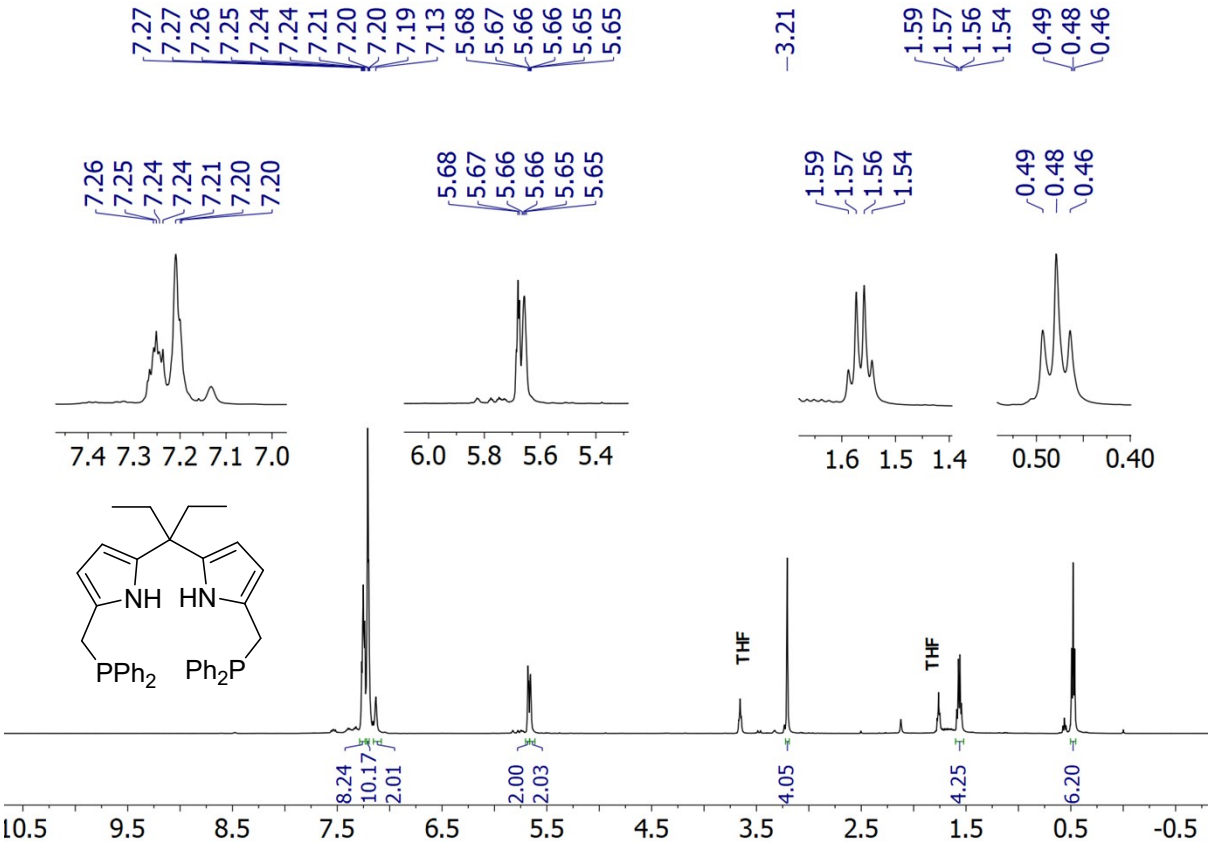

Figure S3. ^{1}H NMR ($CDCl_3$, 500 MHz) spectrum of 1,9-bis(diphenylphosphinomethyl)diethyldipyrrolylmethane, **L2H2**.

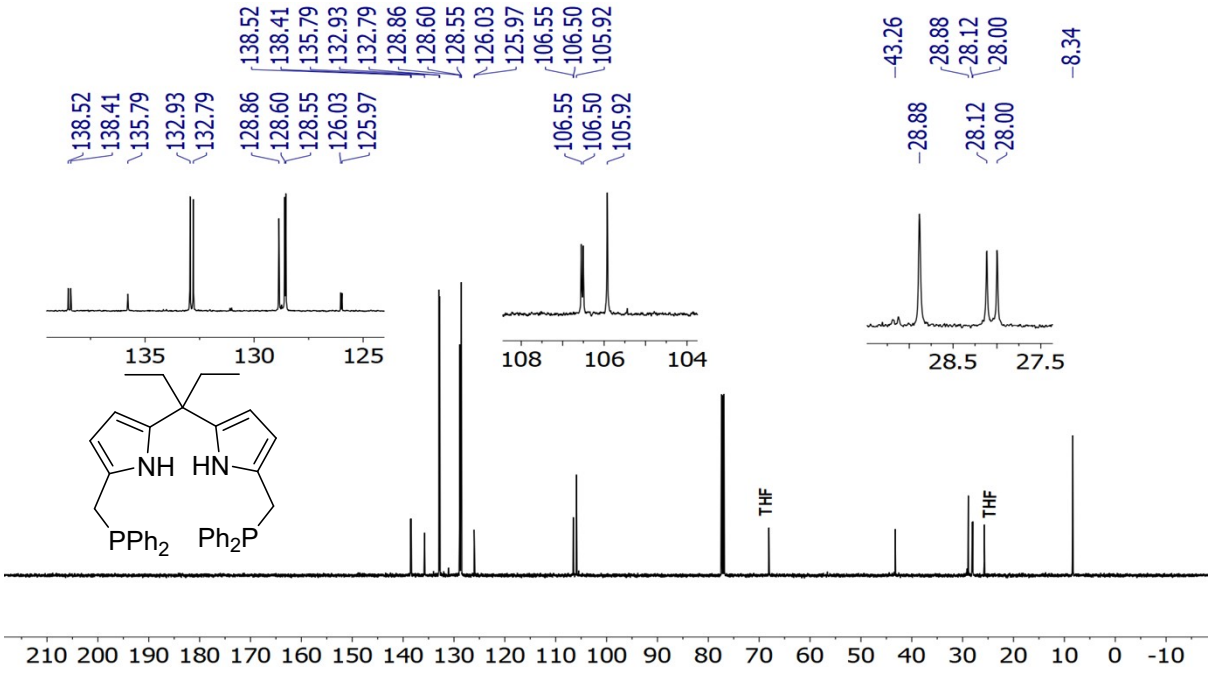

Figure S4. $^{13}C\{^{1}H\}$ NMR ($CDCl_3$, 125.75 MHz) spectrum of 1,9-bis(diphenylphosphinomethyl)diethyldipyrrolylmethane, **L2H2**.

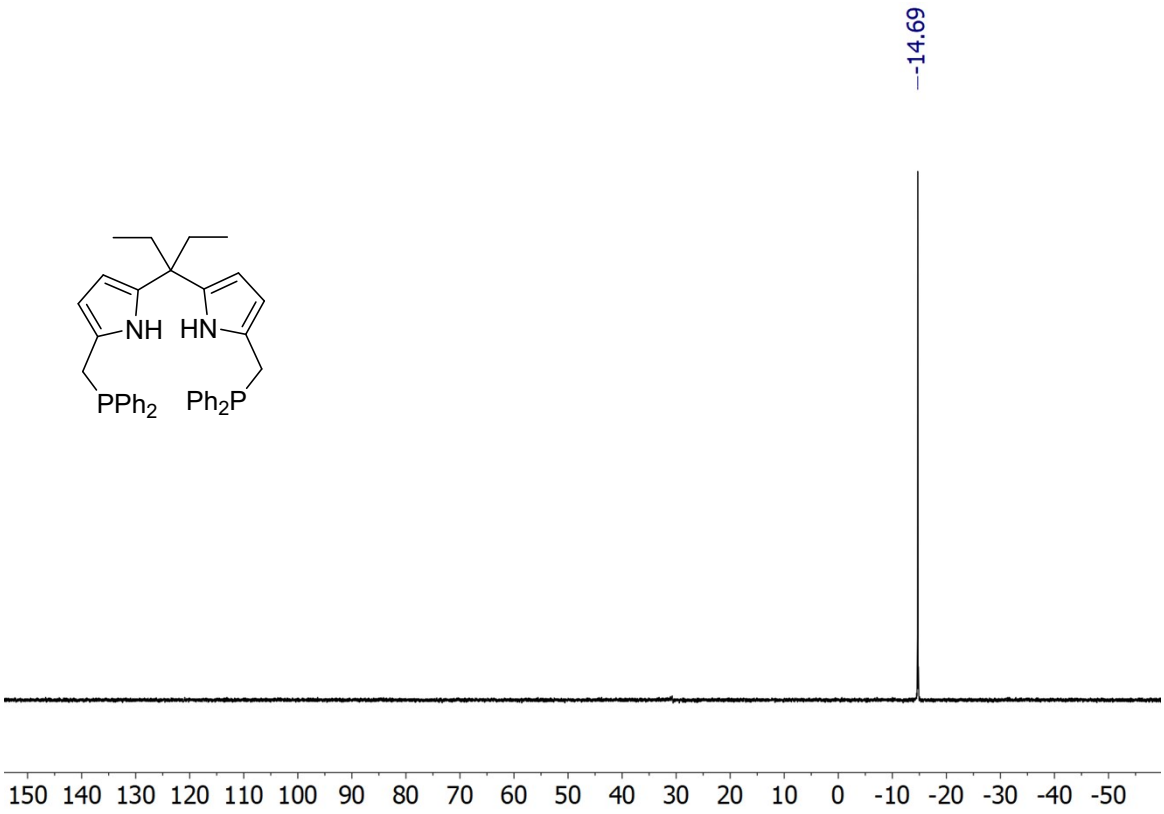

Figure S5. $^{31}P\{^{1}H\}$ NMR ($CDCl_3$, 202.45 MHz) spectrum of 1,9-bis(diphenylphosphinomethyl)diethyldipyrrolylmethane, **L2H2**.

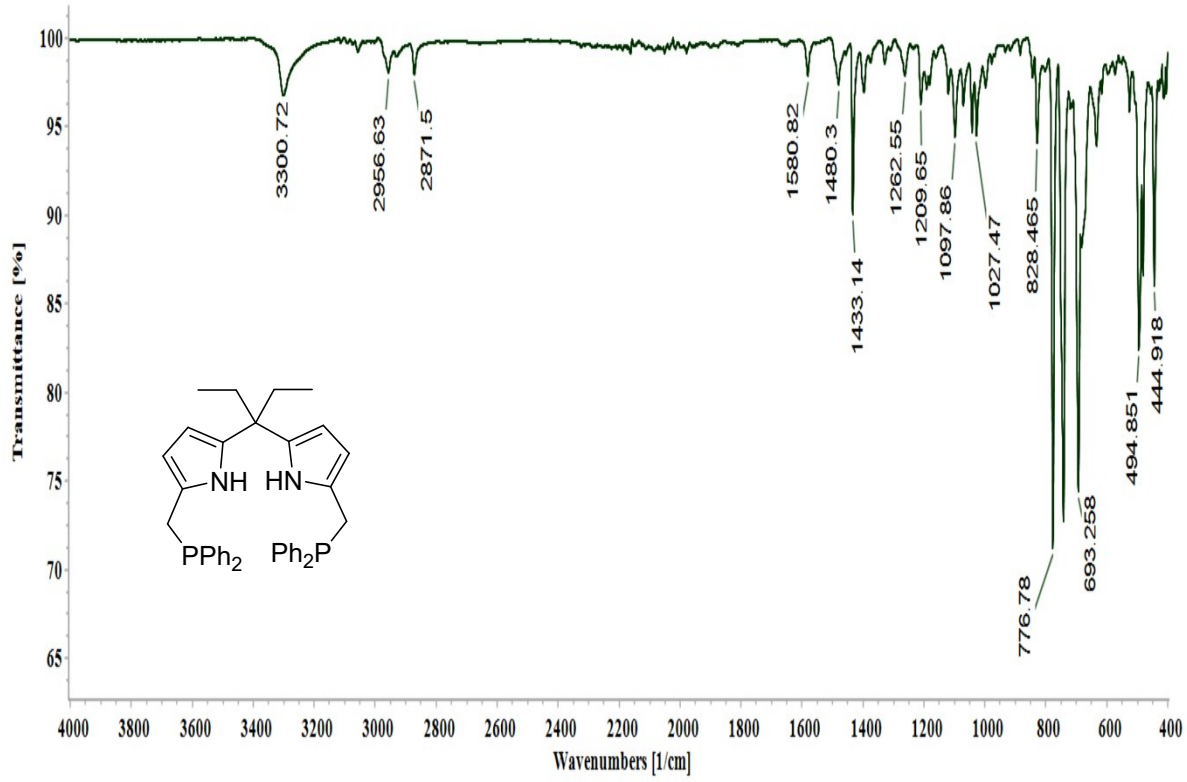

Figure S6. ATR spectrum of 1,9-bis(diphenylphosphinomethyl)diethyldipyrrolylmethane, **L2H2**.

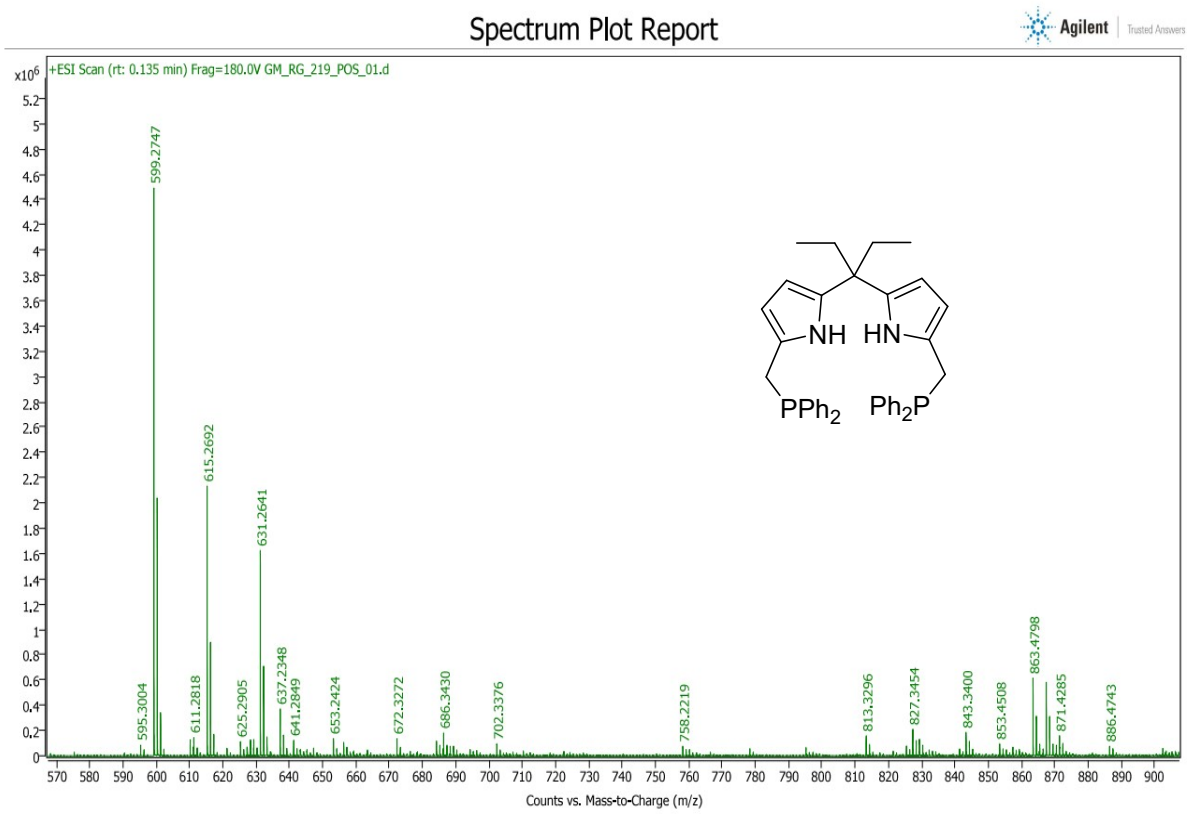

Figure S7. HRMS (ESI+) spectrum of 1,9-bis(diphenylphosphinomethyl)diethyldipyrrolylmethane, **L2H2**.

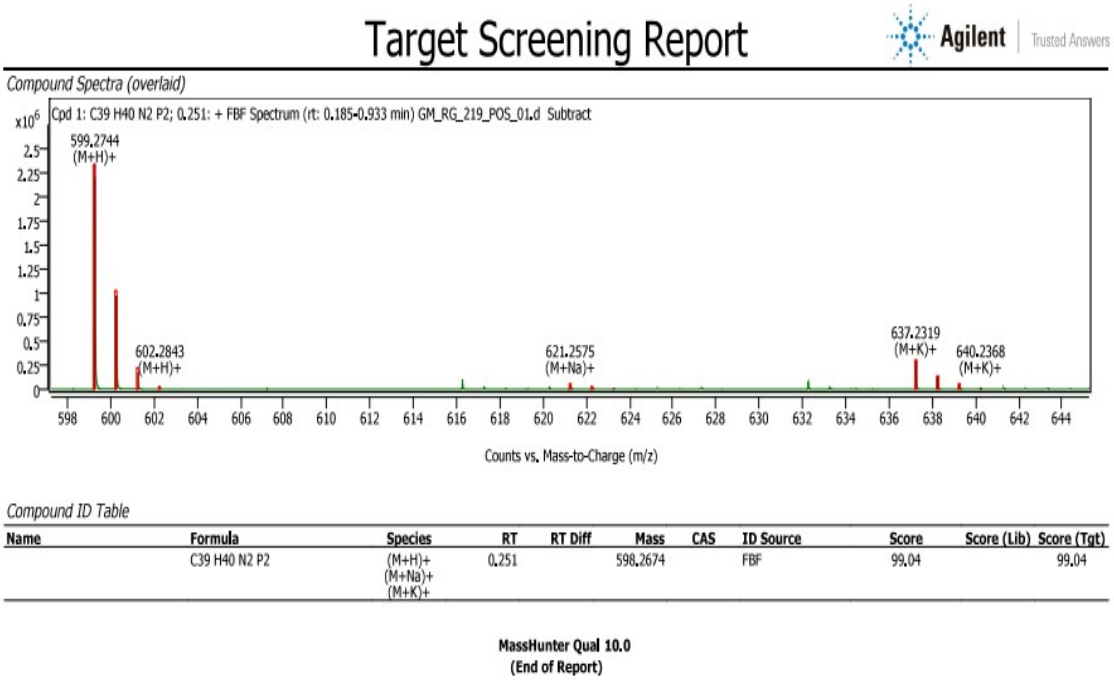

Figure S8. HRMS (ESI+) target screening of 1,9-bis(diphenylphosphinomethyl)diethyldipyrrolylmethane, **L2H2**.

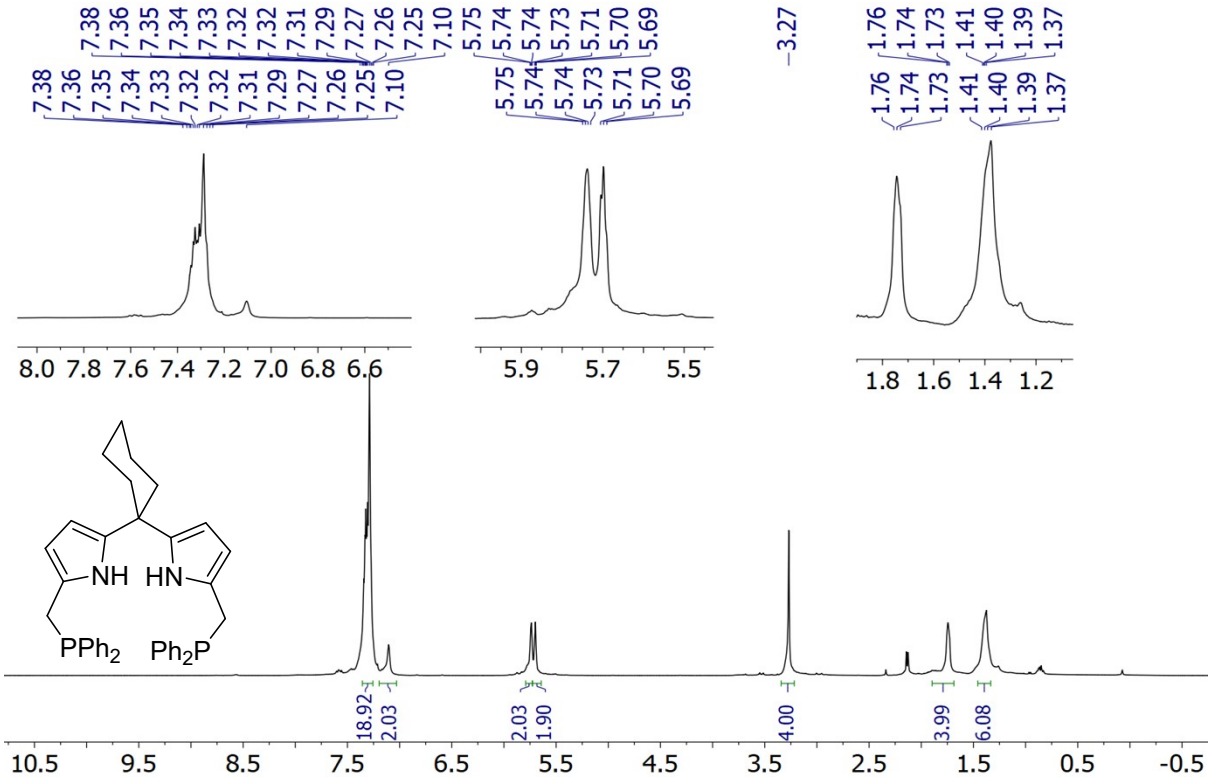

Figure S9. ^{1}H NMR ($CDCl_3$, 400 MHz) spectrum of 1,9-bis(diphenylphosphinomethyl)cyclohexyldipyrrolylmethane, **L3H2**.

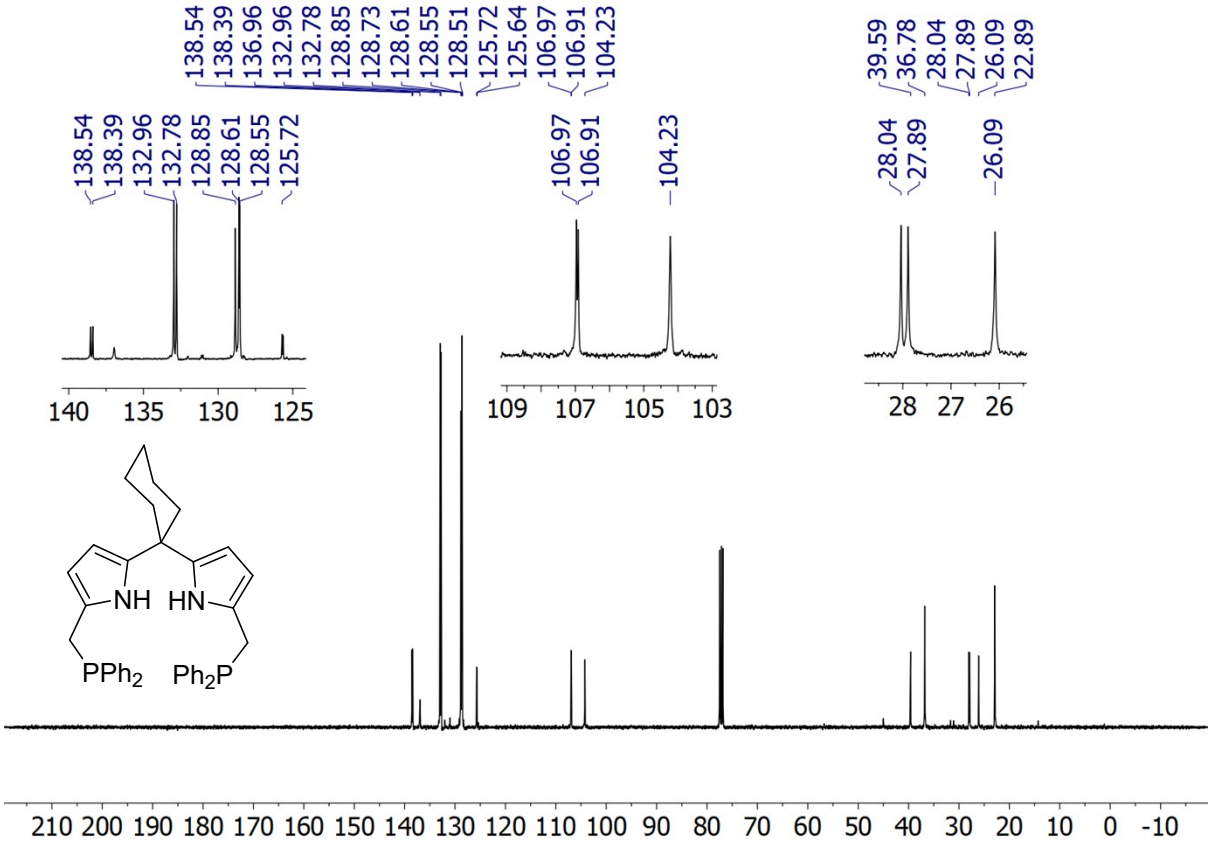

Figure S10. $^{13}C\{^{1}H\}$ NMR ($CDCl_3$, 125.75 MHz) spectrum of 1,9-bis(diphenylphosphinomethyl)cyclohexyldipyrrolylmethane, **L3H2**.

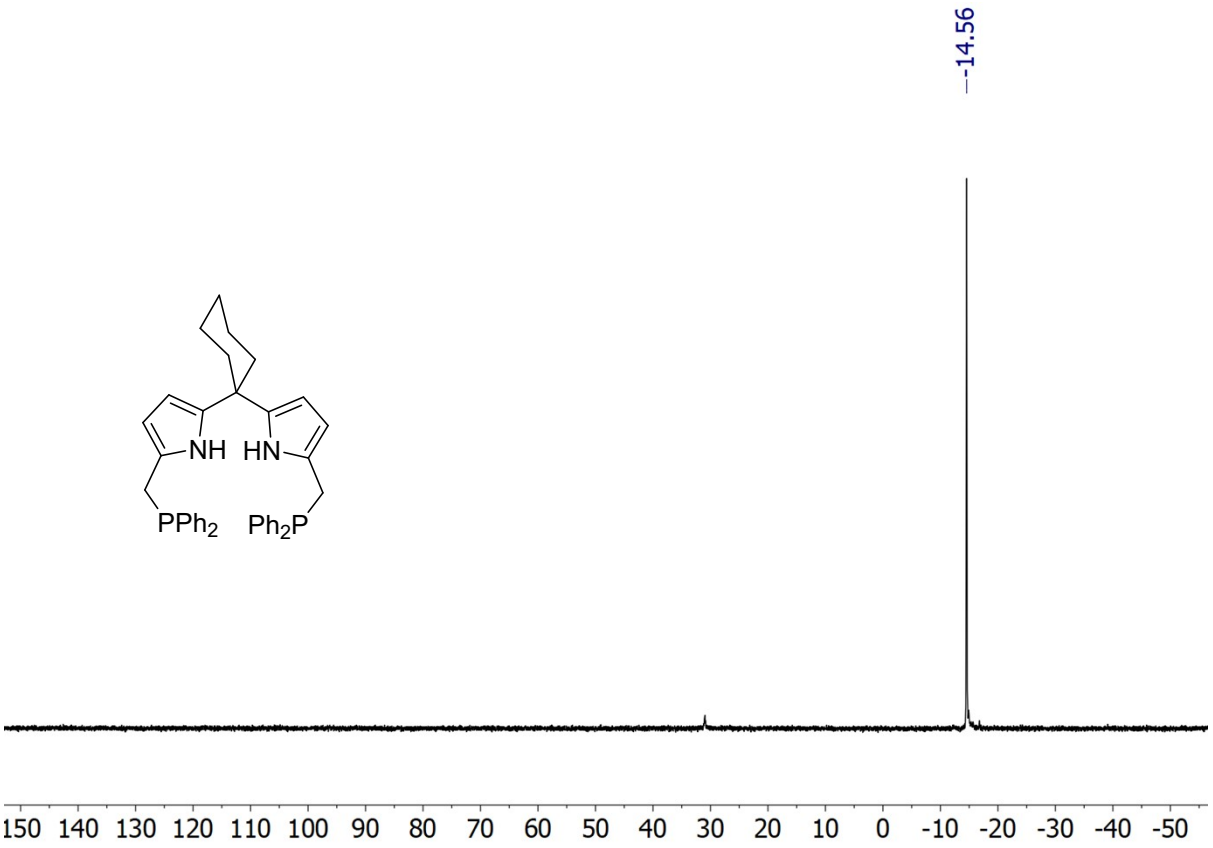

Figure S11. $^{31}P\{^{1}H\}$ NMR ($CDCl_3$, 202.45 MHz) spectrum of 1,9-bis(diphenylphosphinomethyl)cyclohexyldipyrrolylmethane, **L3H2**.

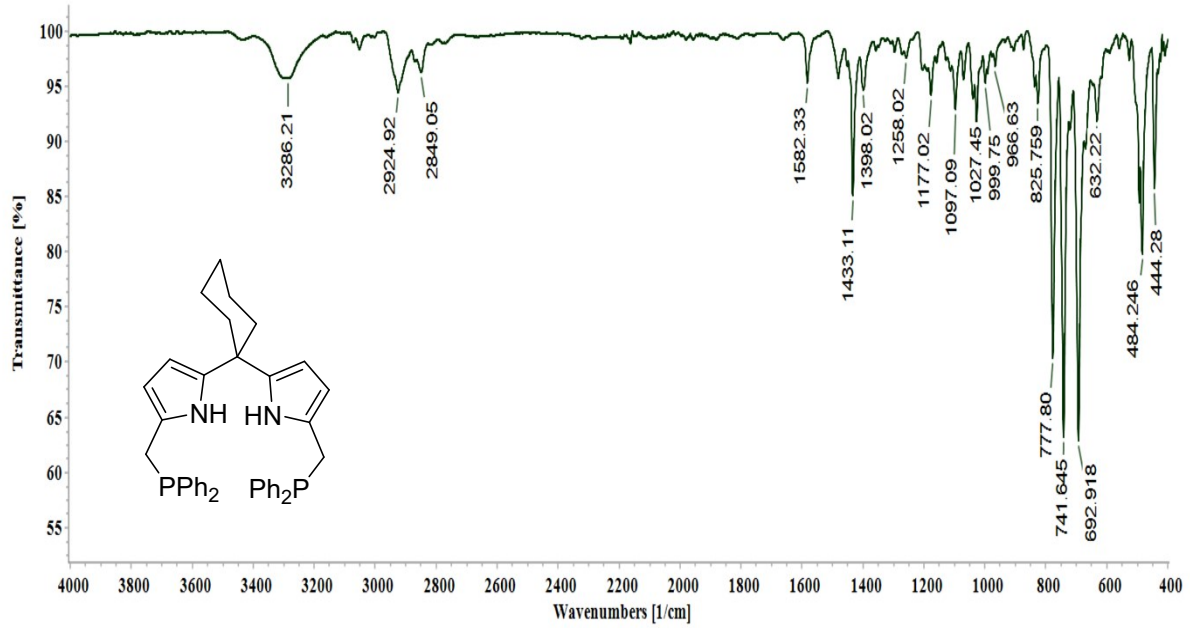

Figure S12. ATR spectrum of 1,9-bis(diphenylphosphinomethyl)cyclohexyldipyrrolylmethane, **L3H2**.

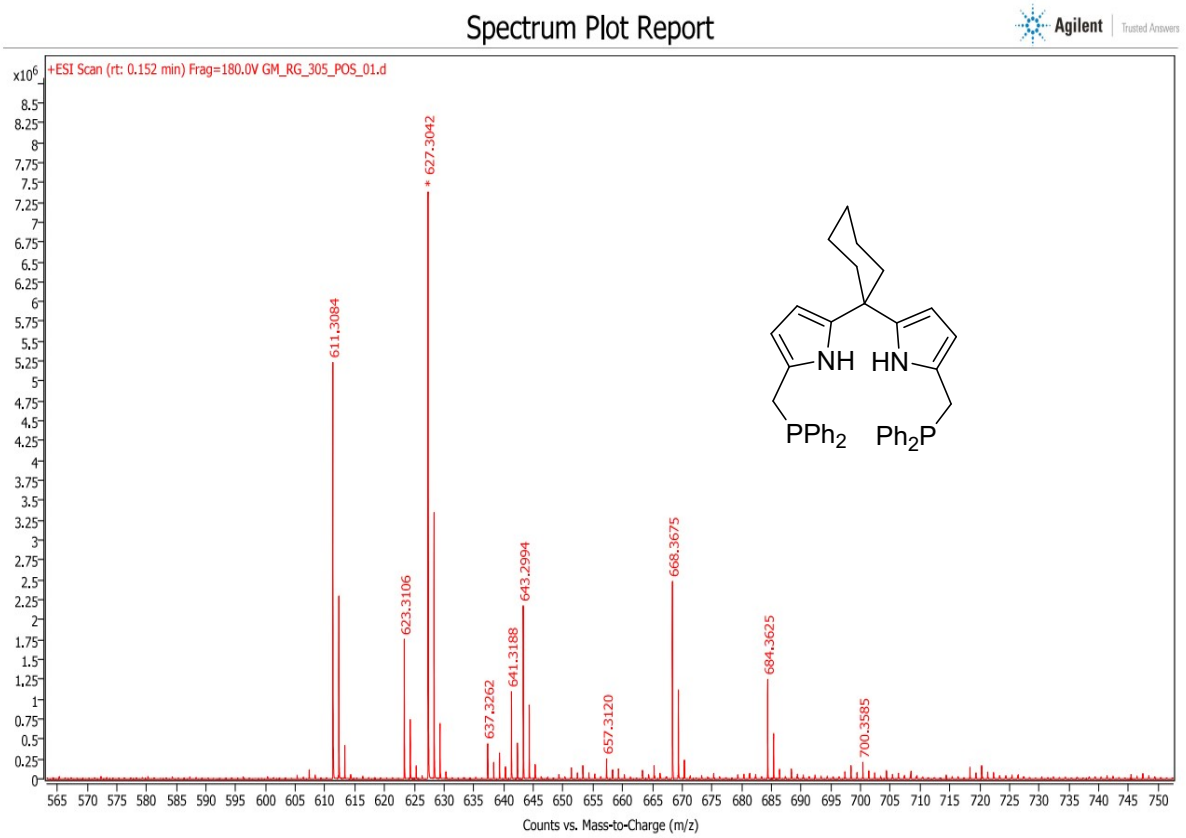

Figure S13. HRMS (ESI+) spectrum of 1,9-bis(diphenylphosphinomethyl)cyclohexyldipyrrolylmethane, **L3H2**.

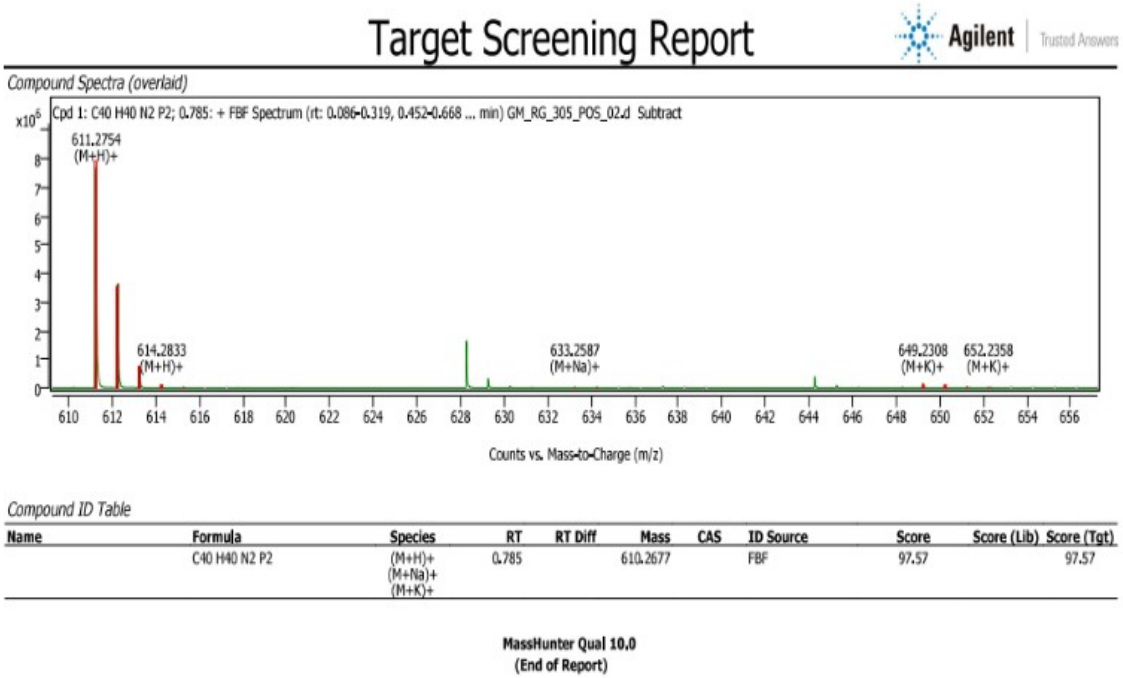

Figure S14. HRMS (ESI+) target screening of 1,9-bis(diphenylphosphinomethyl)cyclohexyldipyrrolylmethane, **L3H2**.

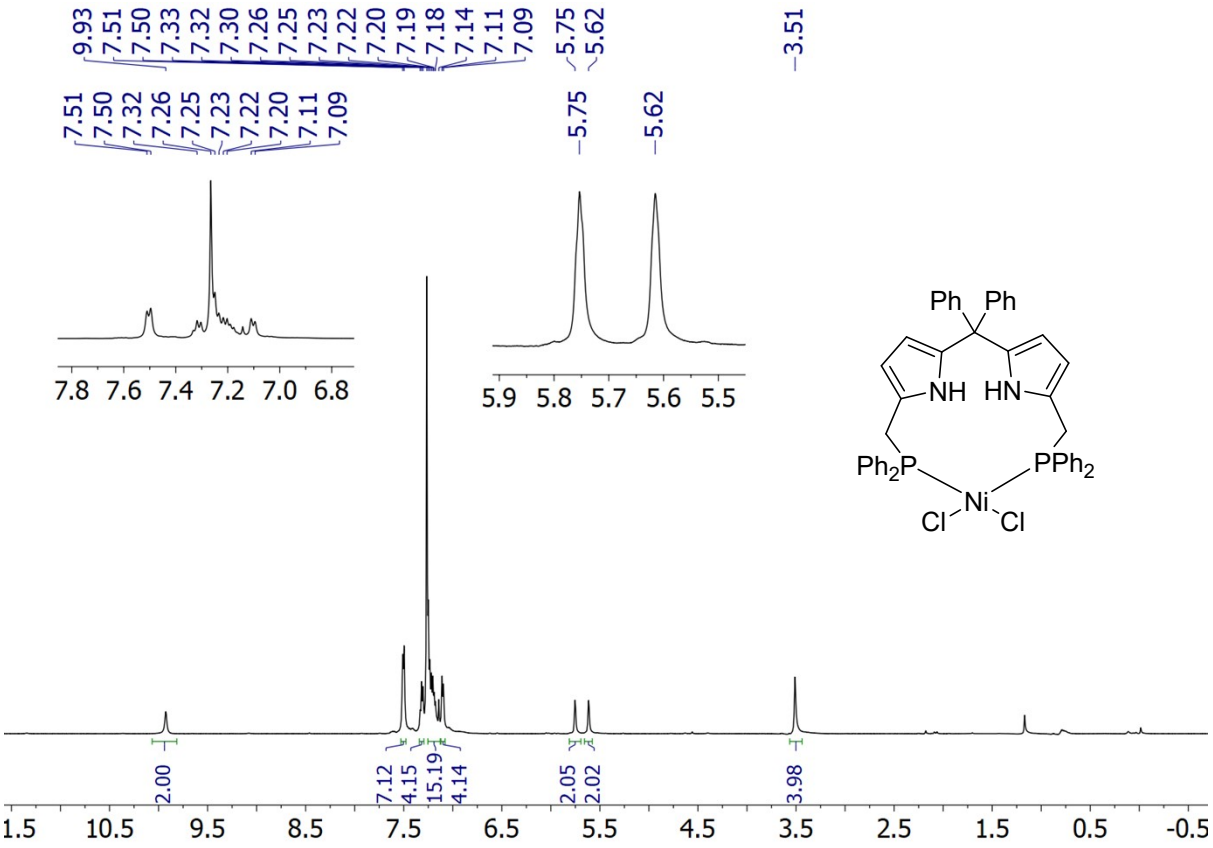

Figure S15. ^{1}H NMR ($CDCl_3$, 500 MHz) spectrum of [$NiCl_2${$Ph_2C(C_4H_3N)_2$-1,9-$(CH_2PPh_2)_2$-κ^2-*P,P*}], **2a**.

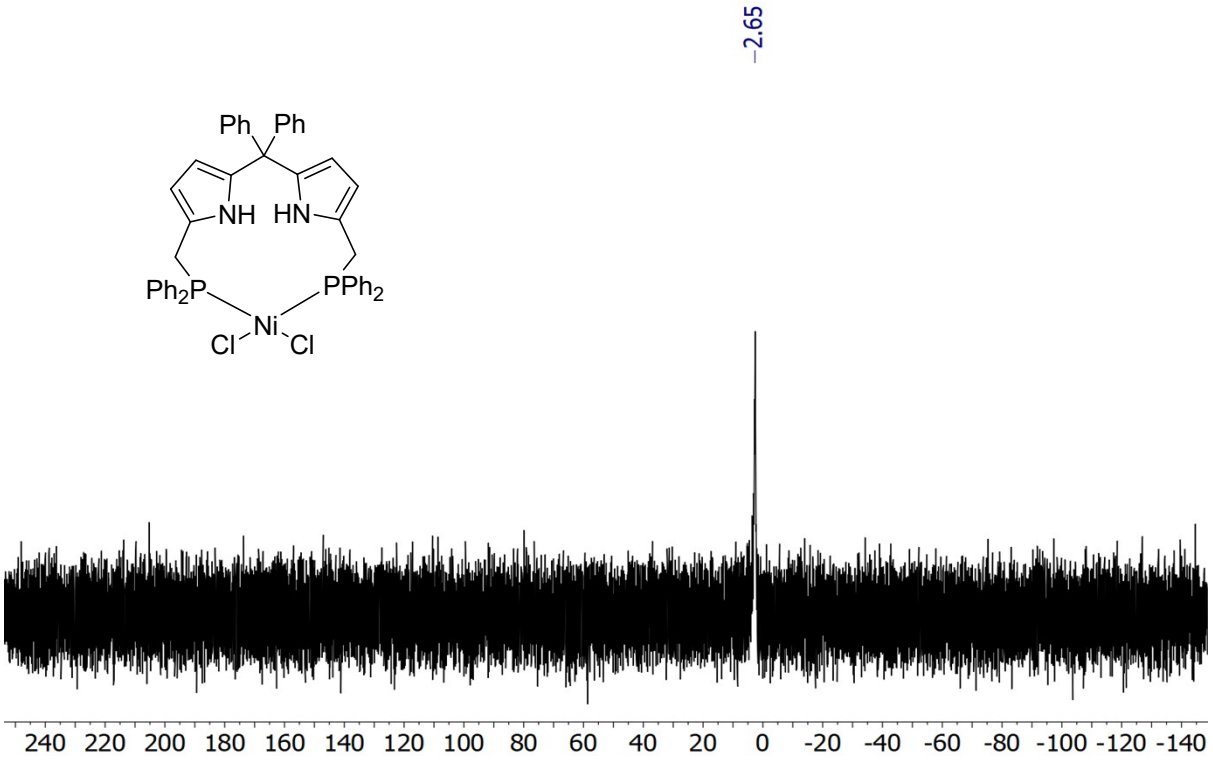

Figure S16. $^{31}P\{^{1}H\}$ NMR ($CDCl_3$, 202.45 MHz) spectrum of [$NiCl_2${$Ph_2C(C_4H_3N)_2$-1,9-$(CH_2PPh_2)_2$-κ^2-*P,P*}], **2a**.

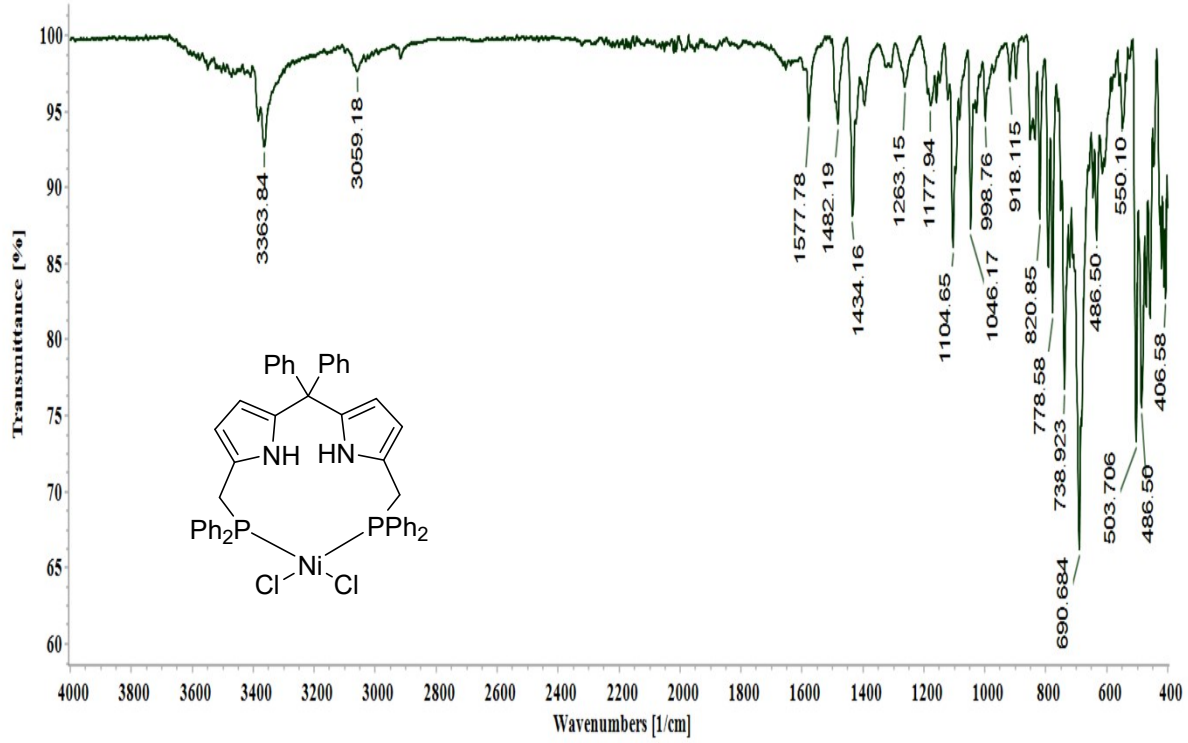

Figure S17. ATR spectrum of [$NiCl_2${$Ph_2C(C_4H_3N)_2$-1,9-$(CH_2PPh_2)_2$-κ^2-*P,P*}], **2a**.

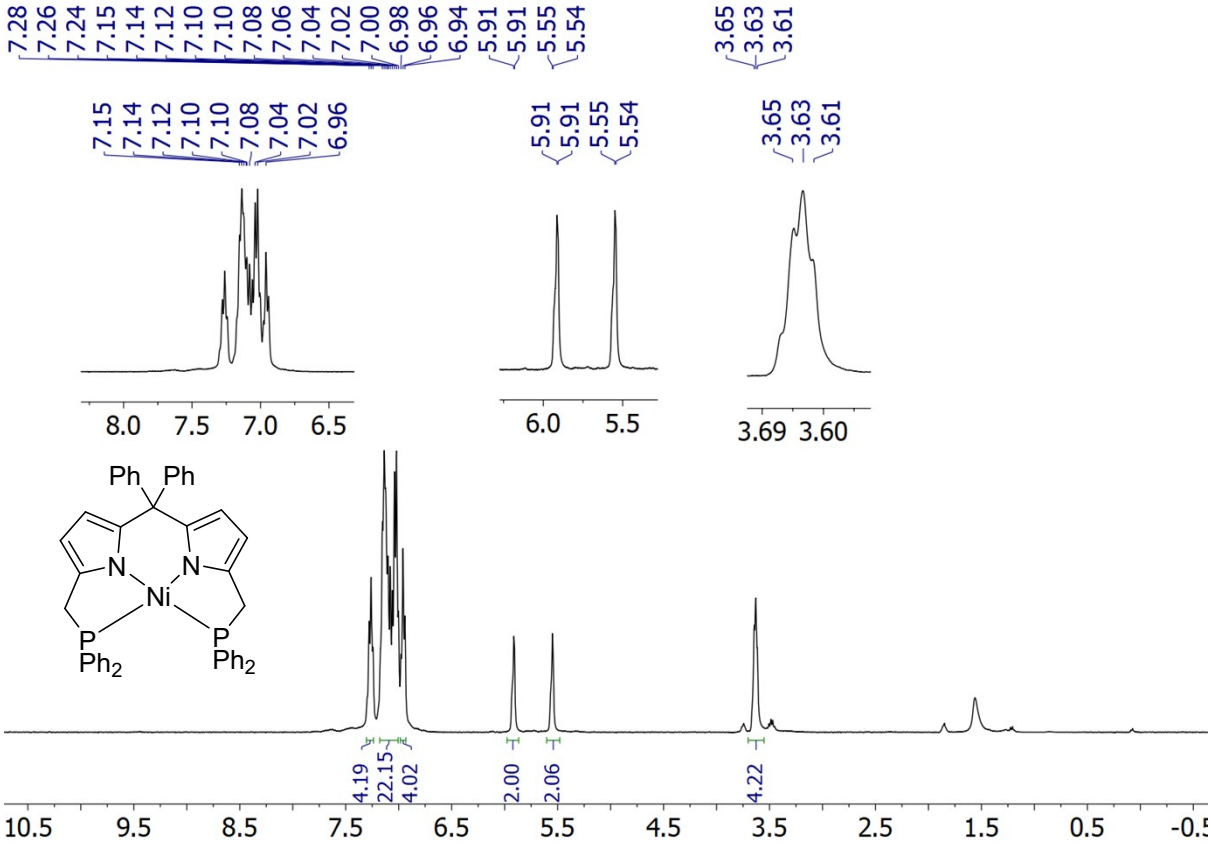

Figure S18. ^1H NMR ($CDCl_3$, 400 MHz) spectrum of [Ni{$Ph_2C(C_4H_2N)_2$-1,9-$(CH_2PPh_2)_2$-κ^4-*P,N,N,P*}], **3a**.

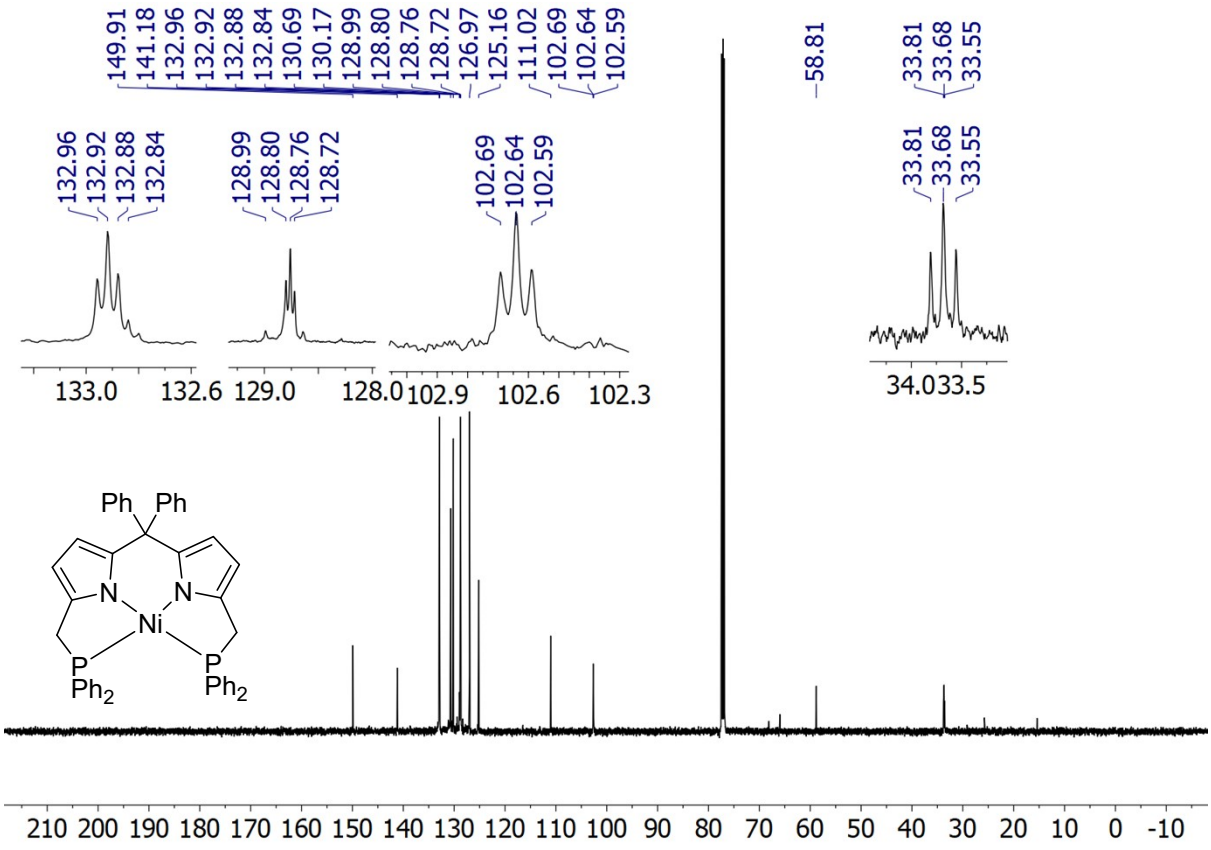

Figure S19. $^{13}C\{^{1}H\}$ NMR ($CDCl_3$, 125.75 MHz) spectrum of Ni{$Ph_2C(C_4H_2N)_2$-1,9-$(CH_2PPh_2)_2$-κ^4-*P,N,N,P*}], **3a**.

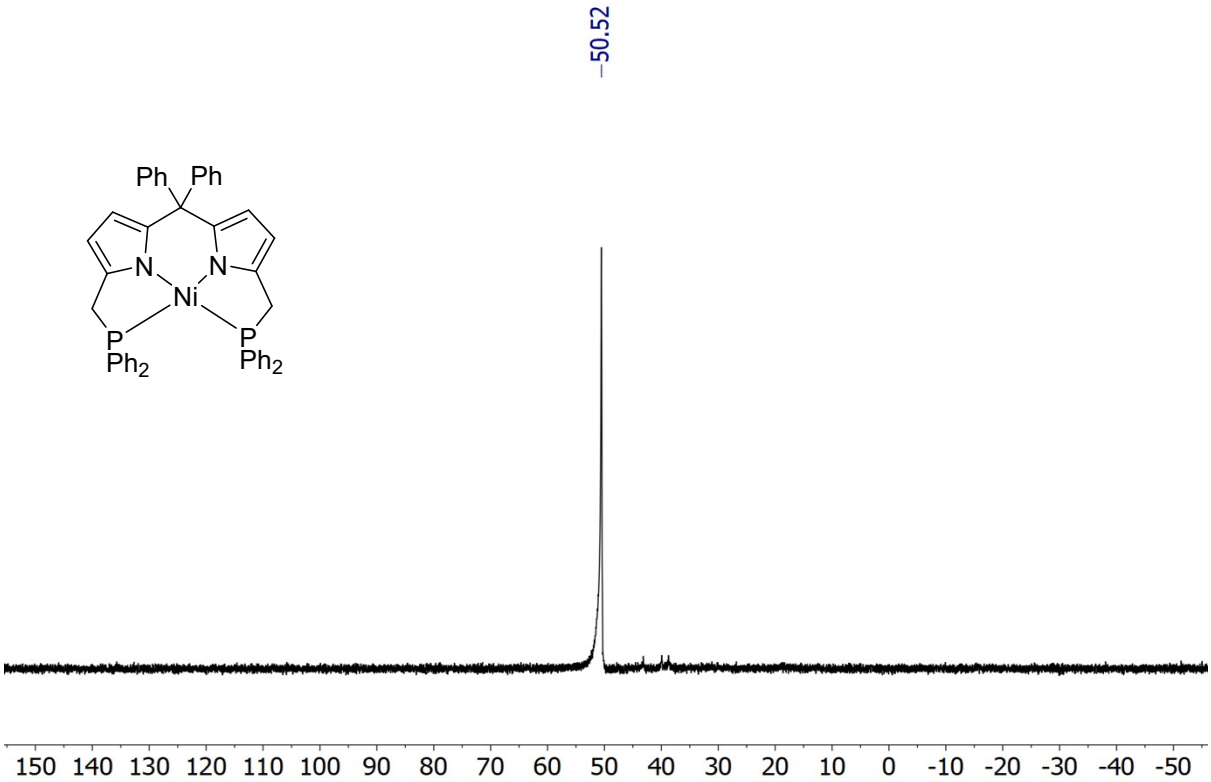

Figure S20. $^{31}P\{^{1}H\}$ NMR ($CDCl_3$, 202.45 MHz) spectrum of [Ni{$Ph_2C(C_4H_2N)_2$-1,9-$(CH_2PPh_2)_2$-κ^4-*P,N,N,P*}], **3a**.

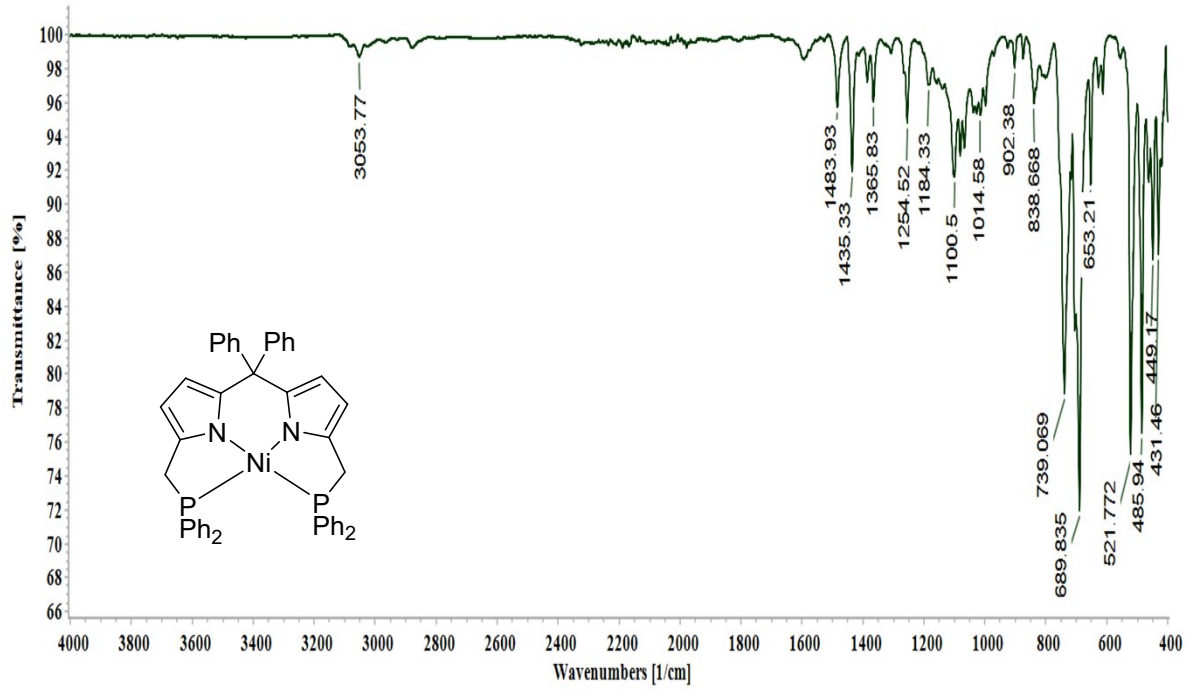

Figure S21. ATR spectrum of [Ni{$Ph_2C(C_4H_2N)_2$-1,9-$(CH_2PPh_2)_2$-κ^4-*P,N,N,P*}], **3a**.

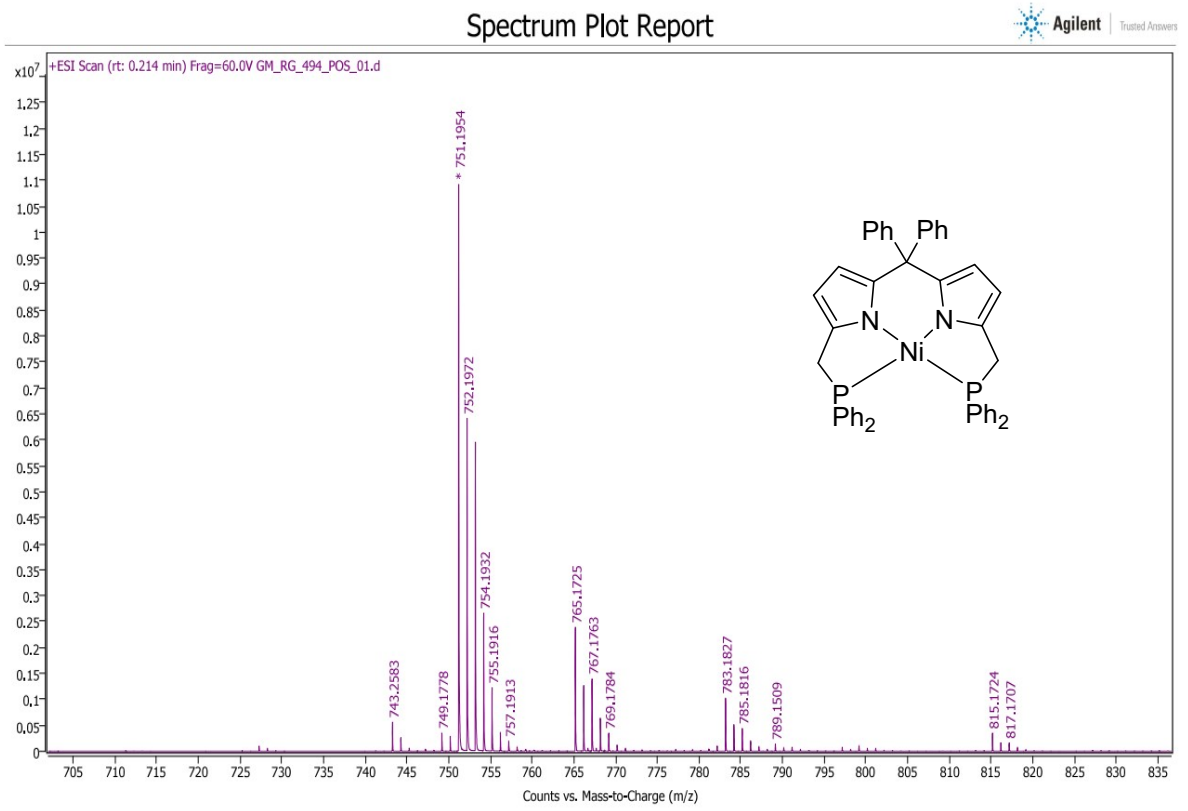

Figure S22. HRMS (ESI+) spectrum of [Ni{$Ph_2C(C_4H_2N)_2$-1,9-$(CH_2PPh_2)_2$-κ^4-*P,N,N,P*}], **3a**.

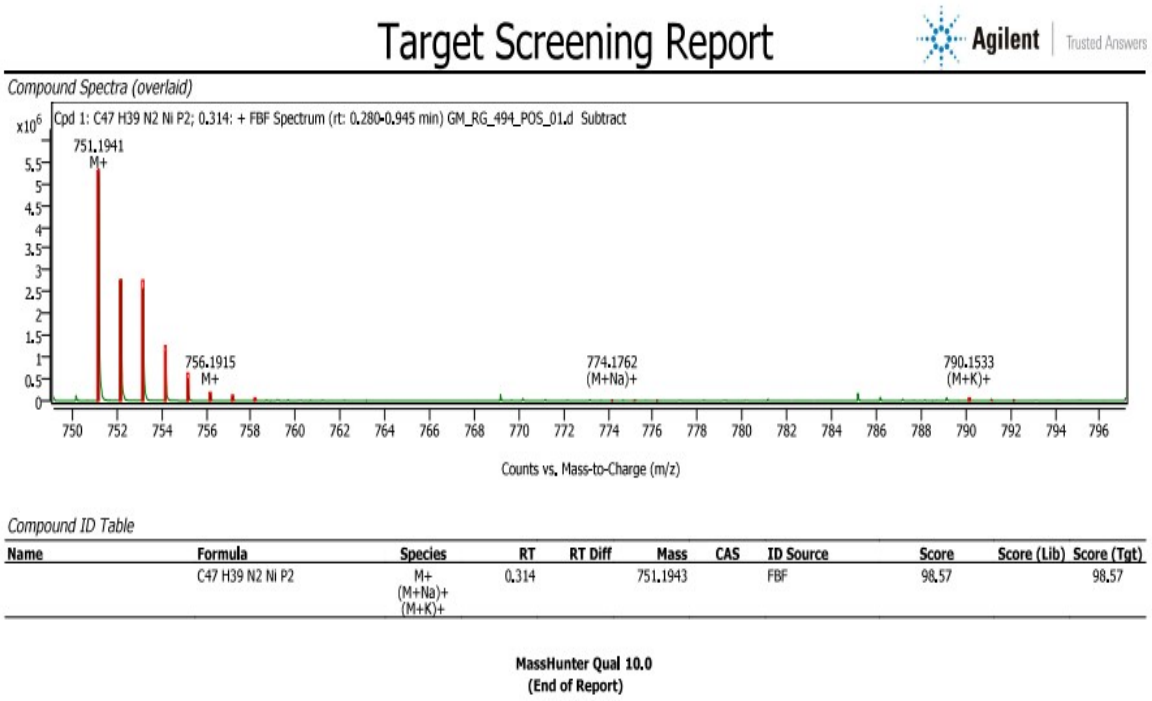

Figure S23. HRMS (ESI+) target screening of [Ni{$Ph_2C(C_4H_2N)_2$-1,9-$(CH_2PPh_2)_2$-κ^4-*P,P*}], **3a.**

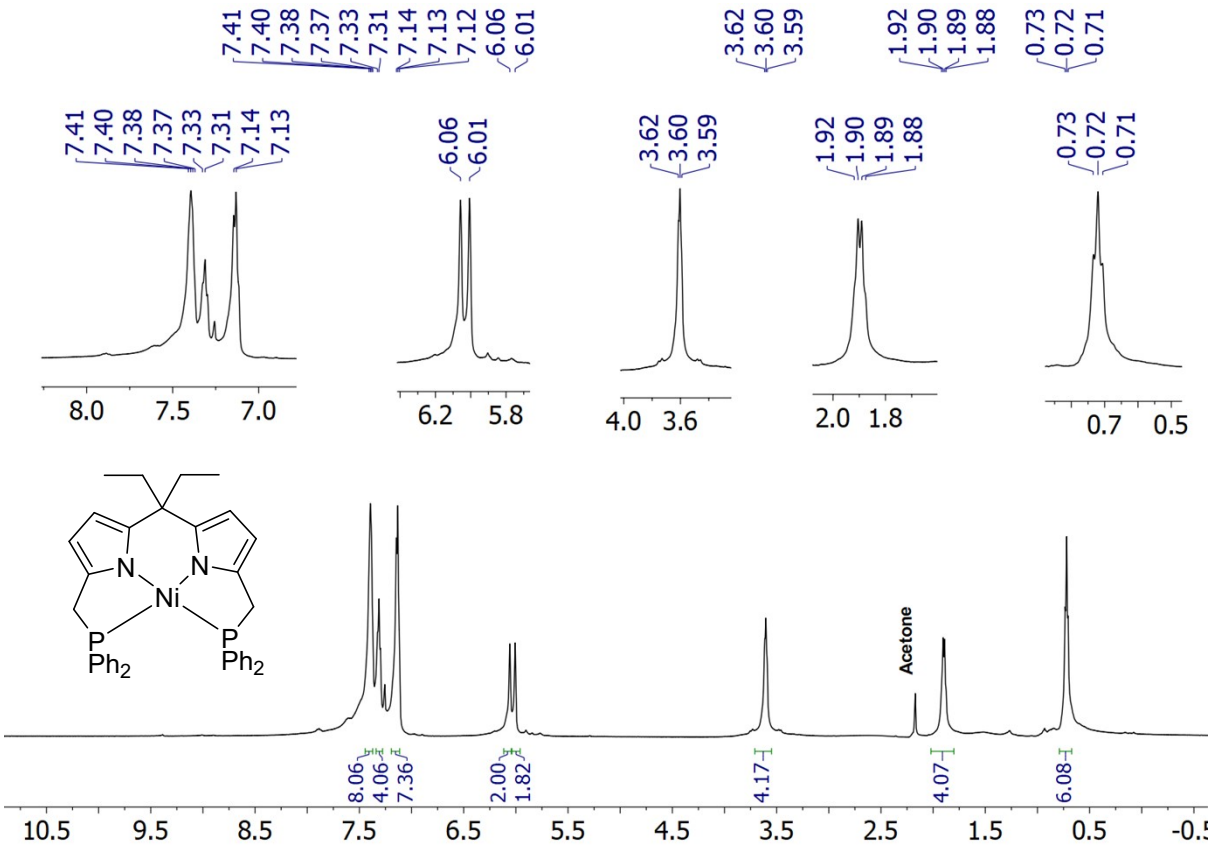

Figure S24. ^{1}H NMR ($CDCl_3$, 500 MHz) spectrum of [Ni{$Et_2C(C_4H_2N)_2$-1,9-$(CH_2PPh_2)_2$-κ^4-*P,N,N,P*}], **3b** (isolated complex).

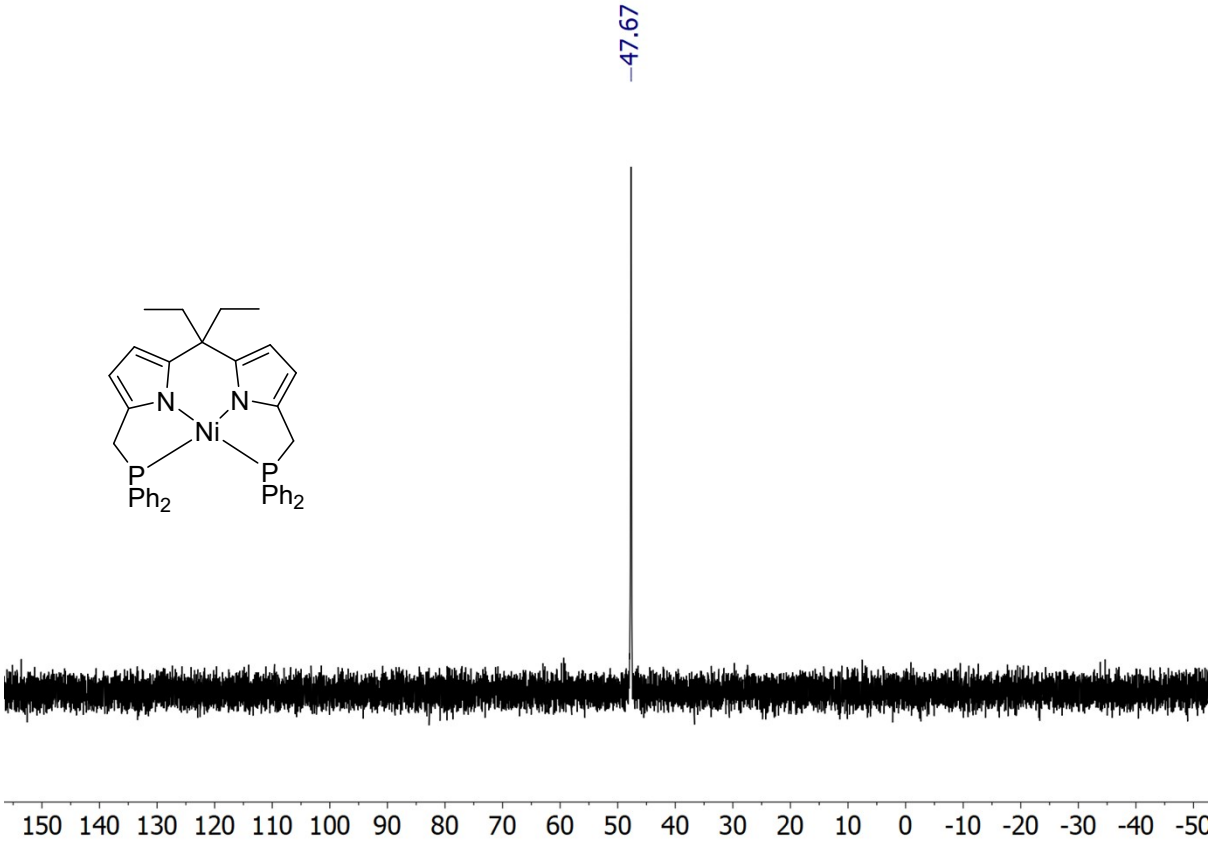

Figure S25. $^{31}P\{^{1}H\}$ NMR ($CDCl_3$, 202.45 MHz) spectrum of [Ni{$Et_2C(C_4H_2N)_2$-1,9-$(CH_2PPh_2)_2$-κ^4-*P,N,N,P*}], **3b** (isolated complex).

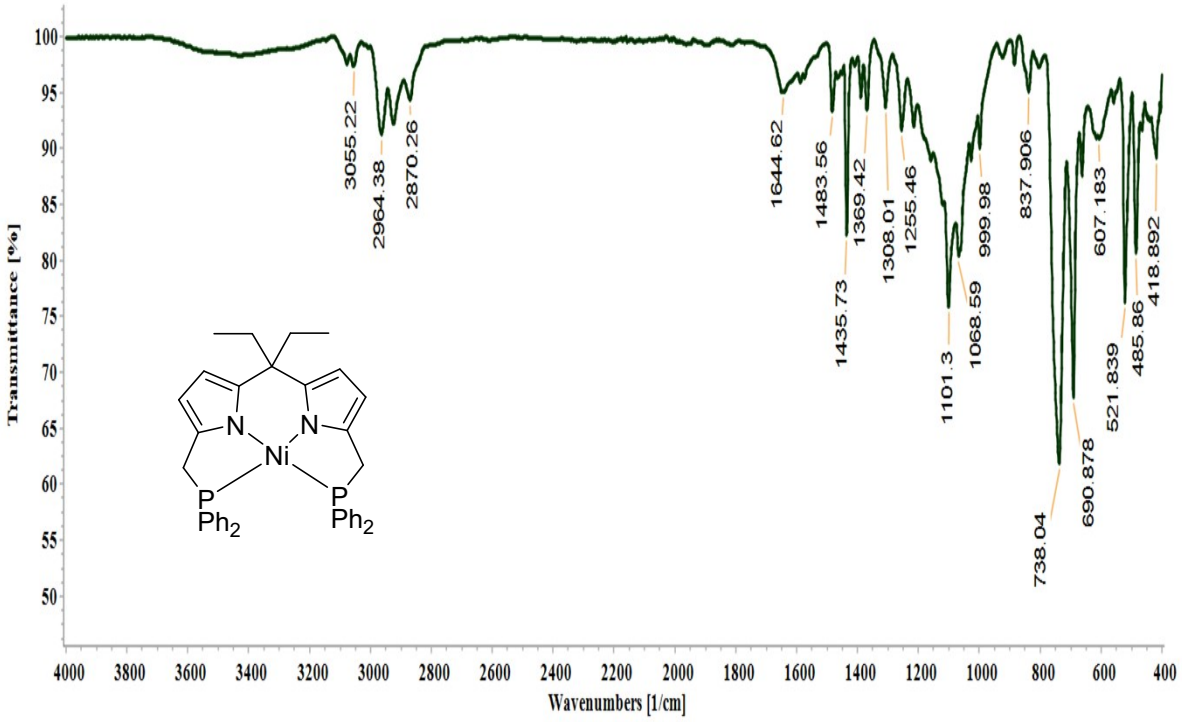

Figure S26. ATR spectrum of [Ni{$Et_2C(C_4H_2N)_2$-1,9-$(CH_2PPh_2)_2$-κ^4-*P,N,N,P*}], **3b** (isolated complex).

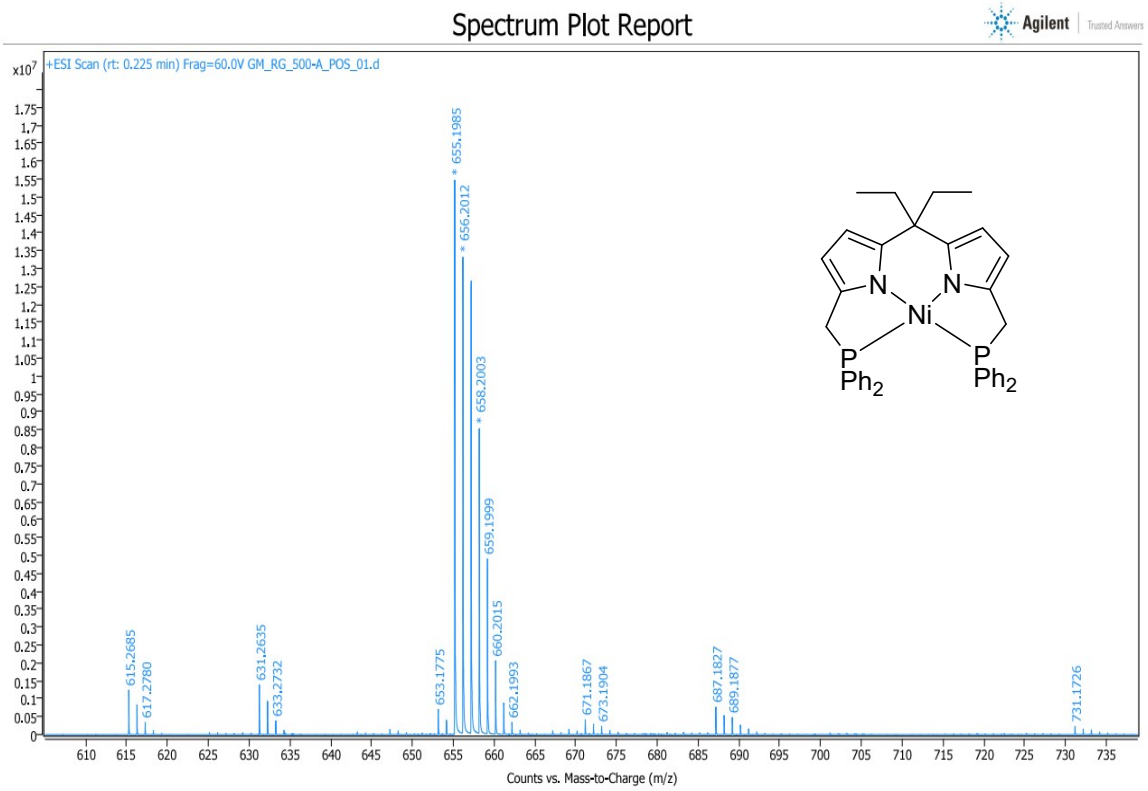

Figure S27. HRMS (ESI+) spectrum of [Ni{$Et_2C(C_4H_2N)_2$-1,9-$(CH_2PPh_2)_2$-κ^4-*P,N,N,P*}], **3b** (isolated complex).

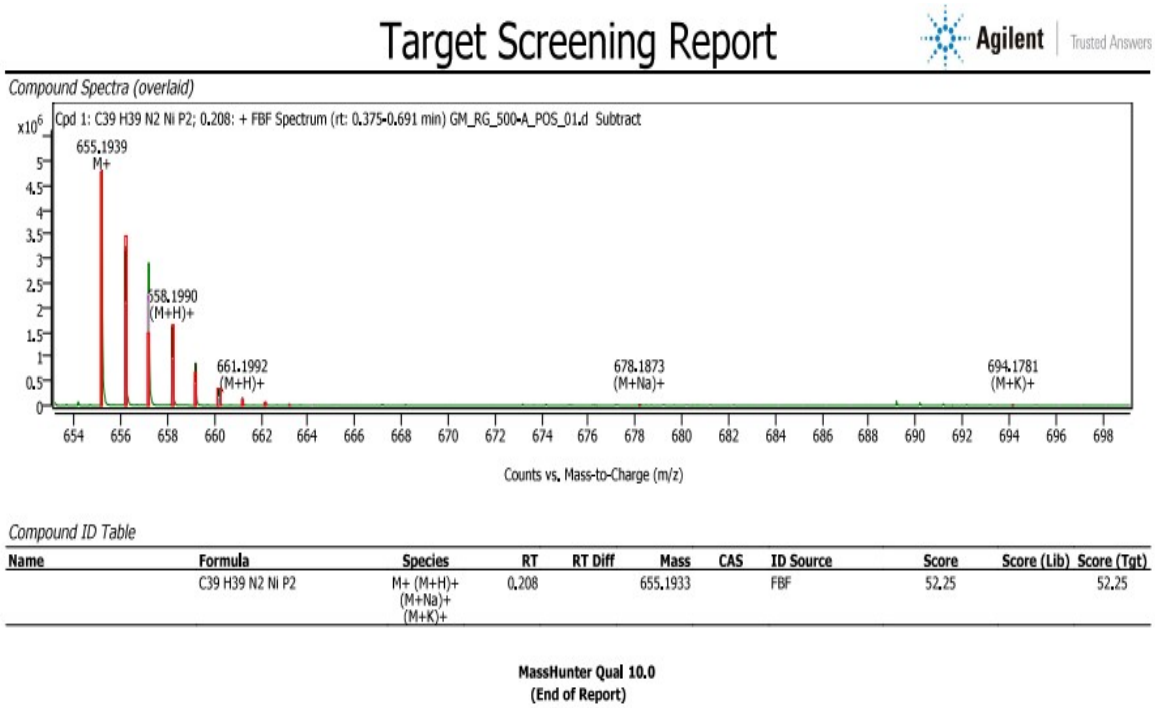

Figure S28. HRMS (ESI+) target screening of [Ni{$Et_2C(C_4H_2N)_2$-1,9-$(CH_2PPh_2)_2$-κ^4-*P,N,N,P*}], **3b** (isolated complex).

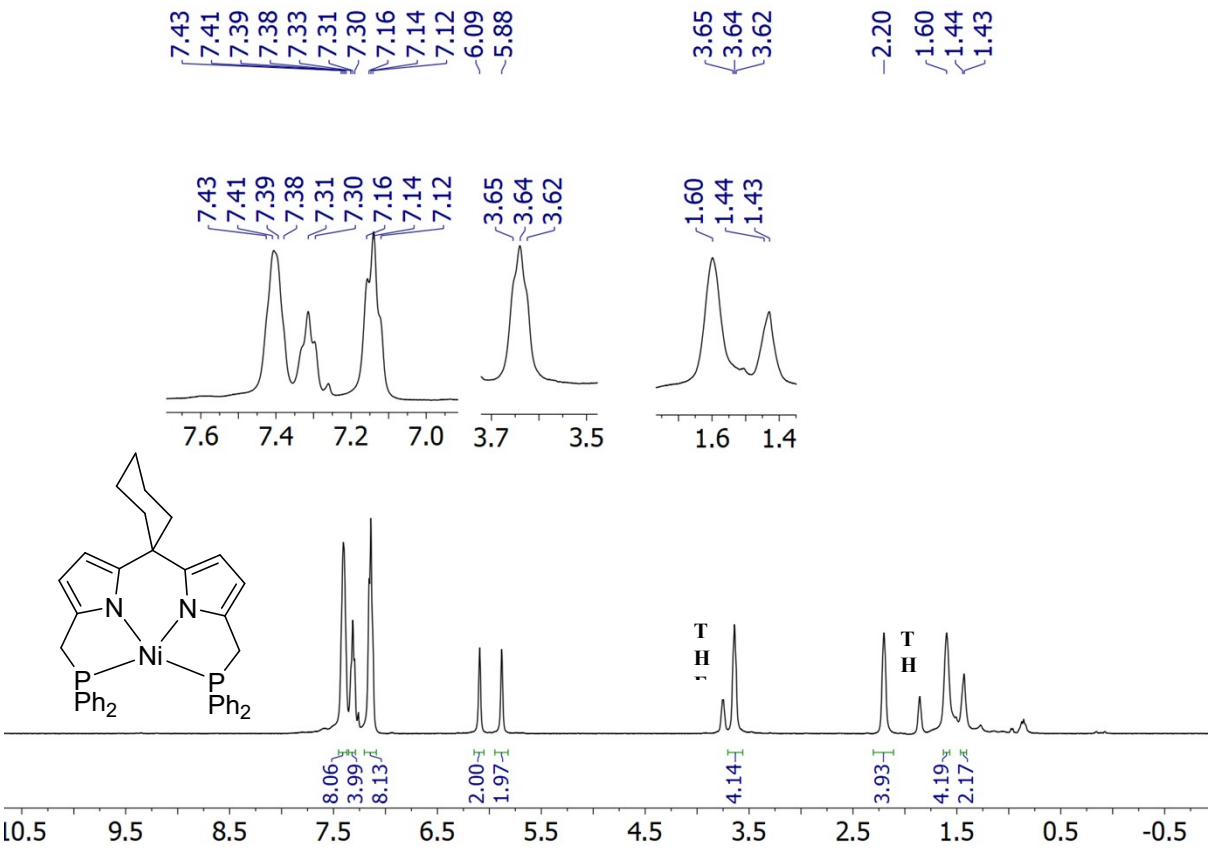

Figure S29. ^{1}H NMR ($CDCl_3$, 400 MHz) spectrum of [Ni{-$(CH_2)_5$-$C(C_4H_2N)_2$-1,9-$(CH_2PPh_2)_2$-κ^4-*P,N,N,P*}], **3c** (isolated complex).

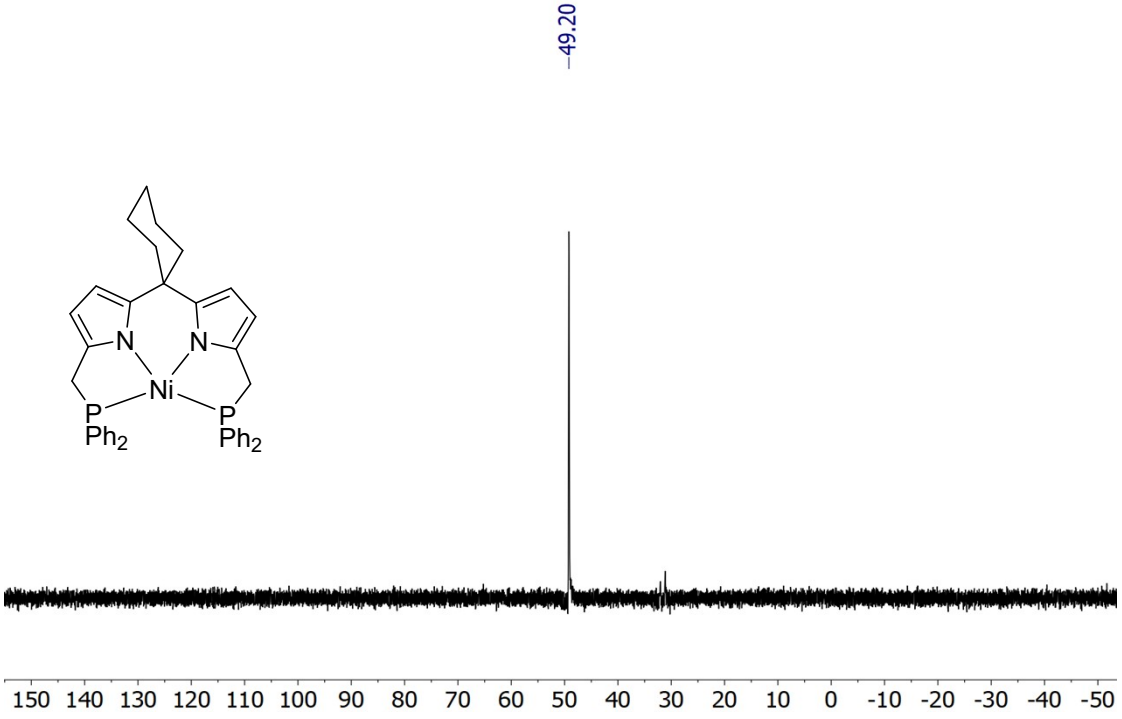

Figure S30. $^{31}P\{^{1}H\}$ NMR ($CDCl_3$, 202.45 MHz) spectrum of [Ni{-$(CH_2)_5$-$C(C_4H_2N)_2$-1,9-$(CH_2PPh_2)_2$-κ^4-*P,N,N,P*}], **3c** (isolated complex).

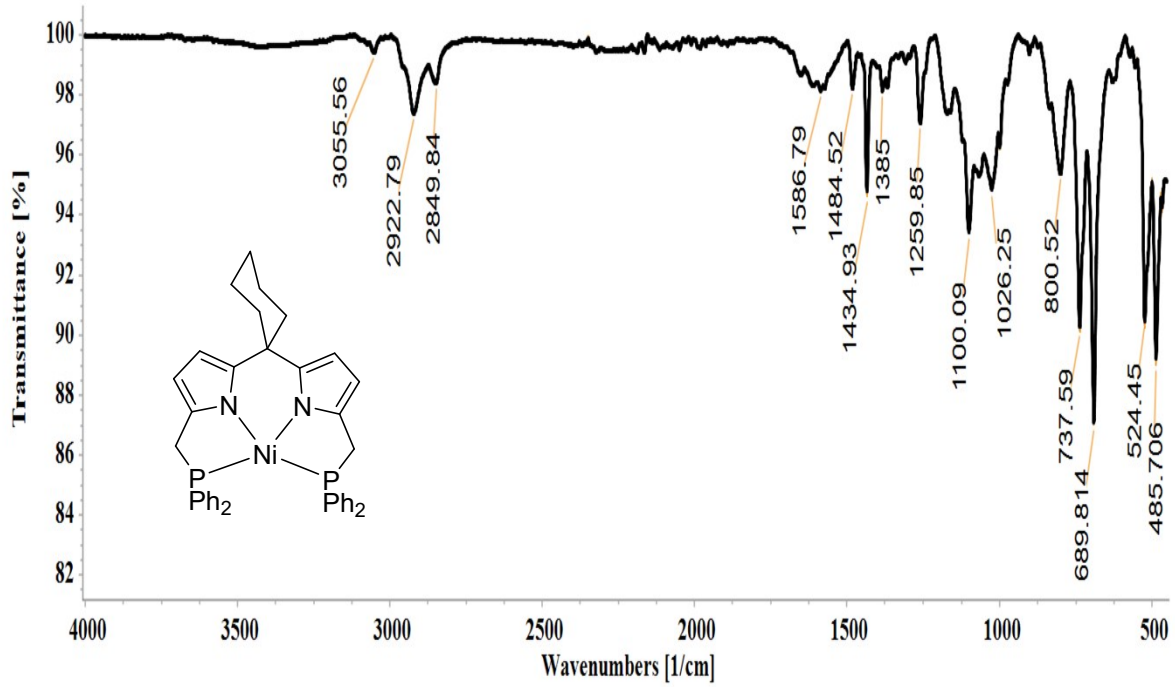

Figure S31. ATR spectrum of [Ni{-$(CH_2)_5$-$C(C_4H_2N)_2$-1,9-$(CH_2PPh_2)_2$-κ^4-*P,N,N,P*}], **3c** (isolated complex).

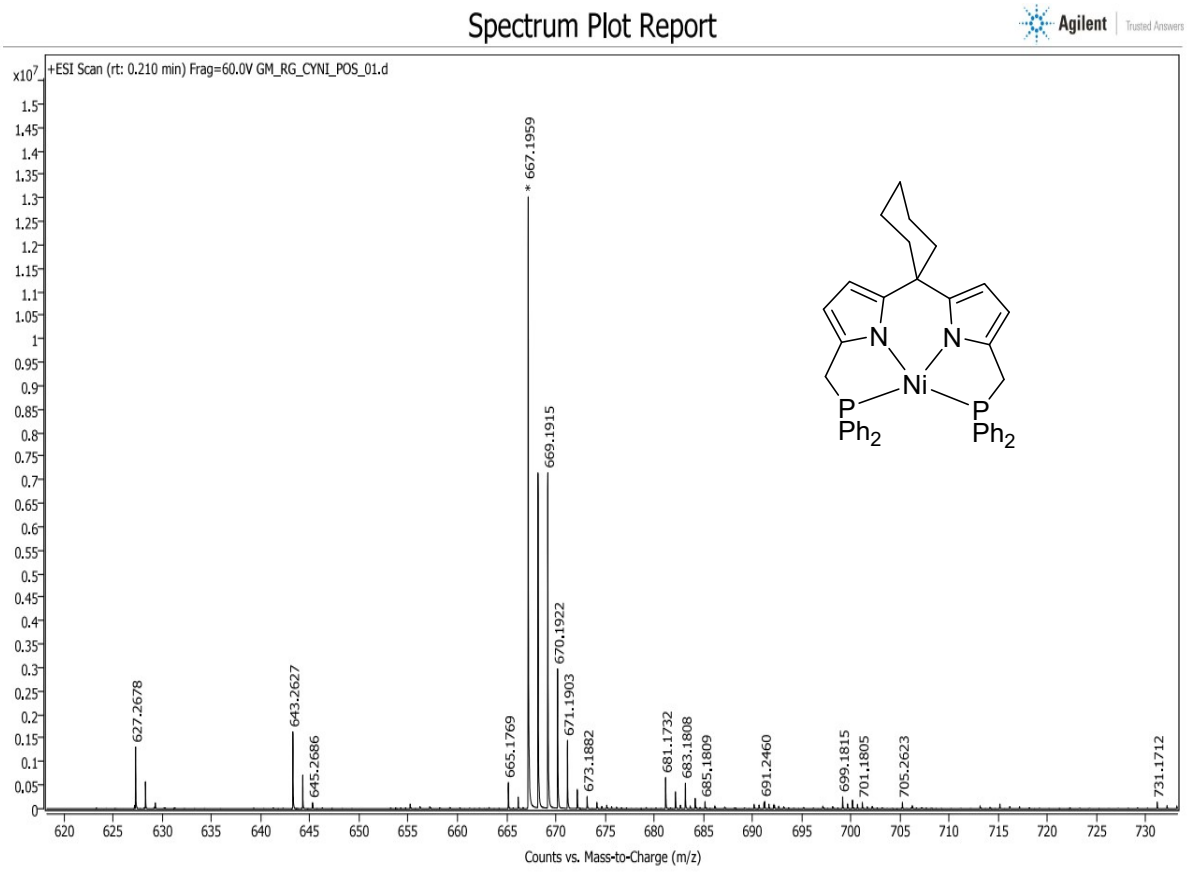

Figure S32. HRMS (ESI+) spectrum of [Ni{-$(CH_2)_5$-$C(C_4H_2N)_2$-1,9-$(CH_2PPh_2)_2$-κ^4-*P,N,N,P*}], **3c** (isolated complex).

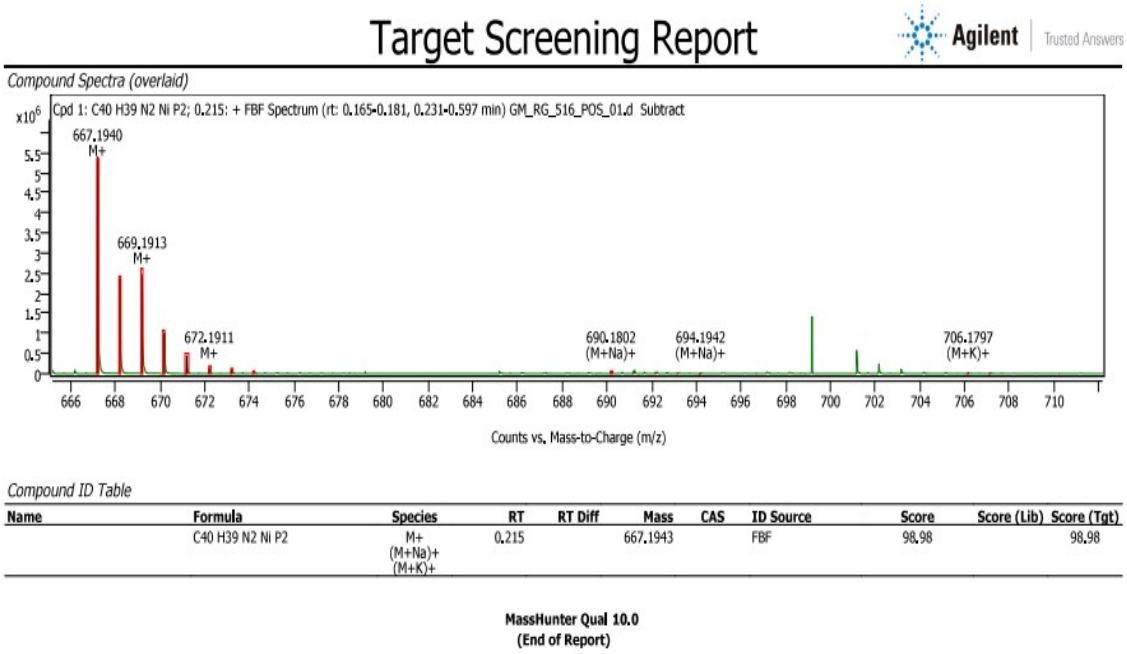

Figure S33. HRMS (ESI+) target screening of [Ni{-$(CH_2)_5$-$C(C_4H_2N)_2$-1,9-$(CH_2PPh_2)_2$-κ^4-*P,N,N,P*}], **3c** (isolated complex).

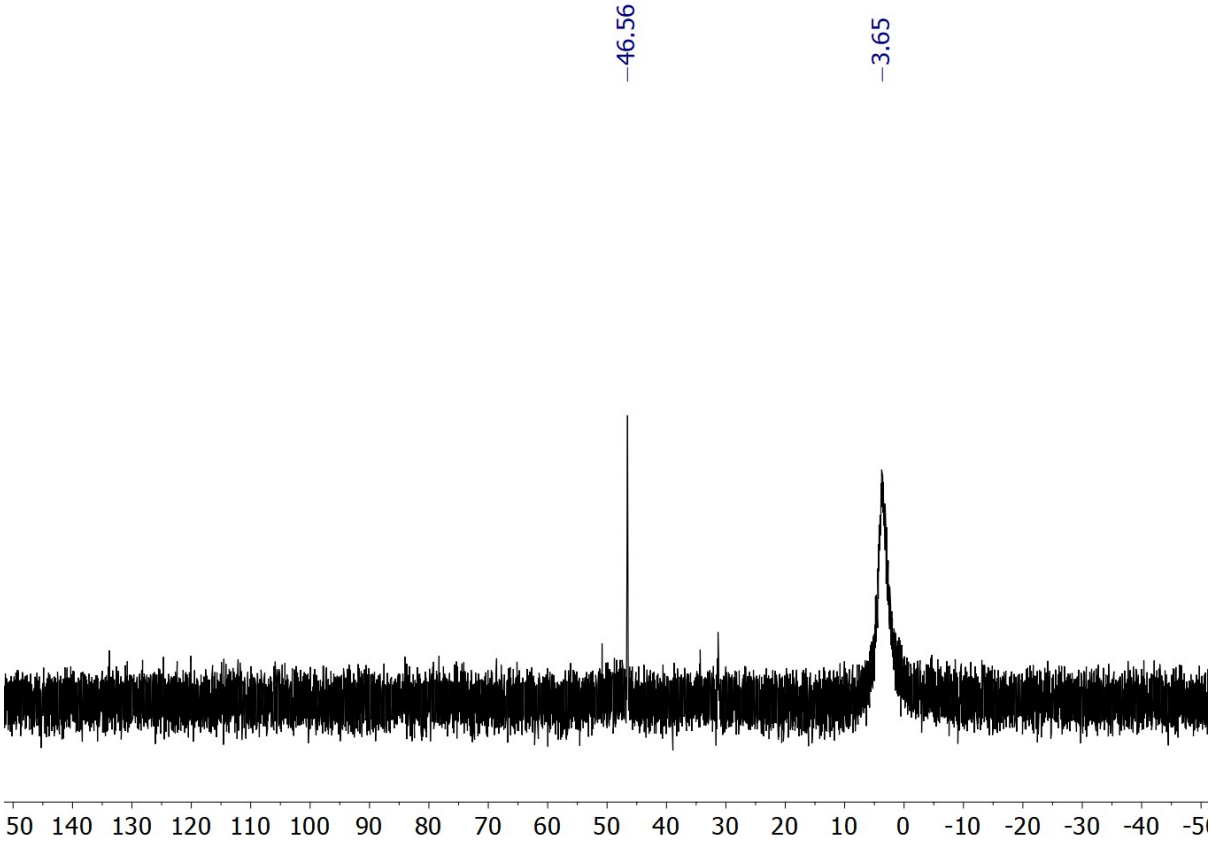

Figure S34. $^{31}P\{^1H\}$ NMR (C_6H_6 with D_2O capillary tube, 202.45 MHz) spectrum of the red solid obtained from the reaction mixture of **L2H2** and $NiCl_2$(DME) in CH_3CN after 1 h. The red solid was obtained after removing all solvents, washing with petroleum ether followed by diethyl ether and then drying.

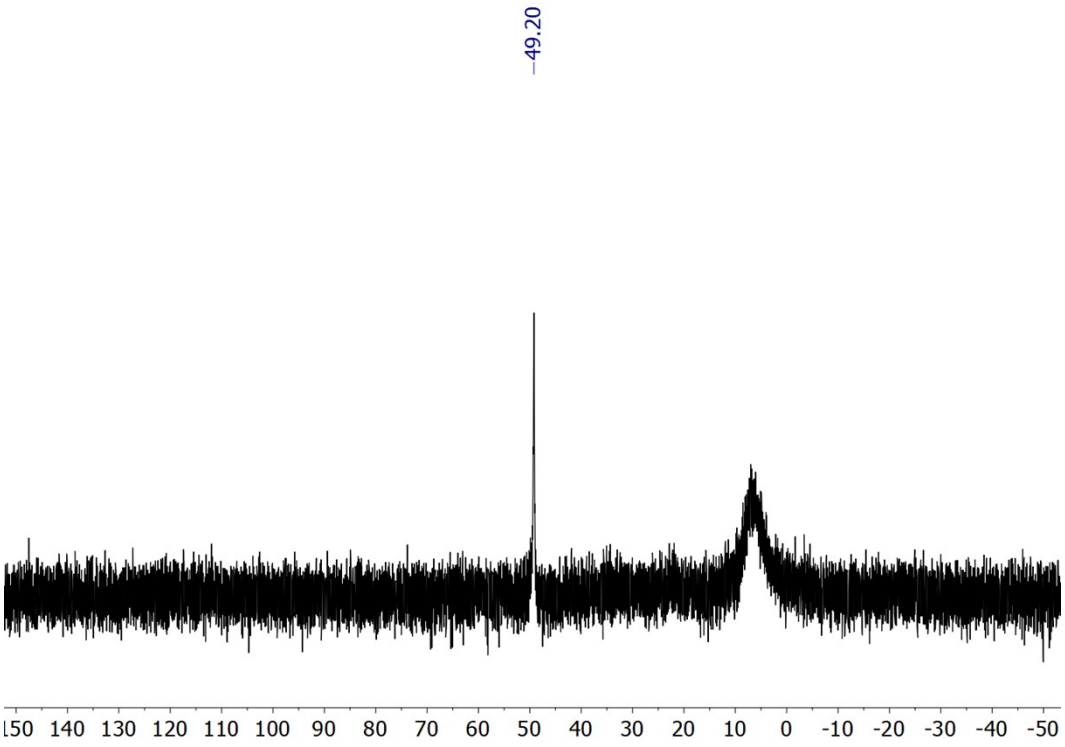

Figure S35. $^{31}P\{^{1}H\}$ NMR (C_6H_6 with D_2O capillary tube, 202.45 MHz) spectrum of the red solid obtained from the reaction of **L3H2** with $NiCl_2$(DME) in CH_3CN after 1 h. The red solid was obtained after removing all solvents, washing with petroleum ether followed by diethyl ether and then drying.

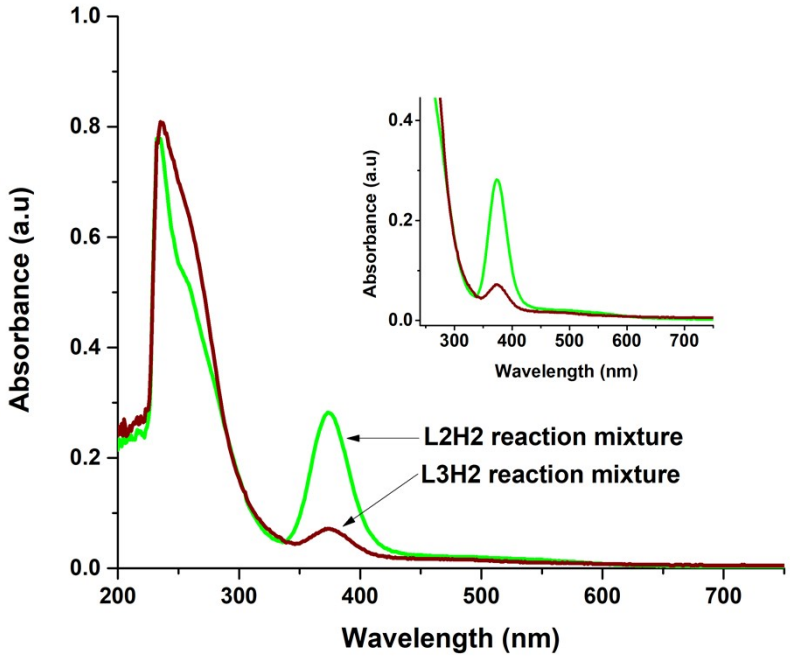

Figure S36. The UV-Vis spectra of the red solid in dichloromethane obtained from the reaction of **L2H2** and **L3H2** with $NiCl_2$(DME) in CH_3CN after 1 h. The red solid was obtained after removing all solvents, washing with petroleum ether followed by diethyl ether and then drying.

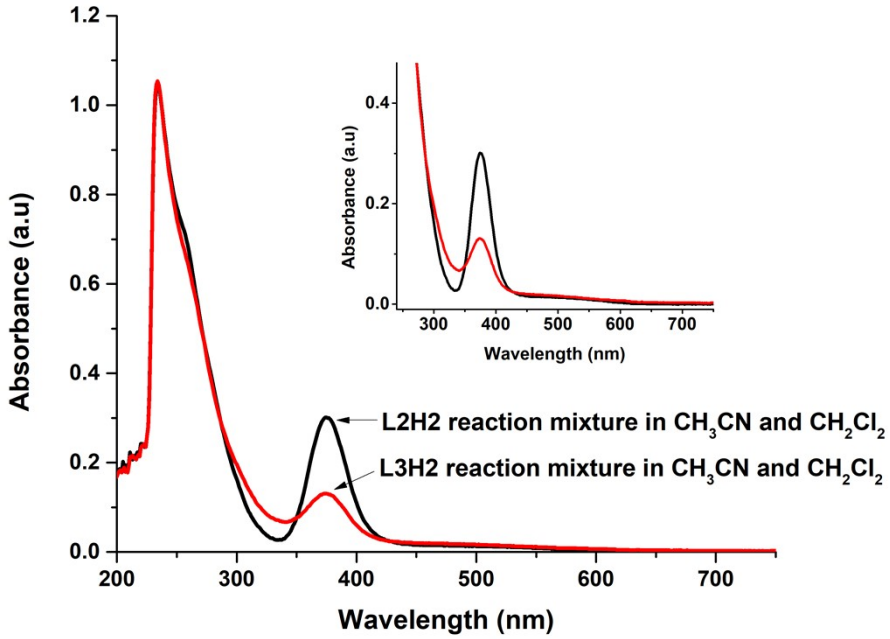

Figure S37. The UV-Vis spectra of the reaction mixtures of **L2H2** and **L3H2** with $NiCl_2$(DME) in CH_3CN and dichloromethane.

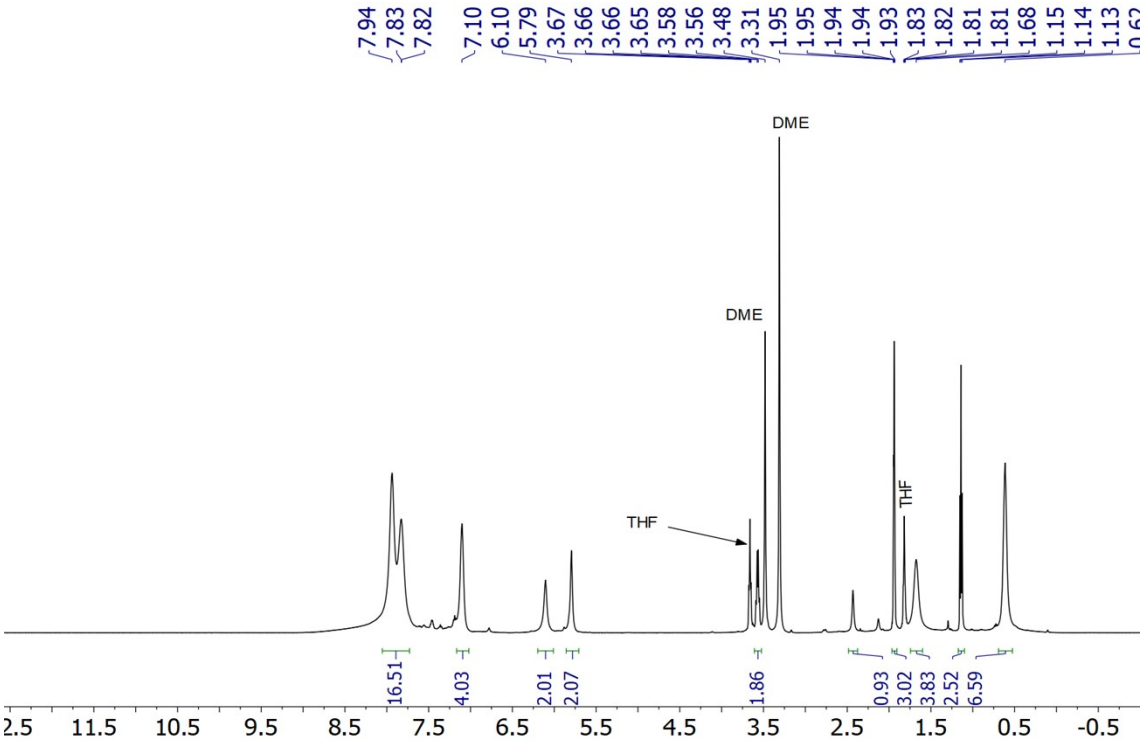

Figure S38. ^1H NMR (CD_3CN, 500 MHz) spectrum of the reaction mixture of **L2H2** and $NiCl_2$(DME) carried out in an NMR tube. Recorded after 1 h.

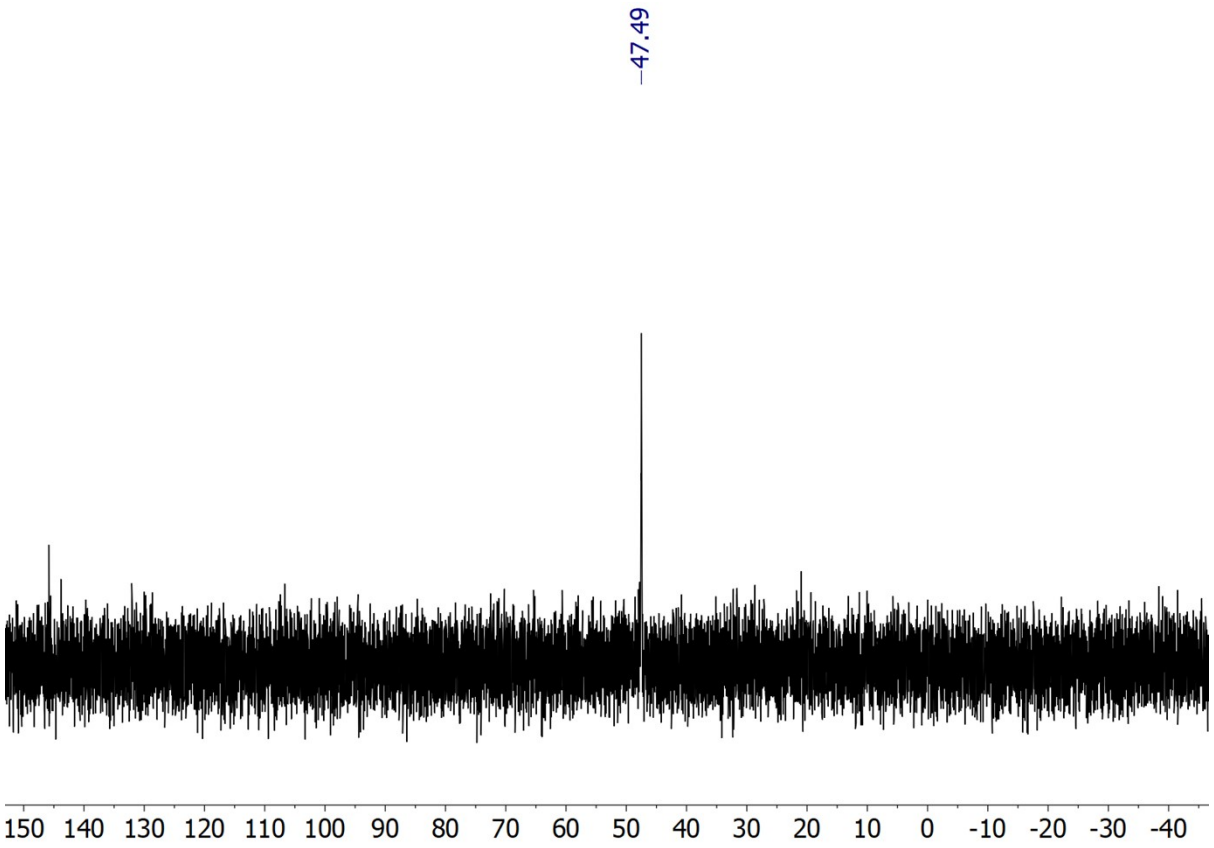

Figure S39. $^{31}P\{^{1}H\}$ NMR (CD_3CN, 202.45 MHz) spectrum of the reaction mixture of **L2H2** and $NiCl_2$(DME) carried out in an NMR tube. Recorded after 1 h.

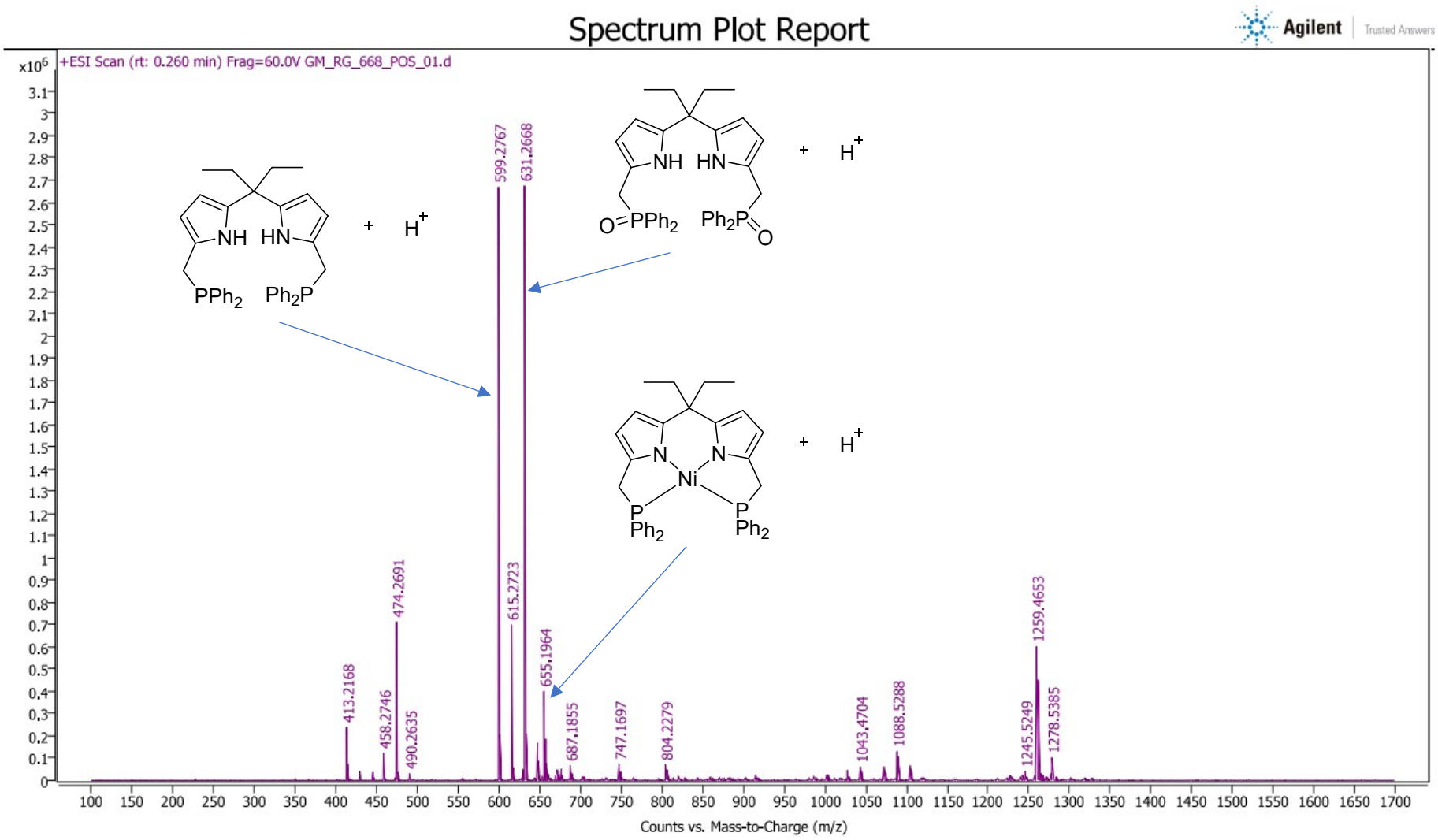

Figure S40. HRMS (ESI+) spectrum of the reaction mixture of **L2H2** and $NiCl_2$(DME) in CD_3CN carried out in an NMR tube.

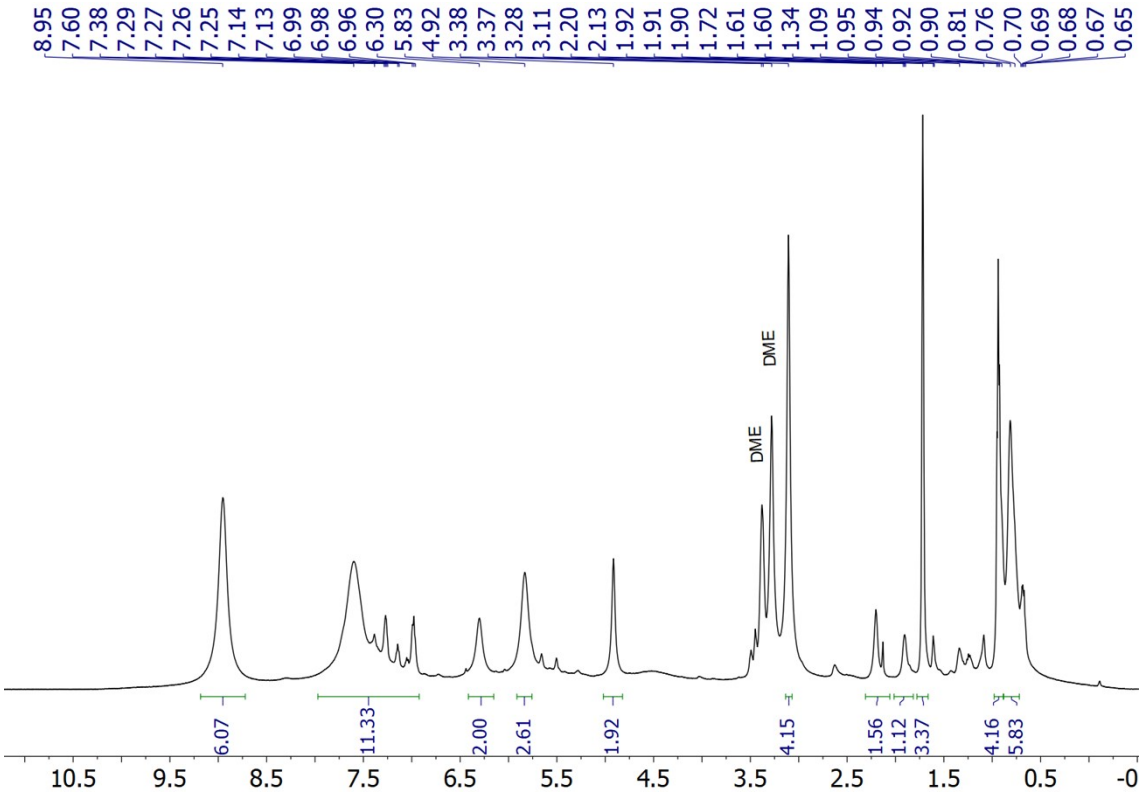

Figure S41. ^{1}H NMR (CD_3CN, 500 MHz) spectrum of the reaction mixture of **L3H2** and $NiCl_2$(DME) carried out in an NMR tube. Recorded after 1 h.

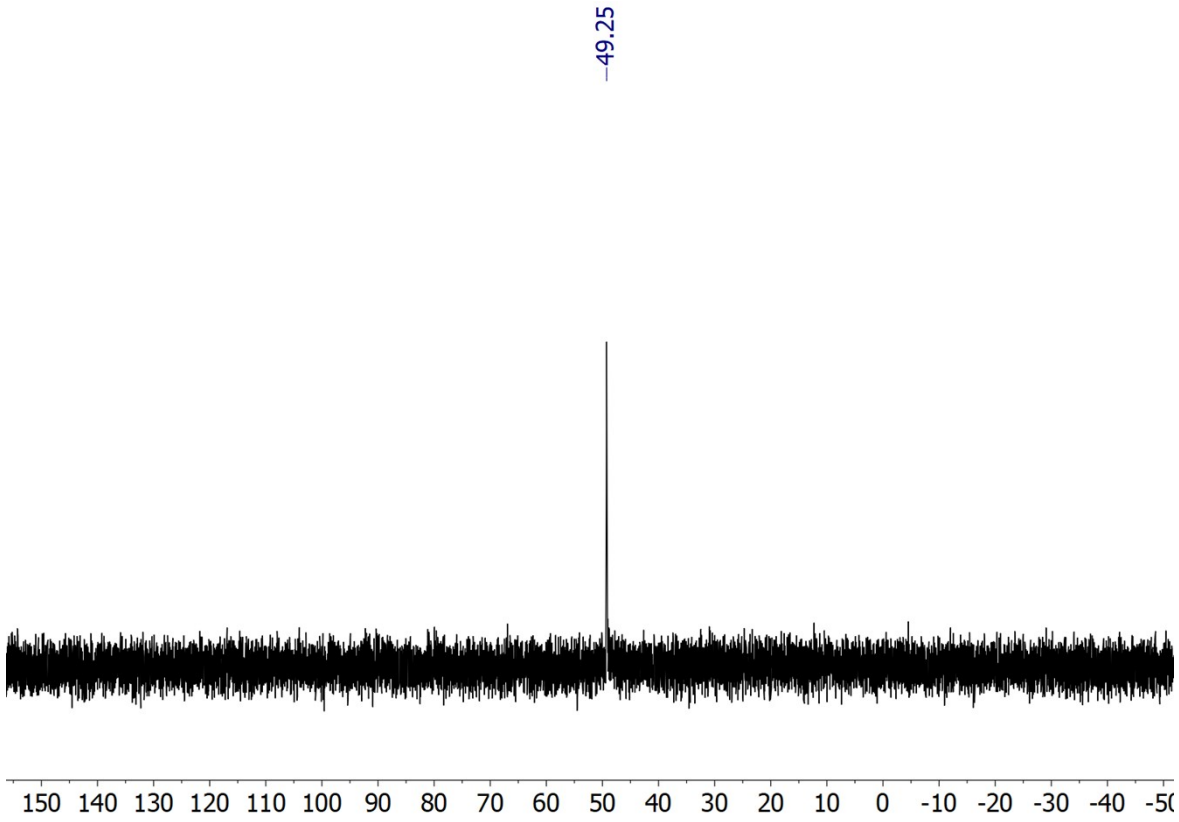

Figure S42. $^{31}P\{^{1}H\}$ NMR (CD_3CN, 202.45 MHz) spectrum of the reaction mixture of **L3H2** and $NiCl_2$(DME) carried out in an NMR tube. Recorded after 1 h.

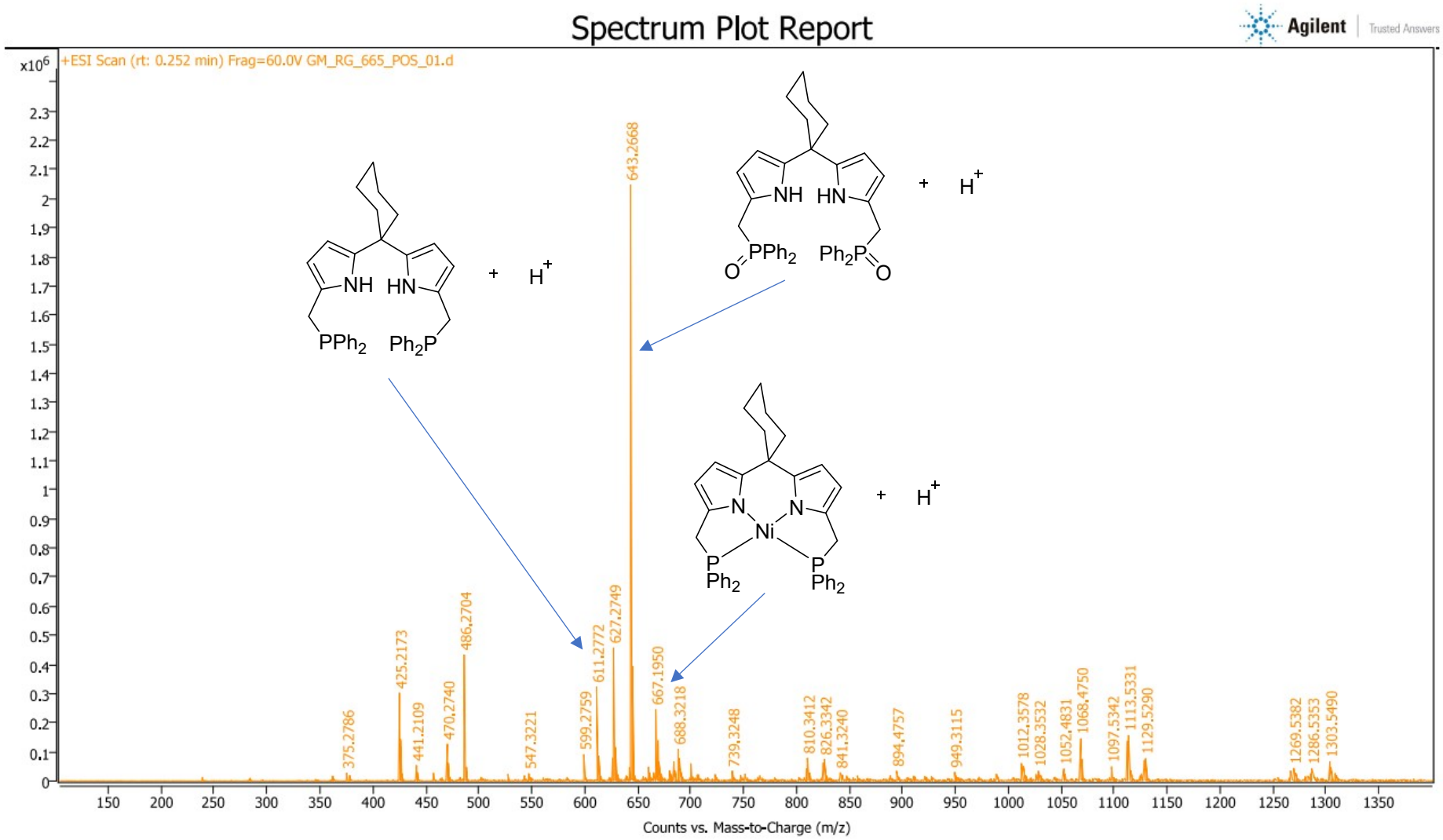

Figure S43. HRMS (ESI+) spectrum of the reaction mixture of **L3H2** and $NiCl_2(DME)$ in CD_3CN carried out in an NMR tube.

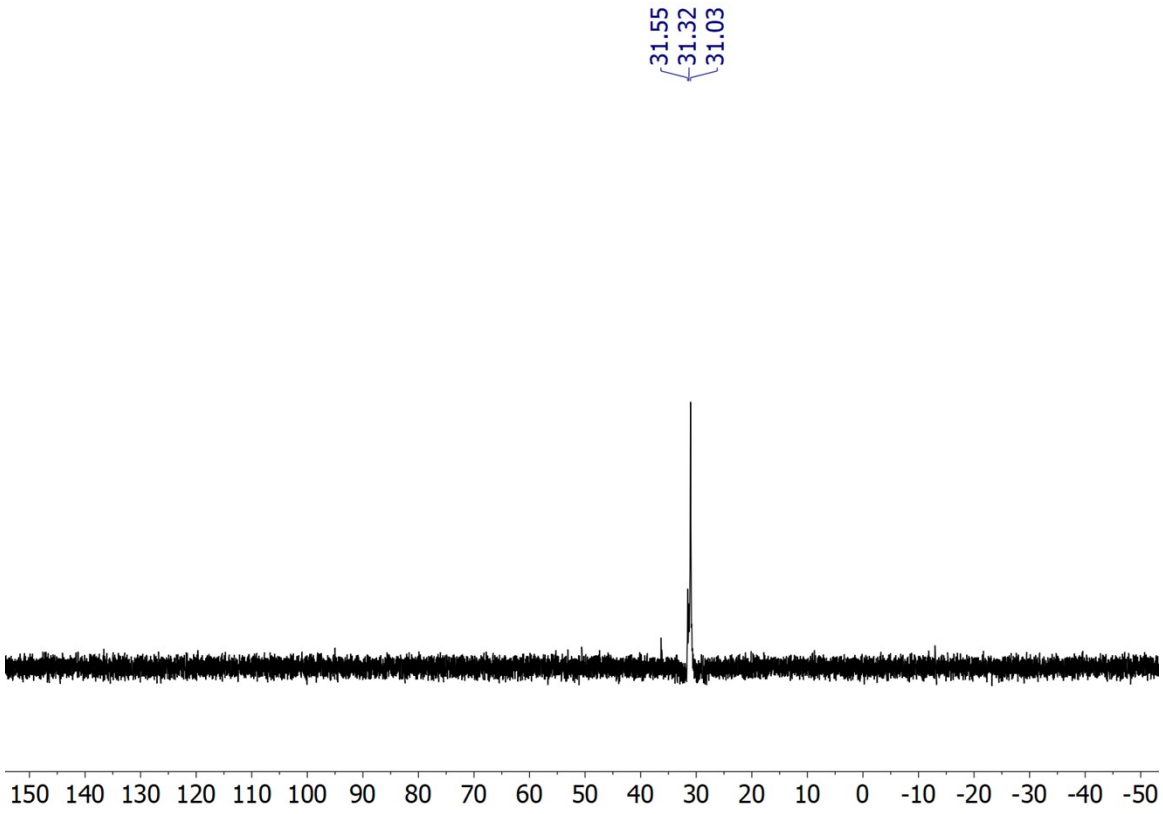

Figure S44. $^{31}P\{^{1}H\}$ NMR ($CHCl_3$ with D_2O capillary, 202.45 MHz) spectrum of solid obtained resulting from the decomposition of **3a** in DCM under the open atmosphere after 10 days.

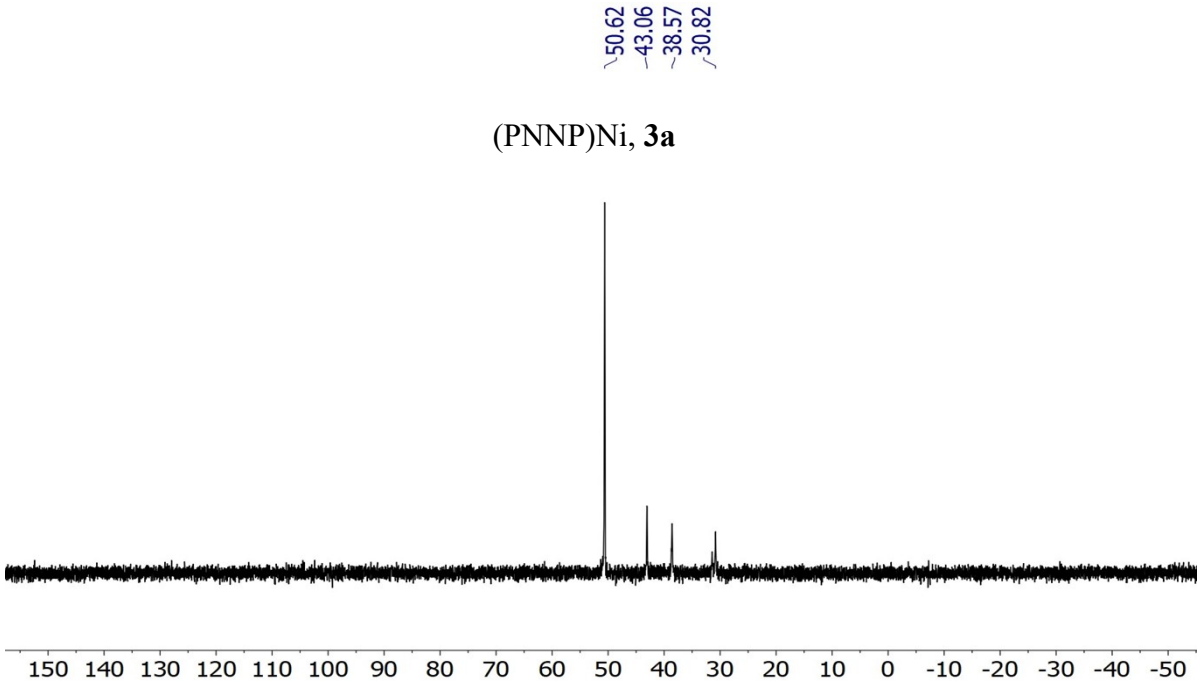

Figure S45. $^{31}P\{^{1}H\}$ NMR (THF with D_2O capillary, 202.45 MHz) spectrum of the yellow precipitate and crystals of complex **4a** obtained by layering **L1H2** and $Ni(COD)_2$ in THF.

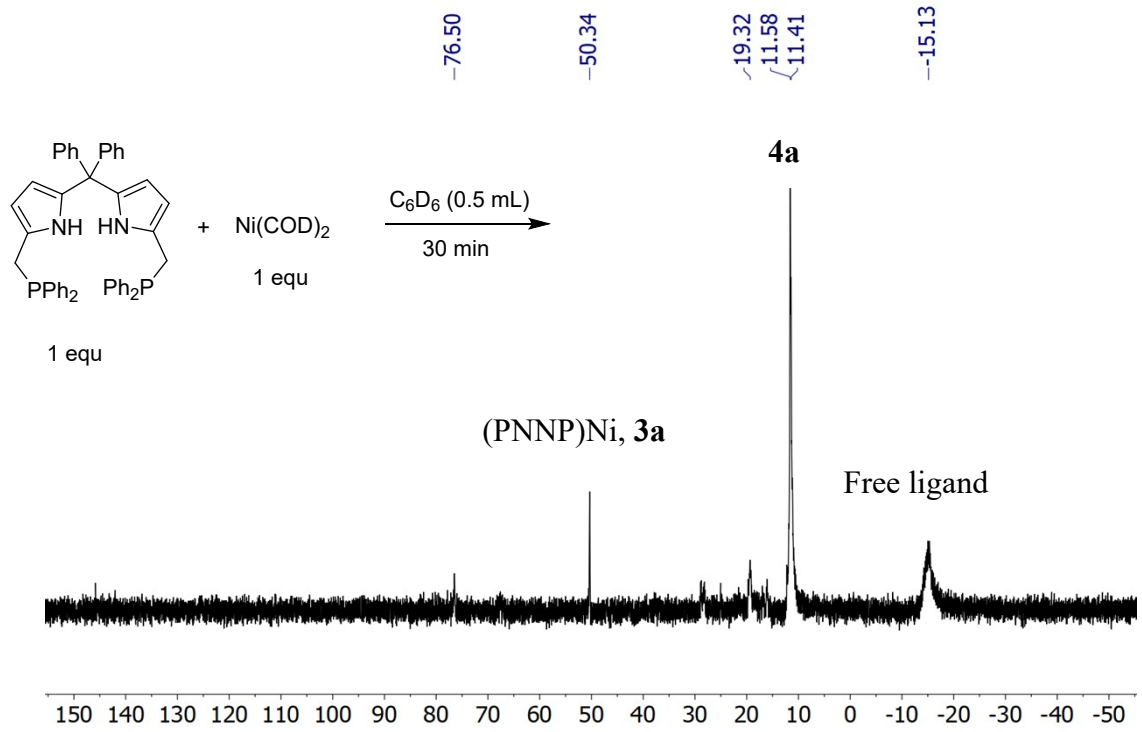

Figure S46. $^{31}P\{^{1}H\}$ NMR (C_6D_6, 202.45 MHz) spectrum of the reaction mixture of **L1H2** and $Ni(COD)_2$ carried out in an NMR tube. The spectrum was recorded after approximately 30 minutes. The major peak at 11.4 ppm is assigned to complex **4a**.

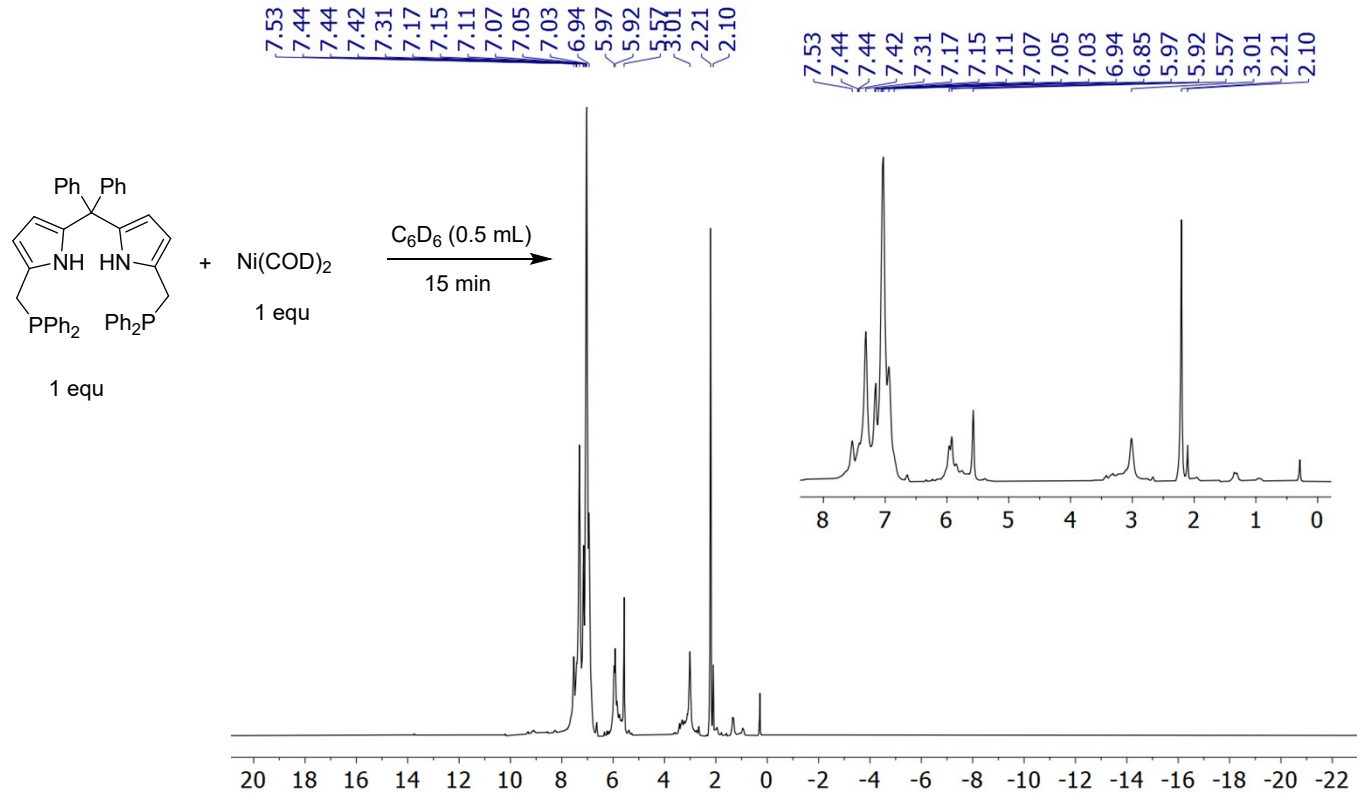

Figure S47. ^{1}H NMR (C_6D_6, 400 MHz) spectrum of the reaction mixture of **L1H2** and $Ni(COD)_2$ carried out in an NMR tube. The spectrum was recorded after approximately 15 minutes. There is no peak in the negative region.

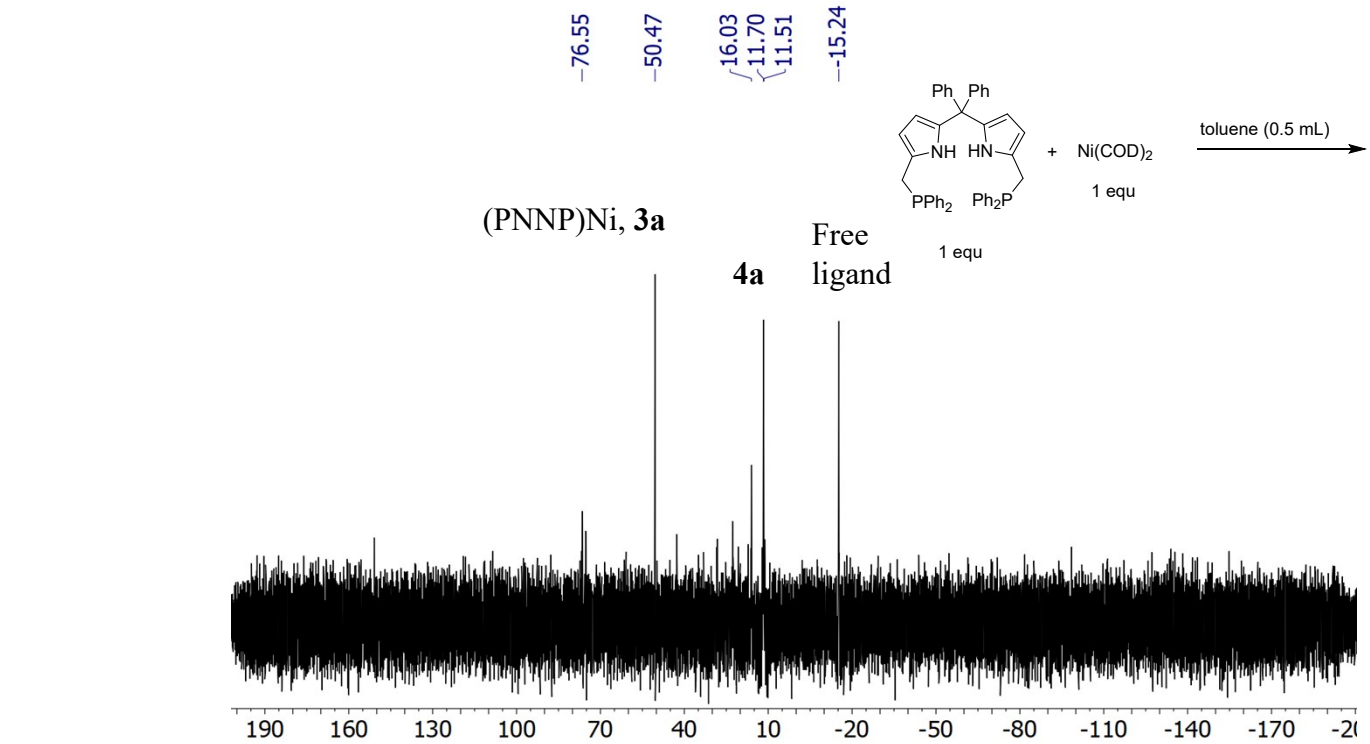

Figure S48. $^{31}P\{^{1}H\}$ NMR (toluene solution with D_2O capillary, 202.45 MHz) spectrum of the reaction mixture of **L1H2** and $Ni(COD)_2$ carried out in an NMR tube.

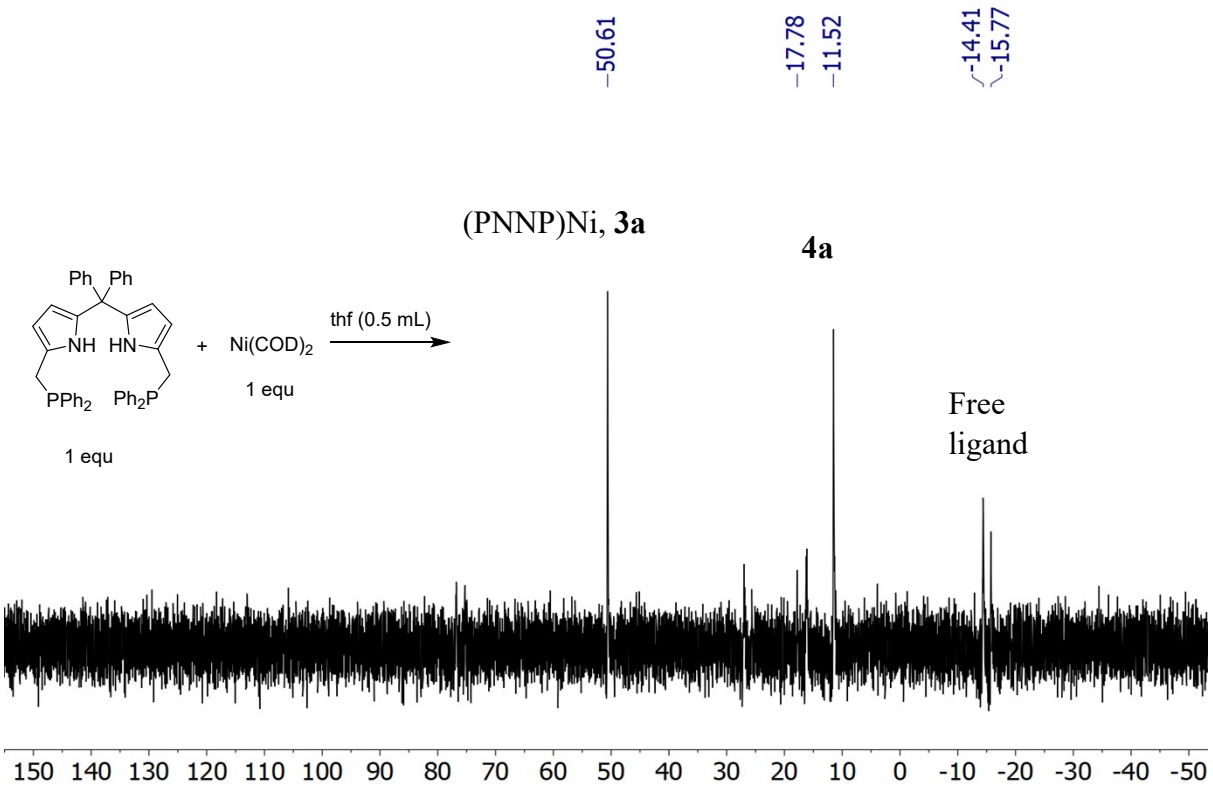

Figure S49. $^{31}P\{^{1}H\}$ NMR (THF solution with D_2O capillary, 202.45 MHz) spectrum of the reaction mixture of **L1H2** and $Ni(COD)_2$ carried out in an NMR tube.

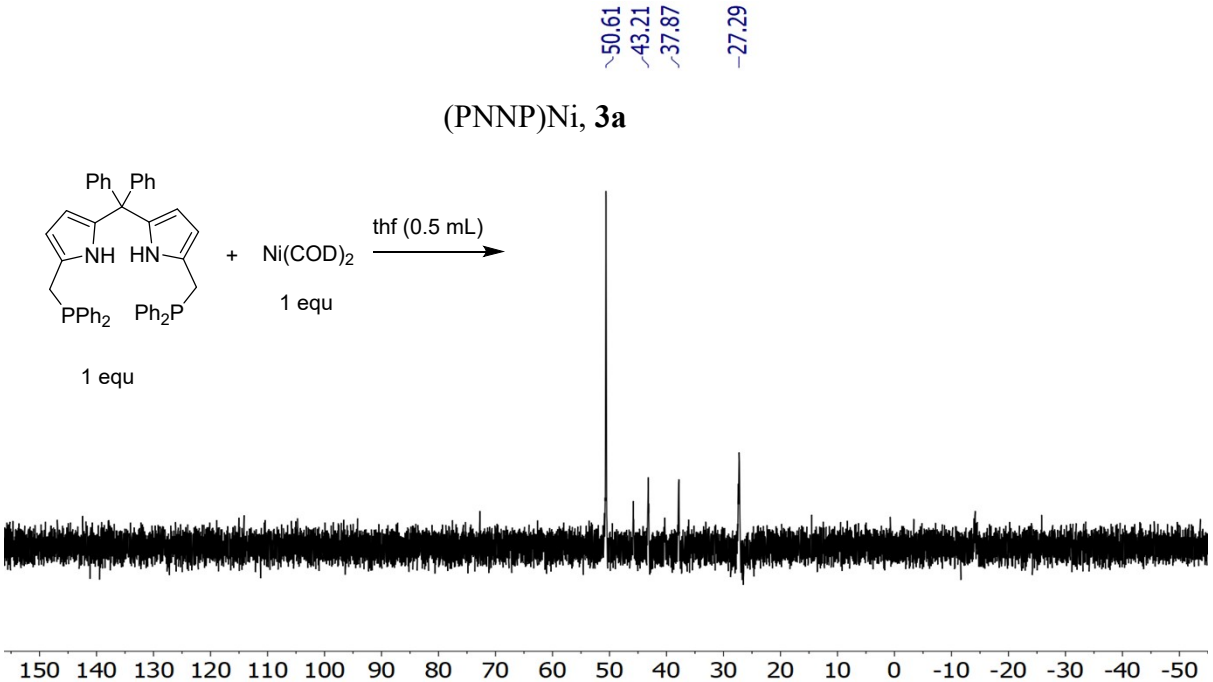

Figure S50. $^{31}P\{^{1}H\}$ NMR (THF solution with D_2O capillary, 202.45 MHz) spectrum of the reaction mixture of **L1H2** and $Ni(COD)_2$ carried out in a NMR tube after 7 days. It shows the disappearance of the signal for the free ligand as well as the signal at around 11 ppm and formation of other unidentified products.

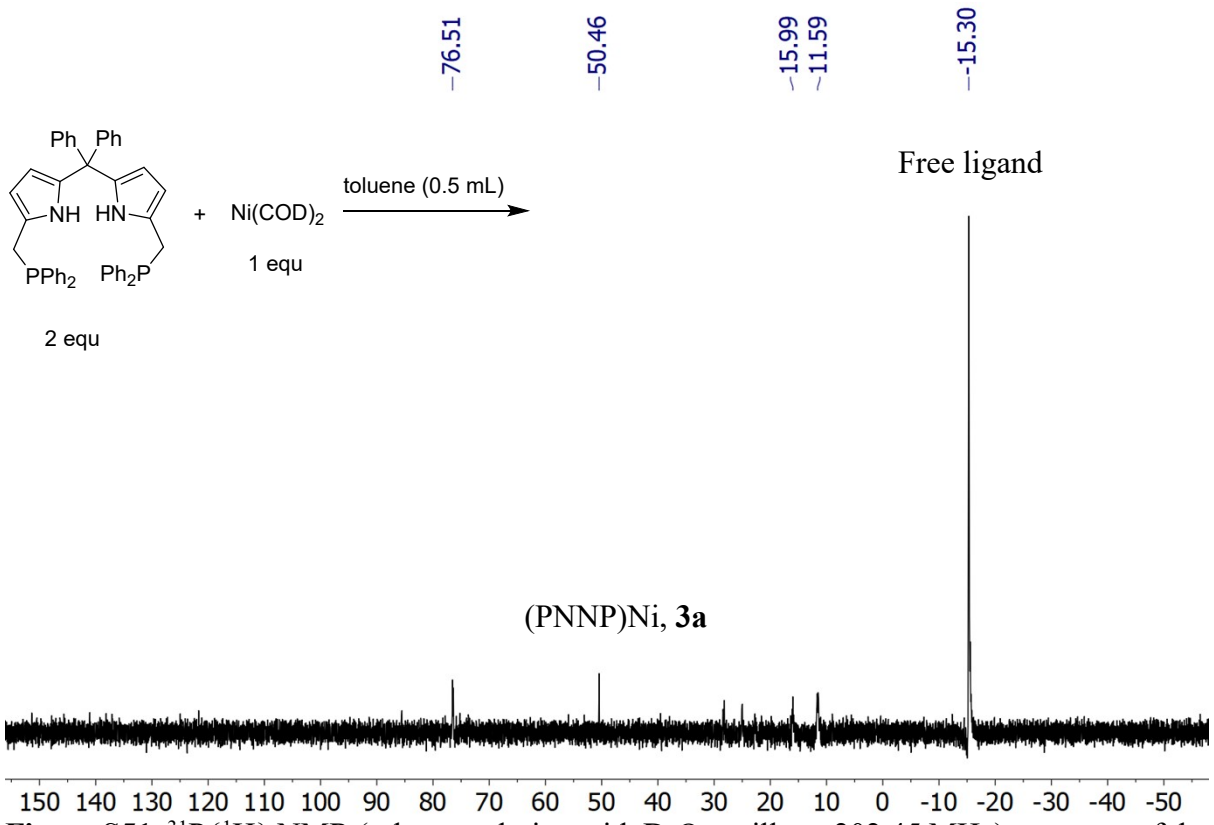

Figure S51. $^{31}P\{^{1}H\}$ NMR (toluene solution with D_2O capillary, 202.45 MHz) spectrum of the reaction mixture of **L1H2** and $Ni(COD)_2$ (2:1) carried out in an NMR tube.

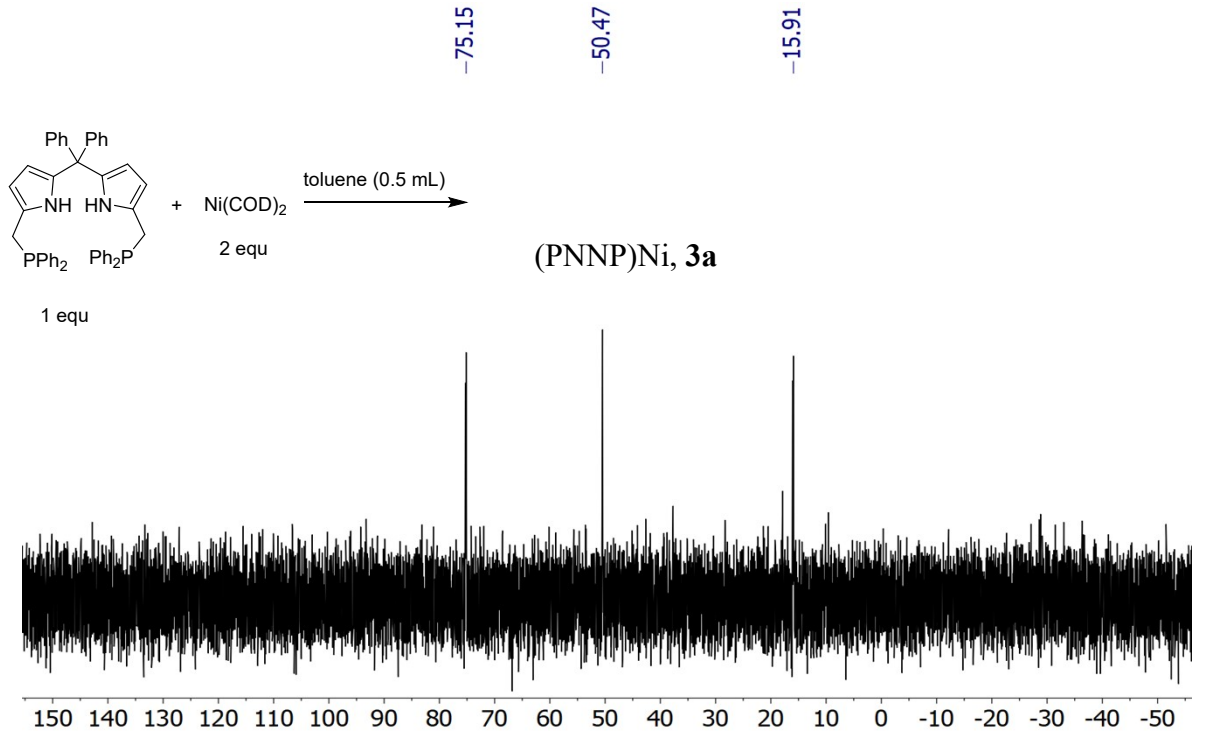

Figure S52. $^{31}P\{^{1}H\}$ NMR (toluene solution with D_2O capillary, 202.45 MHz) spectrum of the reaction mixture of **L1H2** and $Ni(COD)_2$ (1:2) carried out in an NMR tube.

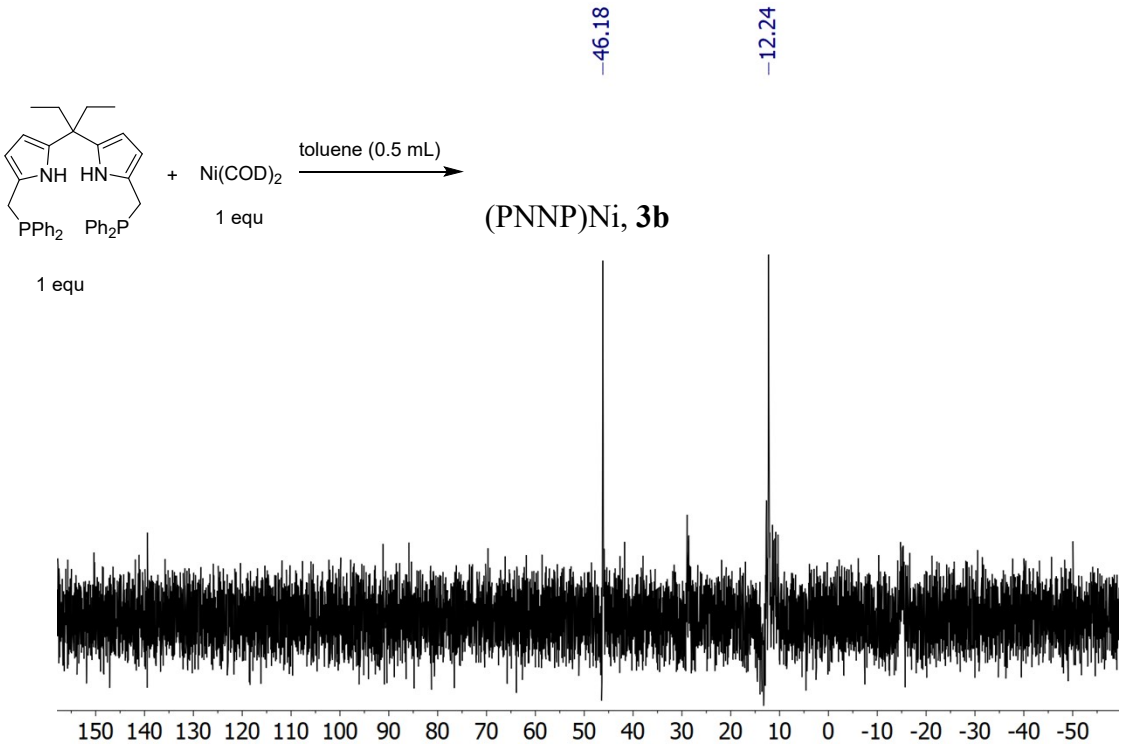

Figure S53. $^{31}P\{^{1}H\}$ NMR (toluene solution with D_2O capillary, 202.45 MHz) spectrum of the reaction mixture of **L2H2** and $Ni(COD)_2$ carried out in an NMR tube. The peaks at 46.2 and 12.2 ppm are assigned to complex **3b** and a nickel(0) complex analogous to complex **4a**, respectively.

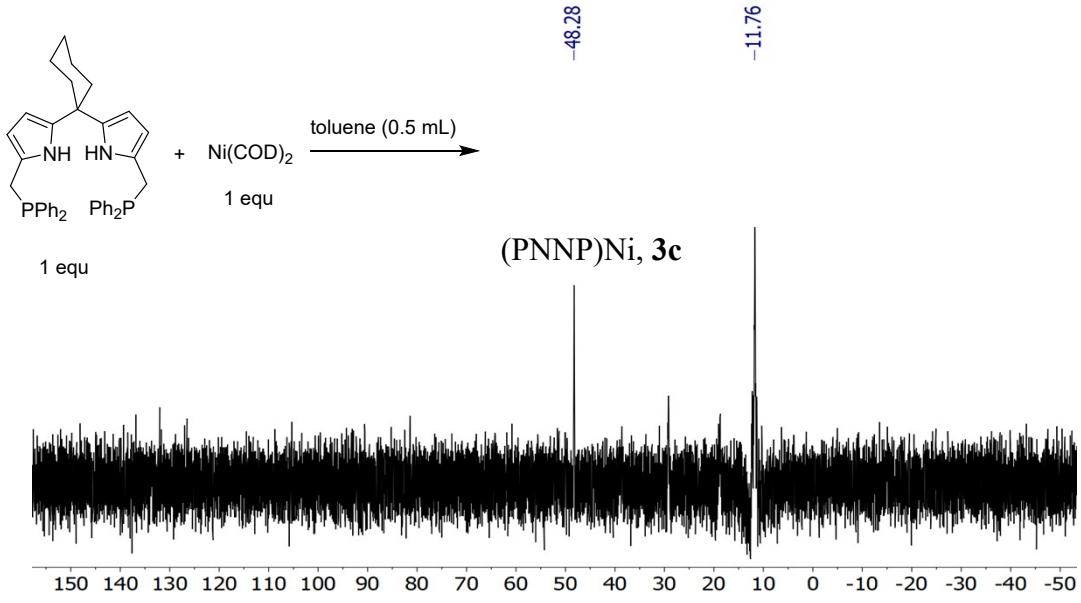

Figure S54. $^{31}P\{^{1}H\}$ NMR (toluene solution with D_2O capillary, 202.45 MHz) spectrum of the reaction mixture of **L3H2** and $Ni(COD)_2$ carried out in a NMR tube. The peaks at 48.3 and 11.8 ppm are assigned to complex **3c** and a nickel(0) complex analogous to complex **4a**, respectively.

Catalytic studies

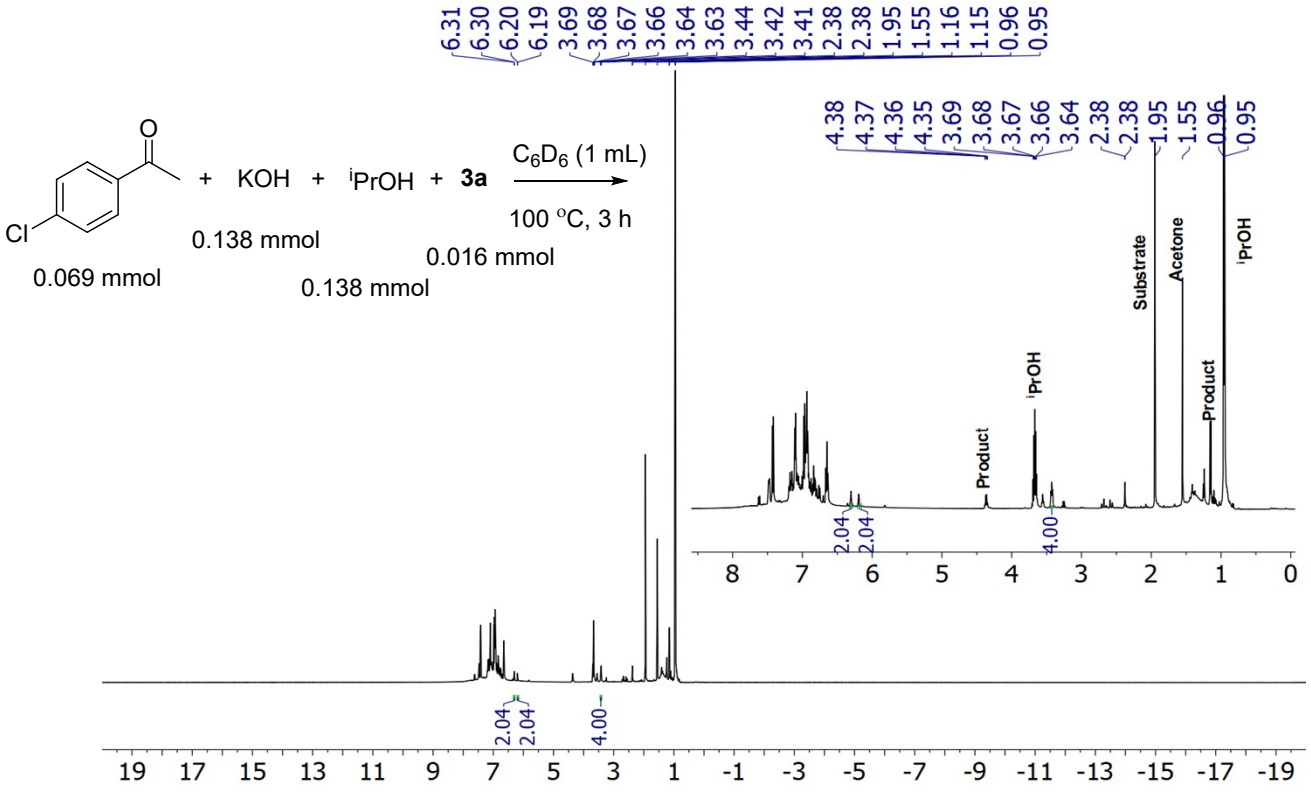

Figure S55. ^{1}H NMR (C_6D_6, 500 MHz) spectrum of the catalytic reaction mixture of complex **3a**, ^{i}PrOH and KOH at 100 °C for 3 h in C_6D_6. No signal in the negative region suggests no nickel hydride species formed.

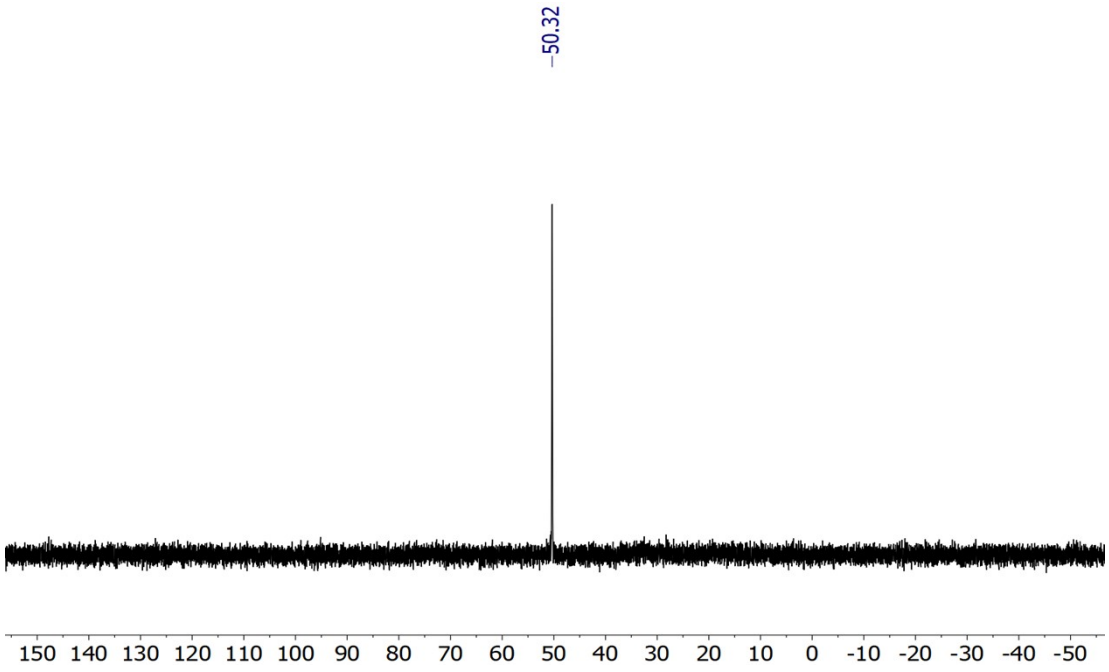

Figure S56. $^{31}P\{^{1}H\}$ NMR (C_6D_6, 202.45 MHz) spectrum of the above catalytic reaction mixture of complex **3a**, ^{i}PrOH and KOH at 100 °C for 3 h in C_6D_6.

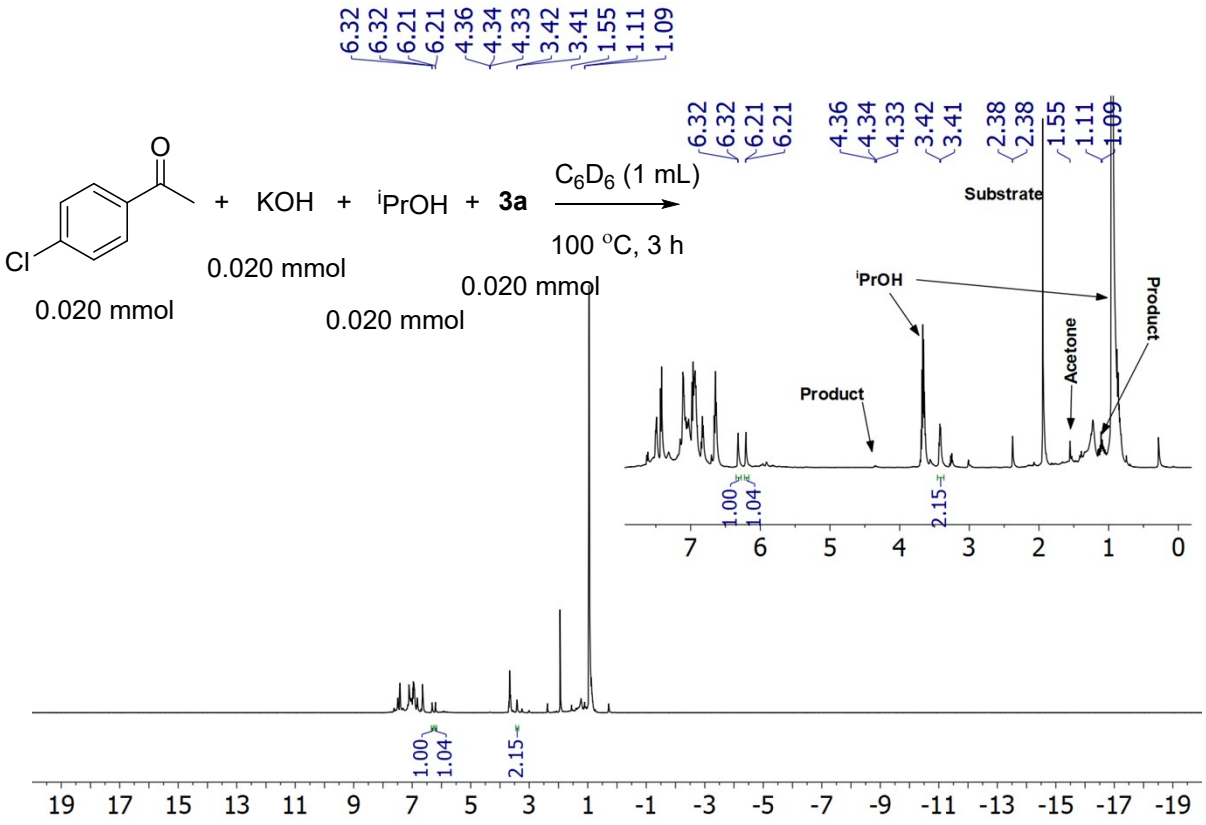

Figure S57. ^{1}H NMR (C_6D_6, 500 MHz) spectrum of the catalytic reaction mixture of complex **3a**, substrate, *i*PrOH and KOH in equiv molar ratio at 100 °C for 3 h in C_6D_6.

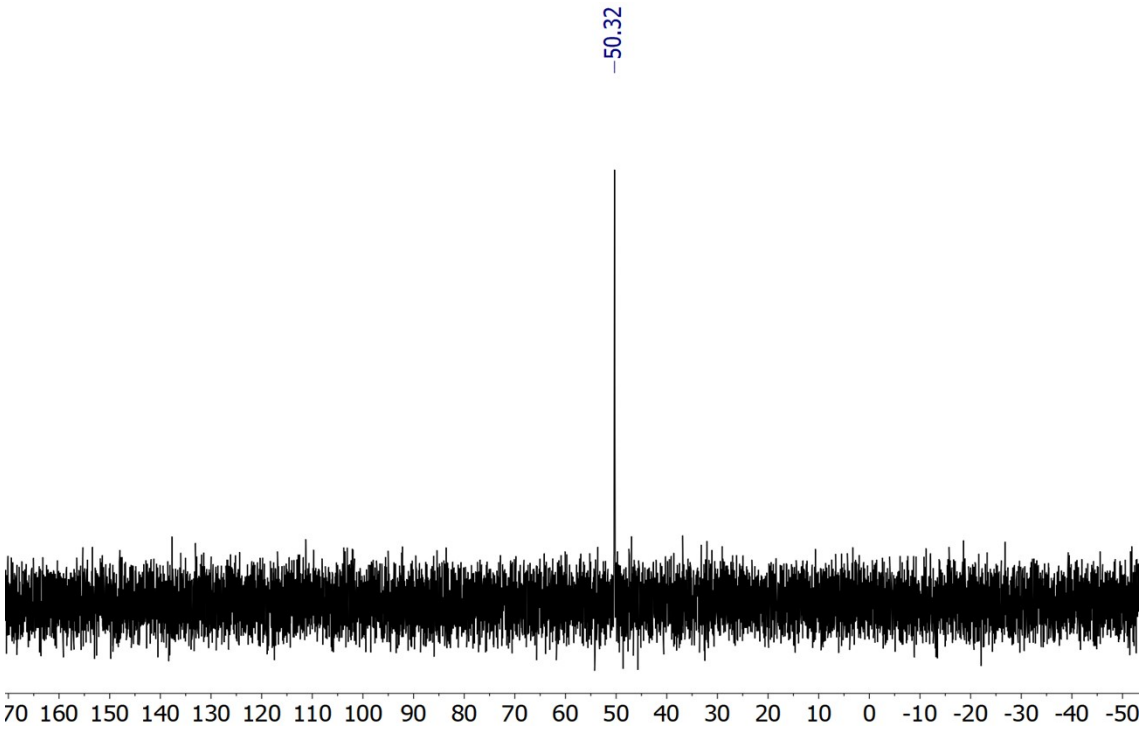

Figure S58. $^{31}P\{^{1}H\}$ NMR (C_6D_6, 202.45 MHz) spectrum of the above catalytic reaction mixture of complex **3a**, substrate, *i*PrOH and KOH in equiv molar ratio at 100 °C for 3 h in C_6D_6.

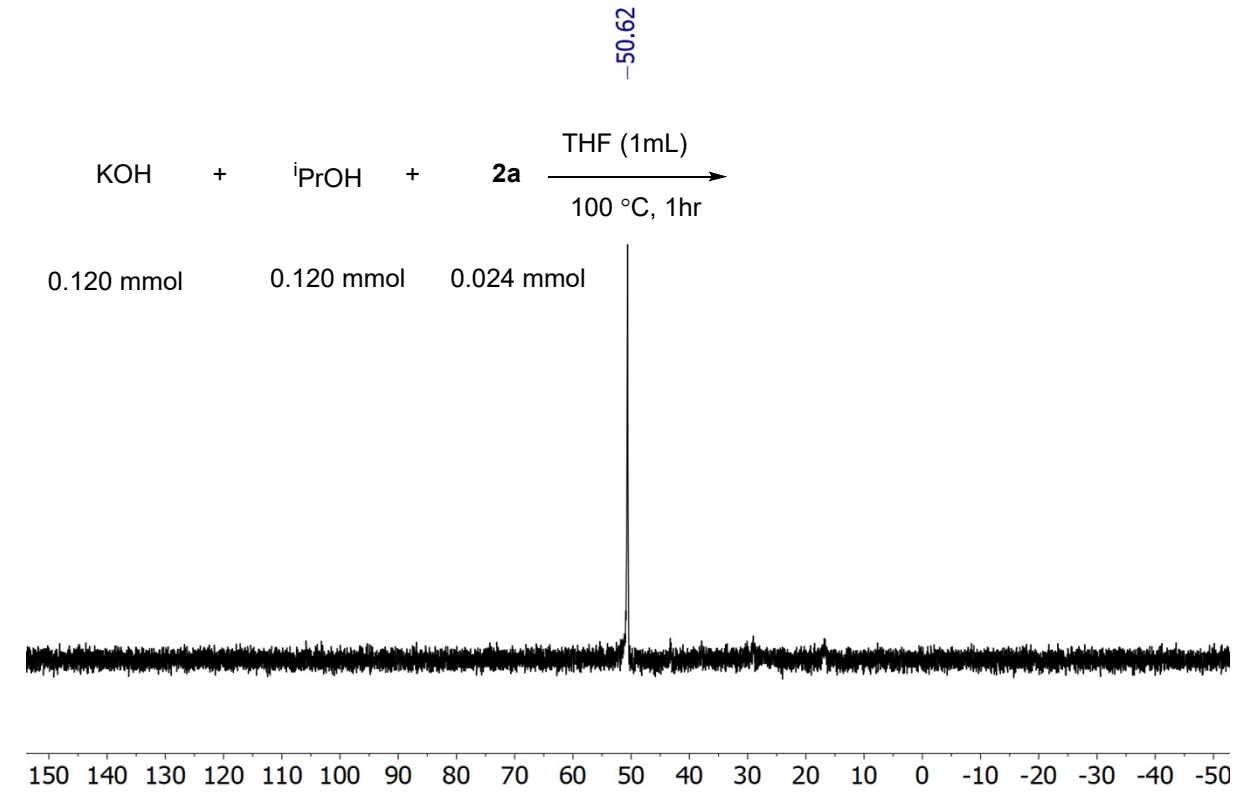

Figure S59. $^{31}P\{^{1}H\}$ NMR (THF solution with D_2O capillary, 202.45 MHz) spectrum of the reaction mixture of complex **2a**, *i*PrOH and KOH in THF after 1 h at 100 °C without substrate. Complex **2a** changed to **3a** under basic conditions.

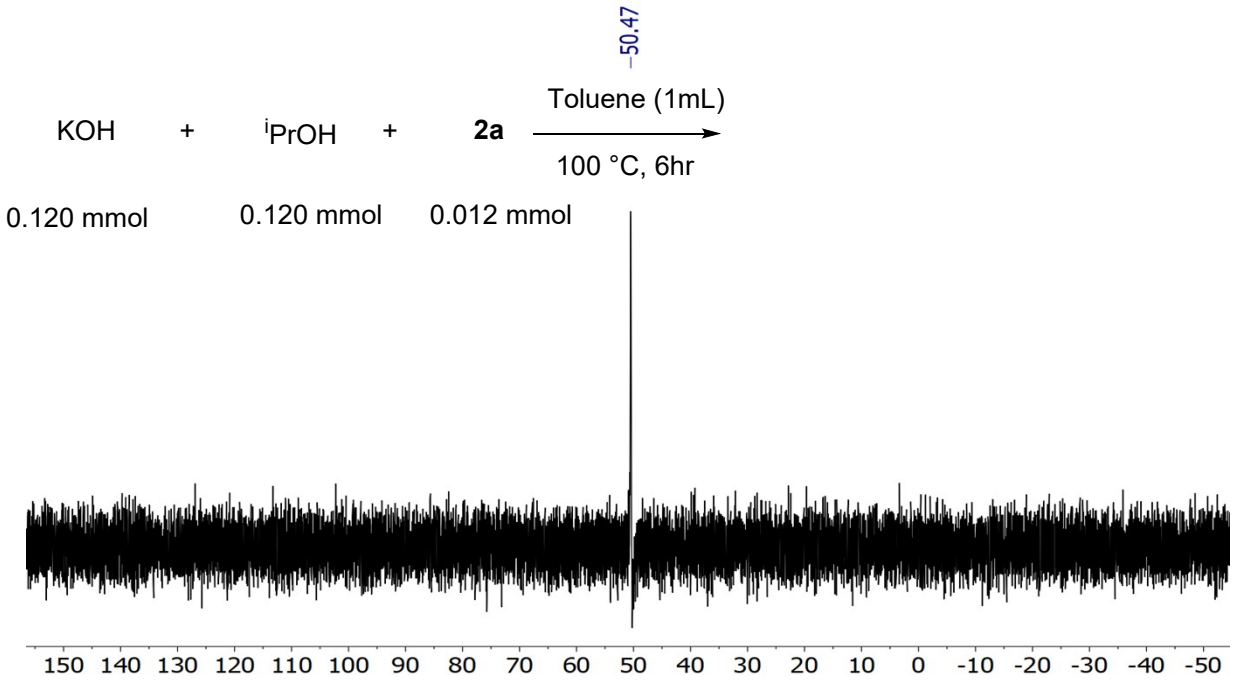

Figure S60. $^{31}P\{^{1}H\}$ NMR (toluene solution with D_2O capillary, 202.45 MHz) spectrum of the reaction mixture of complex **2a**, *i*PrOH and KOH in toluene after 6 h at 100 °C without substrate. Complex **2a** changed to **3a** under basic conditions.

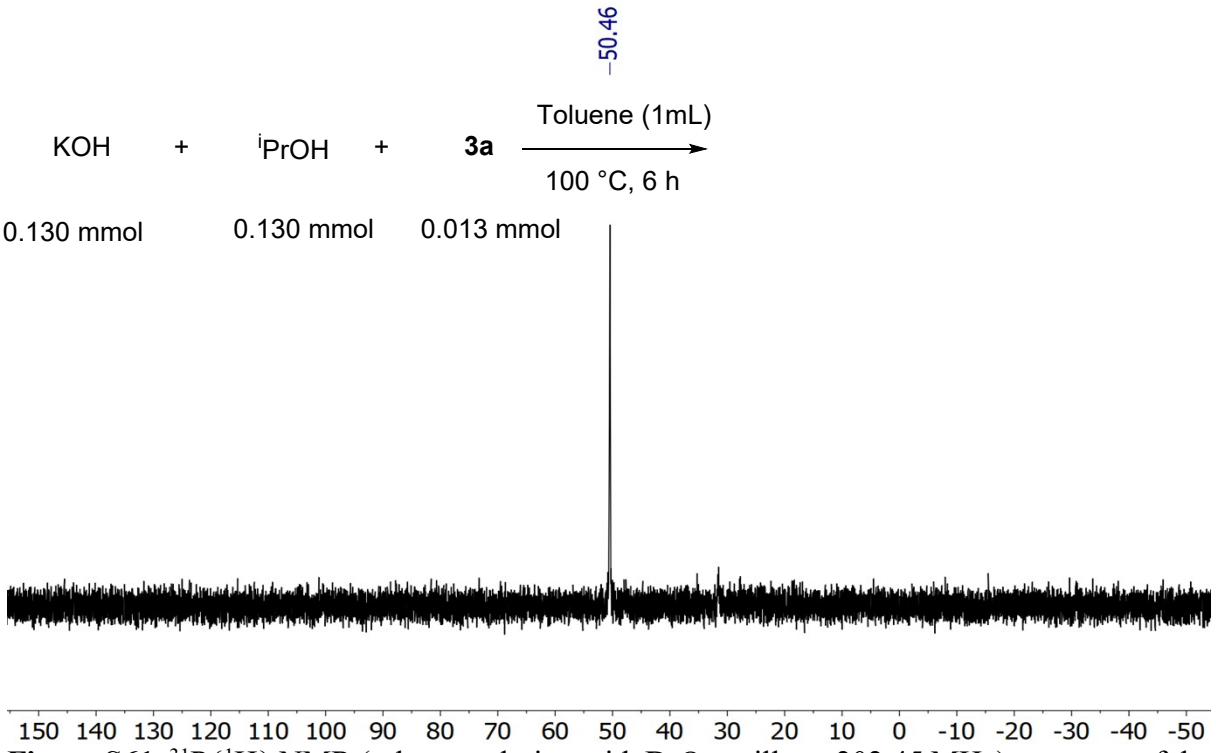

Figure S61. $^{31}P\{^{1}H\}$ NMR (toluene solution with D_2O capillary, 202.45 MHz) spectrum of the catalytic reaction mixture of complex **3a**, *i*PrOH and KOH in toluene after 6 h at 100 °C without substrate.

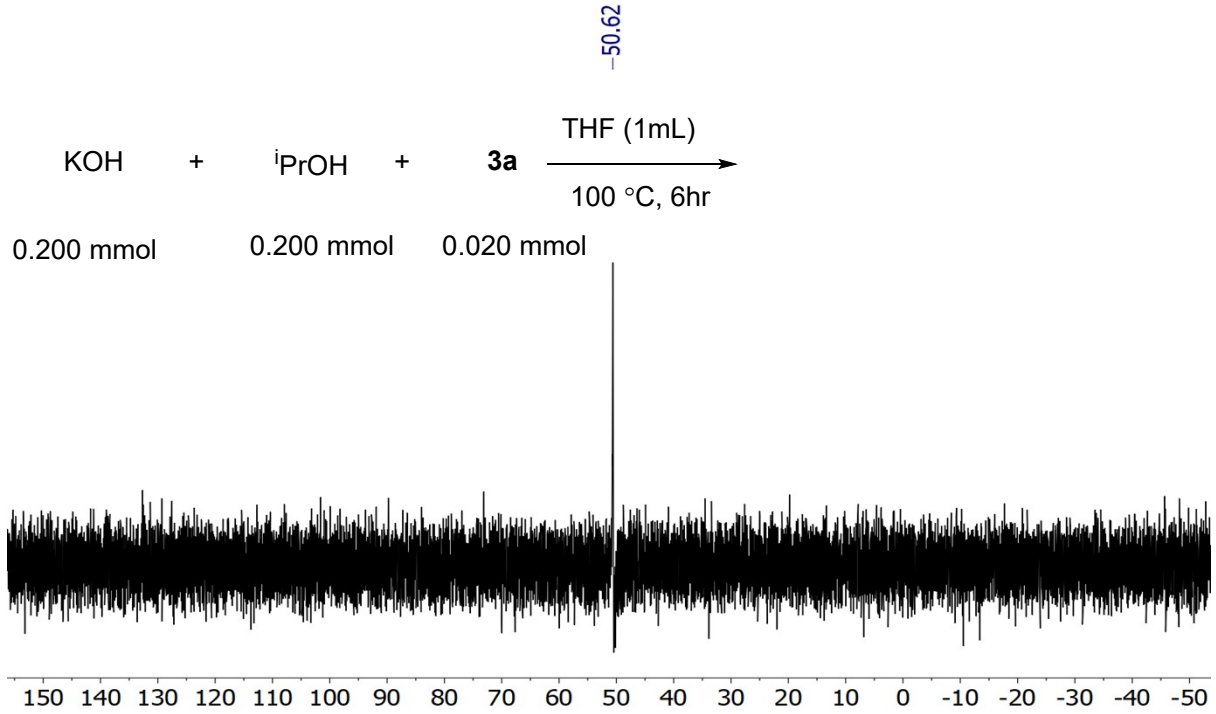

Figure S62. $^{31}P\{^{1}H\}$ NMR (benzene solution with D_2O capillary, 202.45 MHz) spectrum of the catalytic reaction mixture of complex **3a**, *i*PrOH and KOH in THF after 6 h at 100 °C without substrate.

^{1}H and ^{13}C NMR data of alcohols formed by the transfer hydrogenation of ketones

1-Phenylethan-1-ol.[5] Yield: 94%; **^{1}H NMR** ($CDCl_3$, 500 MHz) δ 7.42-7.37 (m, 4H, Ar*H*), 7.30 (t, J_{HH} = 7.5, 1H, Ar*H*), 4.93 (q, $^{3}J_{HH}$ = 6.6, 1H, C*H*), 1.93 (br s, 1H, O*H*), 1.53 (d, $^{3}J_{HH}$ = 5.0, 3H, CH_3). **^{13}C{^{1}H} NMR** ($CDCl_3$, 125.75 MHz): δ 146.0, 128.6, 127.6, 125.5, 70.5, 25.3.

1-(4-Chlorophenyl)ethan-1-ol.[6,7] Yield: 91%; **^{1}H NMR** ($CDCl_3$, 500 MHz) δ 7.29-7.25 (m, 4H, Ar*H*), 4.83 (q, $^{3}J_{HH}$ = 6.6, 1H, C*H*), 2.13 (br s, 1H, O*H*), 1.44 (d, $^{3}J_{HH}$ = 5.0, 3H, CH_3). **^{1}H NMR** (C_6D_6, 400 MHz) δ 7.15-7.09 (m, 2H, Ar*H*), 6.97-6.91 (m, 2H, Ar*H*), 4.43 (q, $^{3}J_{HH}$ = 8.0, 1H, C*H*), 3.30 (br s, 1H, O*H*), 1.16 (d, $^{3}J_{HH}$ = 4.0, 3H, CH_3). **^{13}C{^{1}H} NMR** ($CDCl_3$, 125.75 MHz): δ 144.4, 133.2, 128.7, 126.9, 69.8, 25.4.

1-(3-Chlorophenyl)ethan-1-ol.[6,8] Yield: 90%; **^{1}H NMR** ($CDCl_3$, 500 MHz) δ 7.38 (t, $^{3}J_{HH}$ = 4.8, 1H, Ar*H*), δ 7.29-7.23 (m, 3H, Ar*H*), 4.87 (q, $^{3}J_{HH}$ = 6.6, 1H, C*H*), 2.05 (br s, 1H, O*H*), 1.49 (d, $^{3}J_{HH}$ = 5.0, 3H, CH_3). **^{13}C{^{1}H} NMR** ($CDCl_3$, 125.75 MHz): δ 148.1, 134.5, 129.9, 127.7, 125.8, 123.7, 69.9, 25.4.

1-(2-Chlorophenyl)ethan-1-ol.[6] Yield: 92%; **^{1}H NMR** ($CDCl_3$, 500 MHz) δ 7.59-7.58 (m, 1H, Ar*H*), 7.33-7.27 (m, 2H, Ar*H*), 7.20 (t, $^{3}J_{HH}$ = 4.5, 1H, Ar*H*), 5.29 (q, $^{3}J_{HH}$ = 7.5, 1H, C*H*), 2.04 (br s, 1H, O*H*), 1.49 (d, $^{3}J_{HH}$ = 5.0, 3H, CH_3). **^{13}C{^{1}H} NMR** ($CDCl_3$, 125.75 MHz): δ 143.2, 131.8, 129.5, 128.5, 127.3, 126.6, 67.1, 23.6.

1-(4-Bromophenyl)ethan-1-ol.[6] Yield: 92%; **^{1}H NMR** ($CDCl_3$, 400 MHz): δ 7.48 (t, $^{3}J_{HH}$ = 3.84, 2H, Ar*H*), 7.25 (t, $^{3}J_{HH}$ = 3.76, 2H, Ar*H*), 4.84 (q, $^{3}J_{HH}$ = 5.33, 1H, C*H*), 2.3 (br s, 1H, O*H*), 1.47 (d, $^{3}J_{HH}$ = 3.9, 3H, CH_3). **^{13}C{^{1}H} NMR** ($CDCl_3$, 125.75 MHz): δ 144.9, 131.6, 127.3, 121.2, 69.8, 25.3.

1-(3-Bromophenyl)ethan-1-ol.[6] Yield: 91%; **^{1}H NMR** ($CDCl_3$, 500 MHz): δ 7.47 (t, $^{3}J_{HH}$ = 4.8, 1H, Ar*H*), 7.34 (d, $^{2}J_{HH}$ = 4.6, 1H, Ar*H*), 7.32-7.16 (m, 1H, Ar*H*), 7.14 (t, $^{3}J_{HH}$ = 5.0, 1H, Ar*H*), 4.80 (q, $^{3}J_{HH}$ = 6.6, 1H, C*H*), 1.89 (br s, 1H, O*H*), 1.42 (d, $^{2}J_{HH}$ = 5.0, 3H, CH_3). **^{13}C{^{1}H} NMR** ($CDCl_3$, 125.75 MHz): δ 148.3, 130.6, 130.2, 128.7, 124.1, 122.7, 69.9, 25.4.

1-(2-Bromophenyl)ethan-1-ol.[9] Yield: 89%; **^{1}H NMR** ($CDCl_3$, 500 MHz): δ 7.59-7.57 (m, 1H, Ar*H*), 7.51-7.50 (m, 1H, Ar*H*), 7.35-7.32 (m, 1H, Ar*H*), 7.13-7.10 (m, 1H, Ar*H*), 5.23 (q, $^{3}J_{HH}$ = 6.6, 1H, C*H*), 2.06 (br s, 1H, O*H*), 1.48 (d, $^{2}J_{HH}$ = 6.43, 3H, CH_3). **^{13}C{^{1}H} NMR** ($CDCl_3$, 125.75 MHz): δ 144.8, 132.8, 128.9, 128.0, 126.8, 121.8, 69.3, 23.7.

1-(4-Methoxyphenyl)ethan-1-ol.[6,8,9] Yield: 92%; **^{1}H NMR** ($CDCl_3$, 500 MHz) δ 7.29 (d, $^3J_{HH}$ = 10.0, 2H, Ar*H*), 6.88 (d, $^3J_{HH}$ = 10.0, 2H, Ar*H*), 4.84 (q, $^3J_{HH}$ = 6.6, 1H, C*H*), 3.80 (s, 3H, OCH_3), 2.02 (br s, 1H, O*H*), 1.47 (d, $^3J_{HH}$ = 5.0, 3H, CH_3). **^{13}C{^{1}H} NMR** ($CDCl_3$, 125.75 MHz): δ 159.1, 138.2, 126.8, 114.0, 70.0, 55.4, 25.1.

1-(3-Methoxyphenyl)ethan-1-ol.[6] Yield: 90%; **^{1}H NMR** ($CDCl_3$, 500 MHz) δ 7.27 (t, $^3J_{HH}$ = 7.5, 1H, Ar*H*), 6.96-6.94 (m, 2H, Ar*H*), 6.83-6.81 (m, 1H, Ar*H*), 4.86 (q, $^3J_{HH}$ = 6.4, 1H, C*H*), 3.82 (s, 3H, OCH_3), 2.12 (br s, 1H, O*H*), 1.49 (d, $^3J_{HH}$ = 6.6, 3H, CH_3). **^{13}C{^{1}H} NMR** ($CDCl_3$, 125.75 MHz): δ 159.9, 147.8, 129.6, 117.8, 113.0, 111.1, 70.4, 55.3, 25.2.

1-(2-Methoxyphenyl)ethan-1-ol.[6] Yield: 89%; **^{1}H NMR** ($CDCl_3$, 500 MHz) δ 7.39-7.37 (m, 1H, Ar*H*), 7.29-7.26 (m, 1H, Ar*H*), 7.00 (t, $^3J_{HH}$ = 7.5, 1H, Ar*H*), 6.91 (d, $^3J_{HH}$ = 10.0, 1H, Ar*H*), 5.13 (q, $^3J_{HH}$ = 5.0, 1H, C*H*), 3.89 (s, 3H, OCH_3), 2.75 (br s, 1H, O*H*), 1.53 (d, $^3J_{HH}$ = 5.0, 3H, CH_3). **^{13}C{^{1}H} NMR** ($CDCl_3$, 125.75 MHz): δ 156.7, 133.6, 128.4, 126.2, 120.9, 110.6, 66.7, 55.4, 23.0.

1-(Napthalen-1-yl)ethan-1-ol. Yield: 78%; **^{1}H NMR** ($CDCl_3$, 400 MHz): δ 8.11 (d, $^2J_{HH}$ = 8.0, 1H, Ar*H*), 7.90-7.87 (m, 1H, Ar*H*), 7.79 (d, $^2J_{HH}$ = 10.0, 1H, Ar*H*), 7.67 (d, $^2J_{HH}$ = 5.0, 1H, Ar*H*), 7.55-7.46 (m, 3H, Ar*H*), 5.66 (q, $^3J_{HH}$ = 8.3, 1H, C*H*), 2.07 (br s, 1H, O*H*), 1.67 (d, $^3J_{HH}$ = 10.0, 3H, CH_3). **^{13}C{^{1}H} NMR** ($CDCl_3$, 125.75 MHz): δ 141.5, 134.0, 130.4, 129.0, 128.0, 126.1, 125.7, 123.3, 122.1, 67.2, 24.5.

Diphenylmethanol.[9] Yield: 91%; **^{1}H NMR** ($CDCl_3$, 500 MHz): δ 7.24-7.14 (m, 10H, Ar*H*), 5.65 (1H, C*H*), 2.42 (br s, 1H, O*H*). **^{13}C{^{1}H} NMR** ($CDCl_3$, 125.75 MHz): δ 143.9, 128.5, 127.6, 126.7, 76.3.

(4-Chlorophenyl)(phenyl)methanol.[10] Yield: 94%; **^{1}H NMR** ($CDCl_3$, 500 MHz): δ 7.35-7.30 (m, 9H, Ar*H*), 5.75 (1H, C*H*), 2.69 (br s, 1H, O*H*). **^{13}C{^{1}H} NMR** ($CDCl_3$, 125.75 MHz): δ 143.5,142.4, 133.3, 128.7, 128.7, 128.0, 127.9, 126.6, 75.6.

9H-Fluoren-9-ol.[10] Yield: 89%; **^{1}H NMR** ($CDCl_3$, 400 MHz) δ 7.66-7.62 (m, 4H), 7.41-7.37 (m, 2H), 7.33 – 7.27 (m, 2H), 5.55 (s, 1H), 2.03 (s, 1H). **^{13}C{^{1}H} NMR** ($CDCl_3$, 100 MHz): δ 145.8, 140.1, 129.2, 127.9, 125.2, 112.1, 75.3.

1-(4-Ethynylphenyl)ethan-1-ol. Yield: 70%; **^{1}H NMR** ($CDCl_3$, 500 MHz): δ 7.40-7.39 (m, 2H, Ar*H*), 7.25-7.24 (m, 2H, Ar*H*), 4.81 (q, $^3J_{HH}$ = 6.66, 1H, C*H*), 2.98 (s, 1H, C*H*), 1.84 (br s, 1H, O*H*), 1.84 (d, $^3J_{HH}$ = 5.0, 3H, CH_3). **^{13}C{^{1}H} NMR** ($CDCl_3$, 125.75 MHz): δ 146.7, 132.4, 128.3, 125.5, 121.3, 83.7, 70.2, 25.3.

1,2,3,4-Tetrahydronaphthalen-1-ol.[7,8] Yield: 41%; **^{1}H NMR** ($CDCl_3$, 500 MHz): δ 7.35-7.34 (m, 1H, Ar*H*), 7.14-7.10 (m, 2H, Ar*H*), 7.03-7.01 (m, 1H, Ar*H*), 4.69 (t, $^3J_{HH}$ = 5.0, 1H, C*H*), 2.74-2.63 (m, 2H, CH_2) 1.87-1.81 (m, 2H, CH_2), 1.70-1.69 (m, 2H, CH_2). **^{13}C{^{1}H} NMR** ($CDCl_3$, 125.75 MHz): δ 139.0, 137.2, 129.1, 128.8, 127.7, 126.3, 68.3, 32.4, 29.4, 18.9.

Phenyl(pyridin-2-yl)methanol.[11] Yield: 88%; **^{1}H NMR** ($CDCl_3$, 500 MHz): δ 8.49 (d, $^3J_{HH}$ = 5.0, 1H, ArH), 7.57-7.53 (m, 1H, ArH), 7.36 (d, $^3J_{HH}$ = 10.0, 2H, ArH), 7.29 (t, $^3J_{HH}$ = 10.0, 2H, ArH), 7.23 (t, J_{HH} = 7.5, 1H, ArH), 7.16 (d, $^3J_{HH}$ = 5.0, 1H, ArH), 7.13-7.09 (m, 1H, ArH), 5.74 (s, 1H, C*H*), 5.31 (br s, 1H, O*H*). **^{13}C{^{1}H} NMR** ($CDCl_3$, 125.75 MHz): δ 161.3, 161.2, 147.9, 143.3, 136.9, 128.5, 127.8, 127.0, 122.4, 121.3, 75.2.

1-(Thiophen-2-yl)ethan-1-ol.[6] Yield: 86%; **^{1}H NMR** ($CDCl_3$, 500 MHz): δ 7.25-7.23 (m, 1H, thiol CH), 6.99-6.96 (m, 2H, thiol CH), 5.13 (q, $^3J_{HH}$ = 6.66, 1H, C*H*), 2.17 (br s, 1H, O*H*), 1.60 (d, $^3J_{HH}$ = 5.0, 3H, CH_3). **^{13}C{^{1}H} NMR** ($CDCl_3$, 125.75 MHz): δ 150.0, 126.8, 124.5, 123.3, 66.3, 25.4.

6-Methylhept-5-en-2-ol.[8] Yield: 87%; **^{1}H NMR** ($CDCl_3$, 500 MHz): δ 5.12 (t, $^3J_{HH}$ = 7.5, 1H, alkene-C*H*), 3.80-3.77 (m, 1H, C*H*), 2.09-2.02 (m, 2H, CH_2), 1.67 (s, 3H, CH_3), 1.61 (s, 3H, CH_3), 1.59-1.44 (m, 2H, CH_2), 1.17 (d, $^3J_{HH}$ = 10.0, 3H, CH_3). **^{13}C{^{1}H} NMR** ($CDCl_3$, 125.75 MHz): δ 132.1, 124.2, 68.0, 39.4, 25.8, 24.6, 23.5, 17.8.

4-Methylpentan-2-ol. ^{13}C{^{1}H} NMR ($CDCl_3$, 125.75 MHz): δ 66.0, 68.6, 24.8, 23.9, 23.1, 22.4.

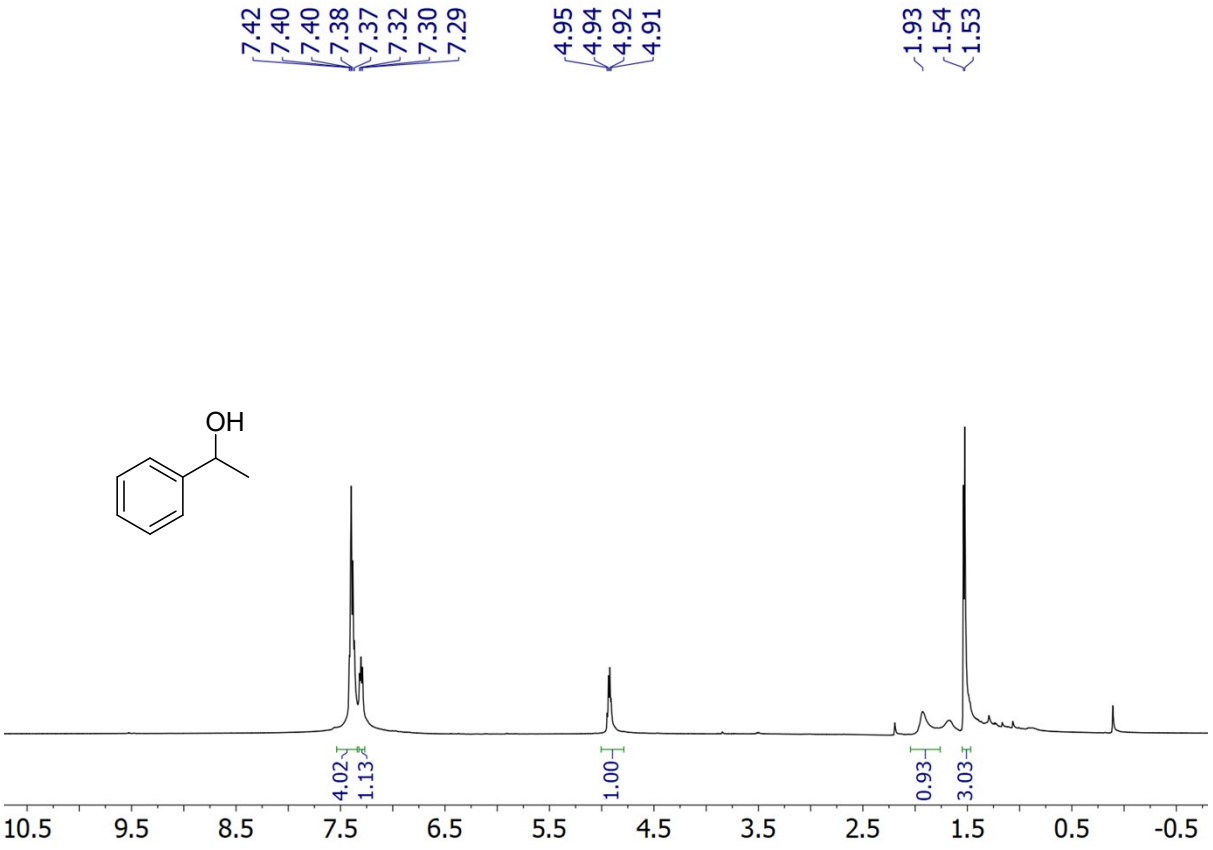

Figure S63. ^{1}H NMR ($CDCl_3$, 500 MHz) spectrum of 1-phenylethan-1-ol.

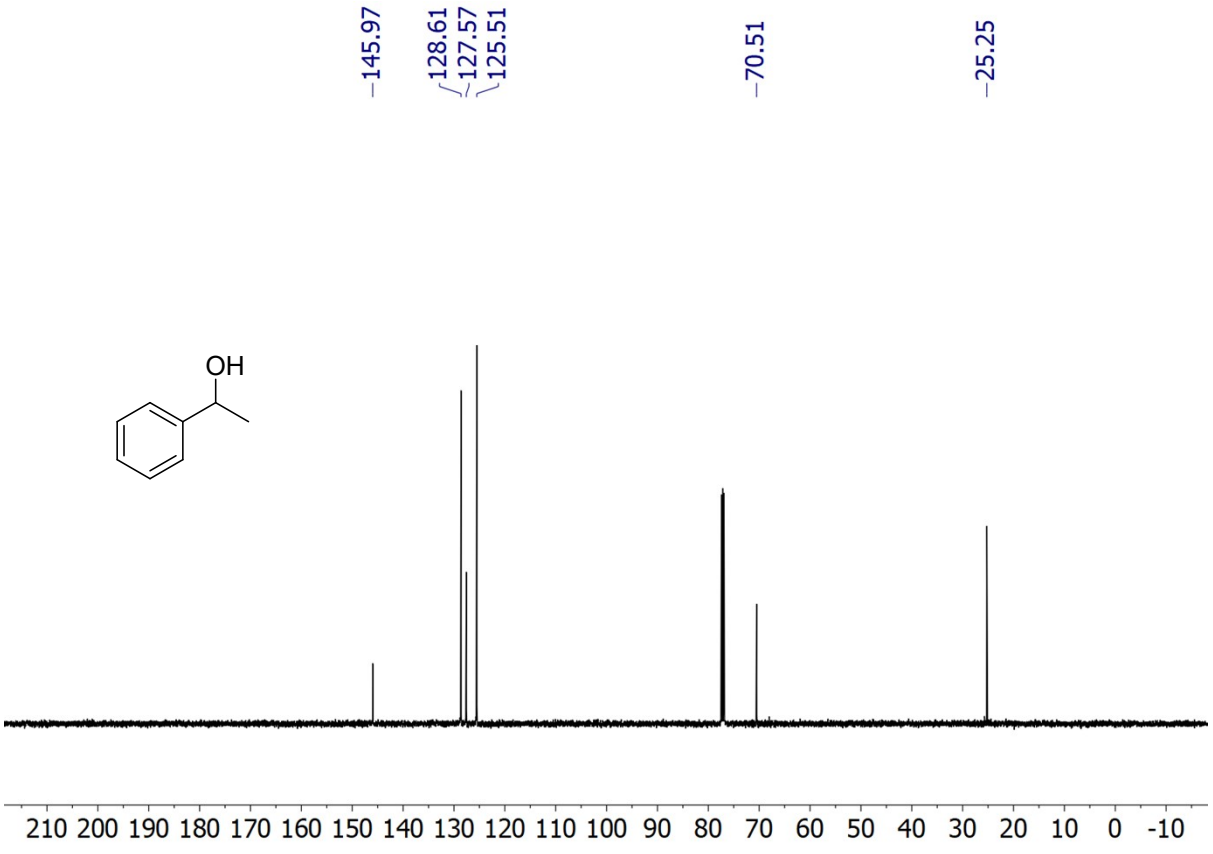

Figure S64. $^{13}C\{^{1}H\}$ NMR ($CDCl_3$, 125.75 MHz) spectrum of 1-phenylethan-1-ol.

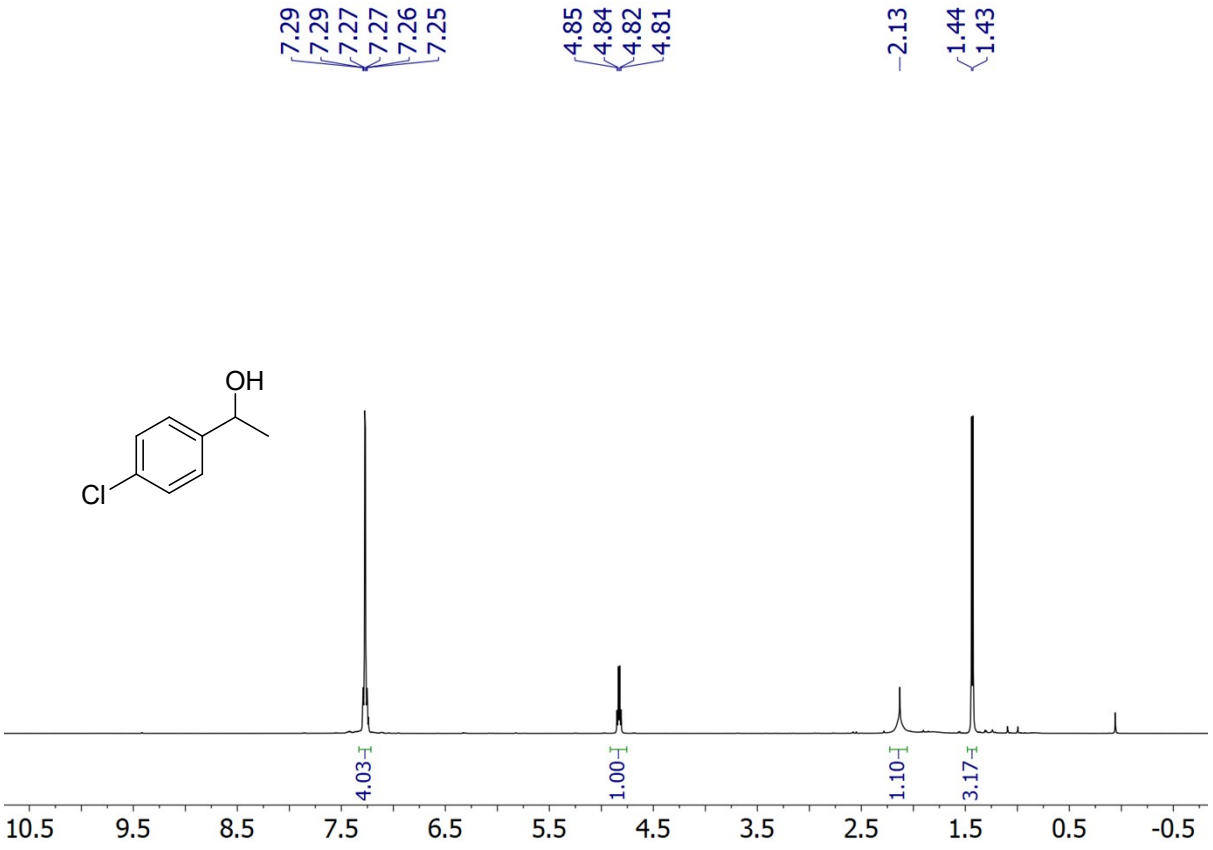

Figure S65. ^{1}H NMR ($CDCl_3$, 500 MHz) spectrum of 1-(4-chlorophenyl)ethan-1-ol.

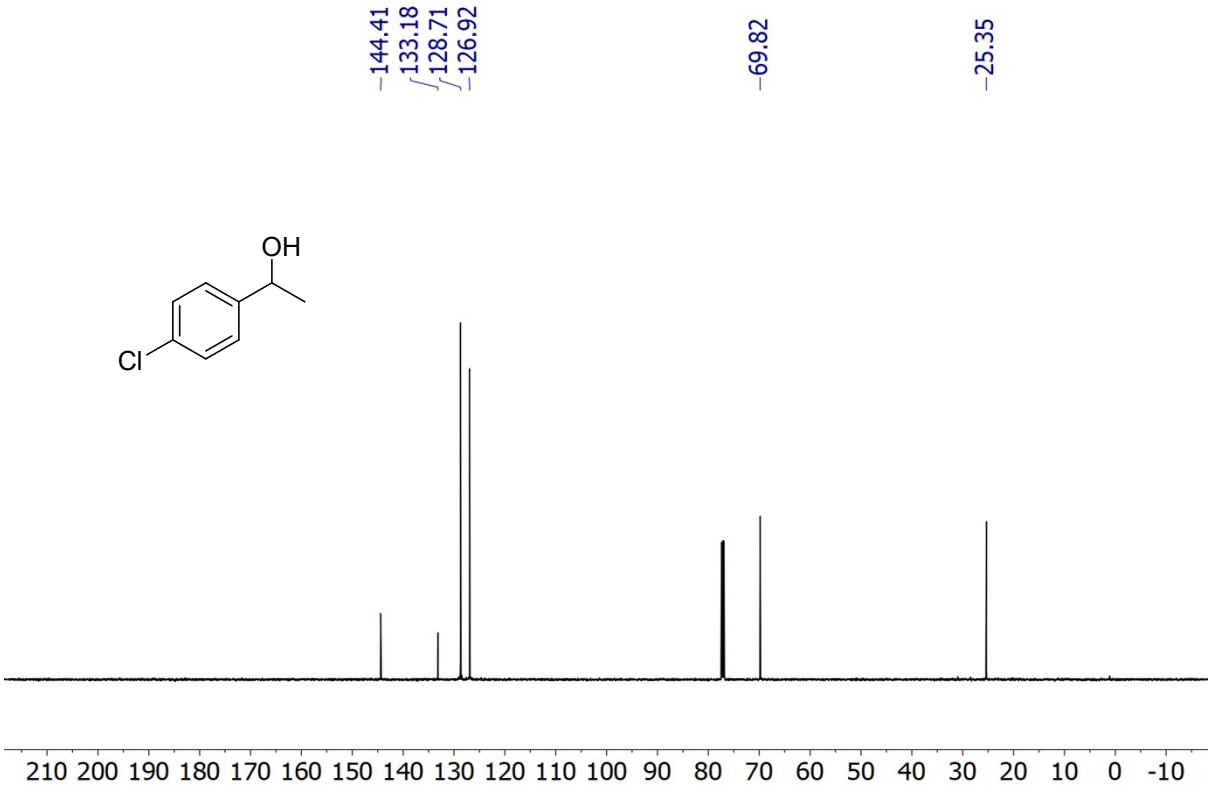

Figure S66. $^{13}C\{^{1}H\}$ NMR ($CDCl_3$, 125.75 MHz) spectrum of 1-(4-chlorophenyl)ethan-1-ol.

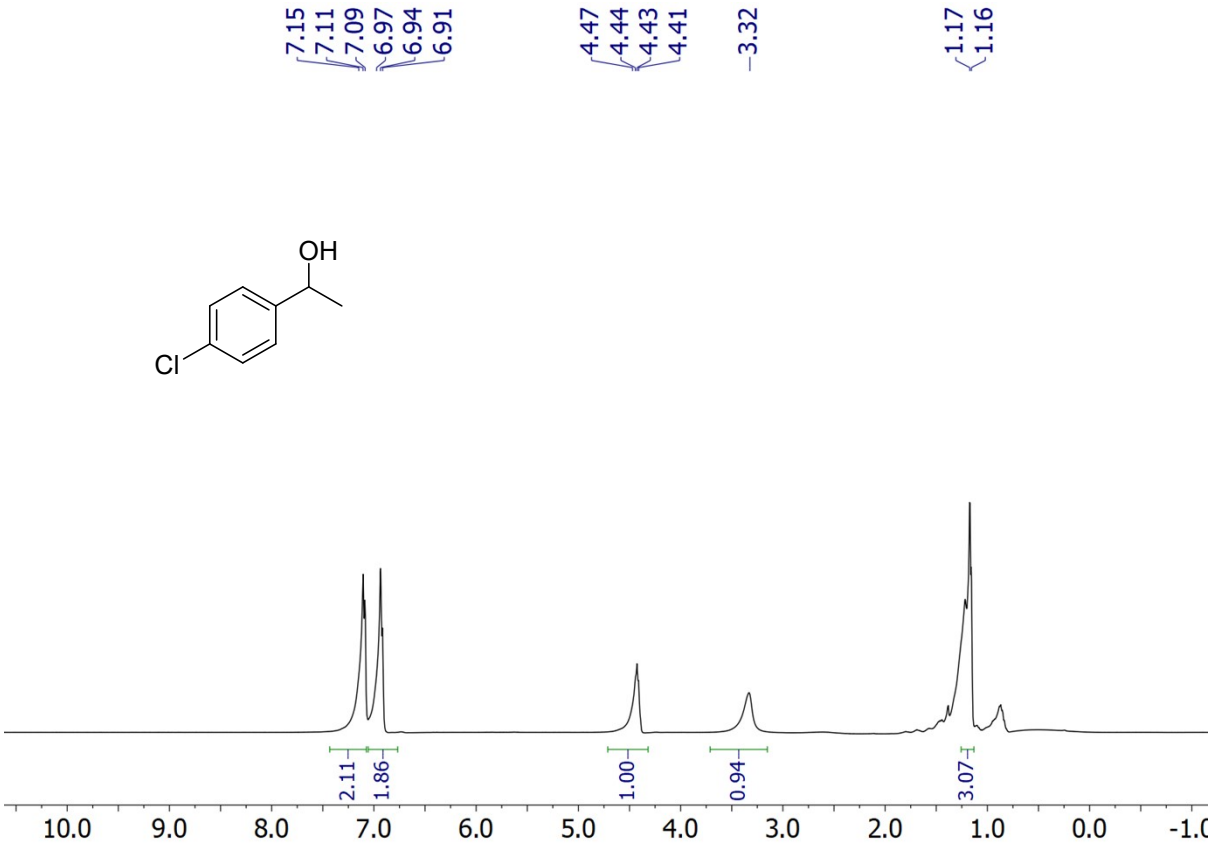

Figure S67. ^{1}H NMR (C_6D_6, 400 MHz) spectrum of 1-(4-chlorophenyl)ethan-1-ol.

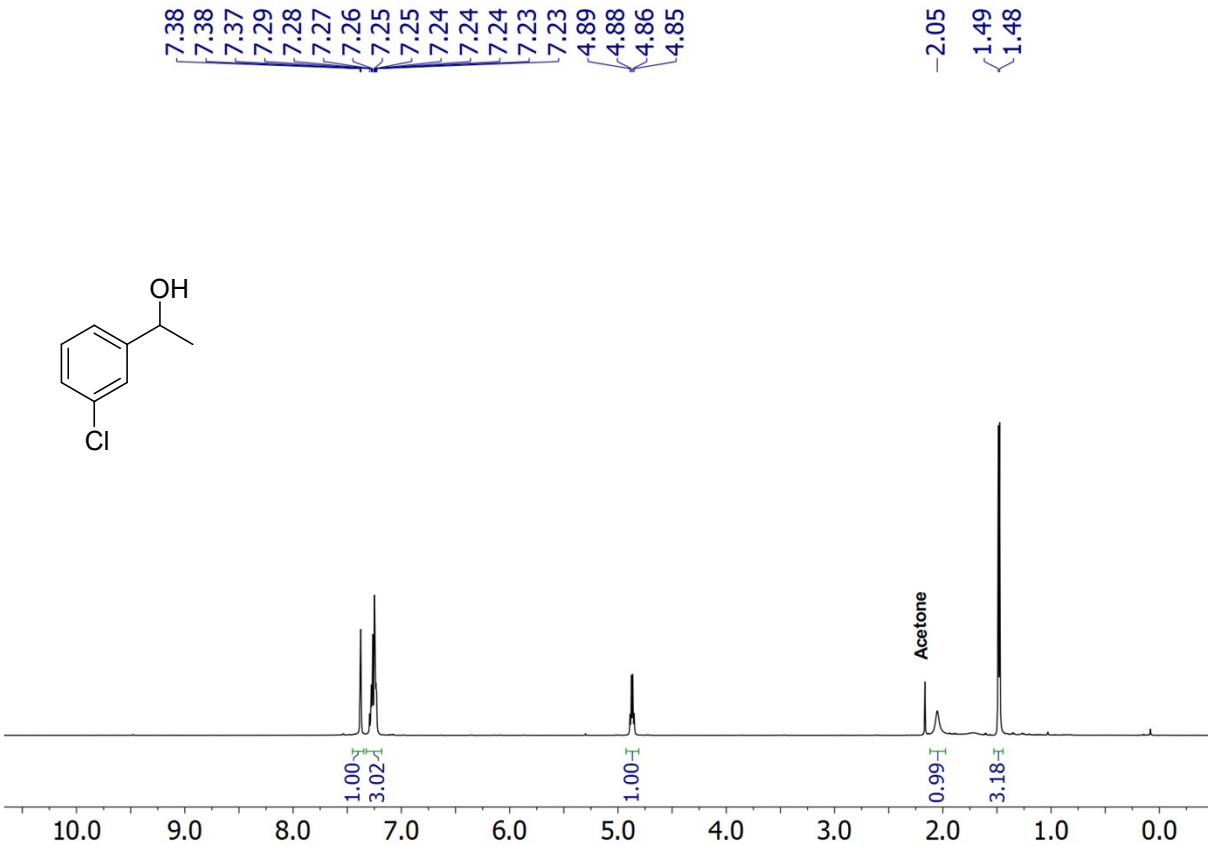

Figure S68. ^{1}H NMR ($CDCl_3$, 500 MHz) spectrum of 1-(3-chlorophenyl)ethan-1-ol.

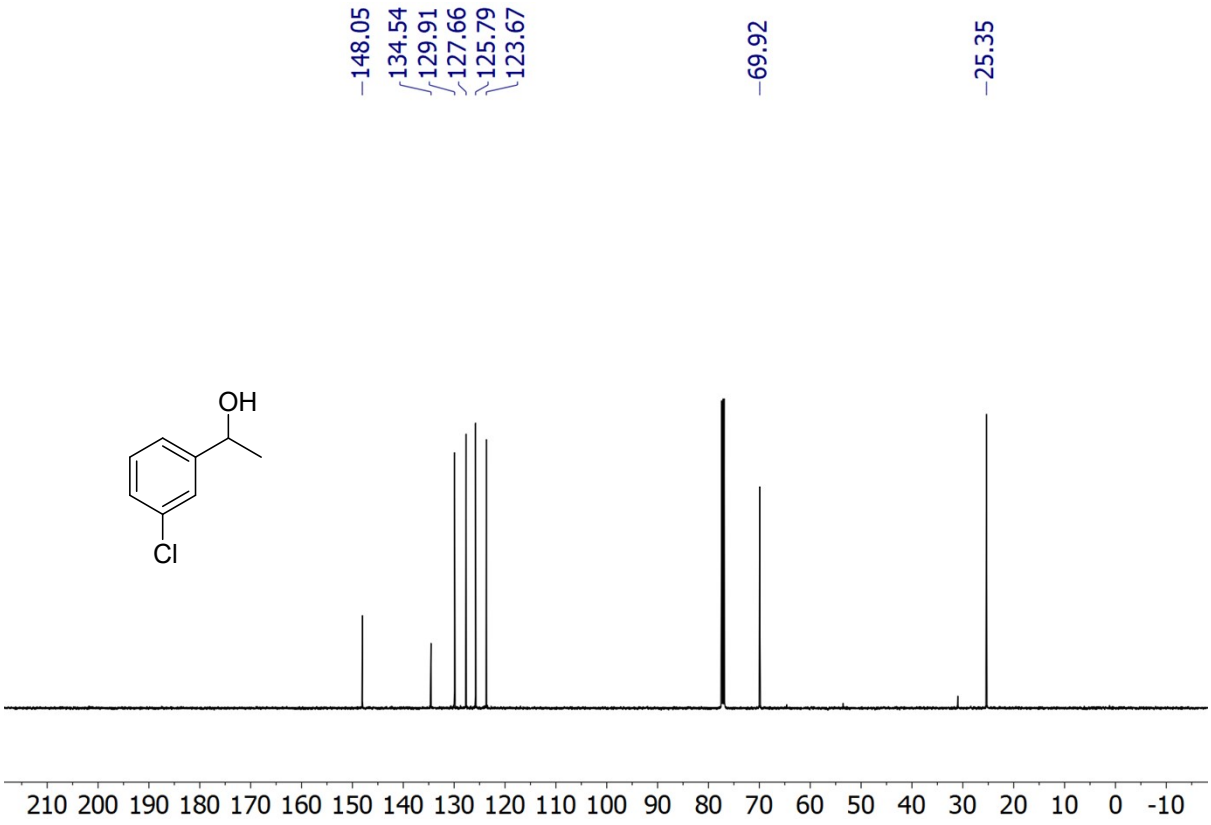

Figure S69. $^{13}C\{^{1}H\}$ NMR ($CDCl_3$, 125.75 MHz) spectrum of 1-(3-chlorophenyl)ethan-1-ol.

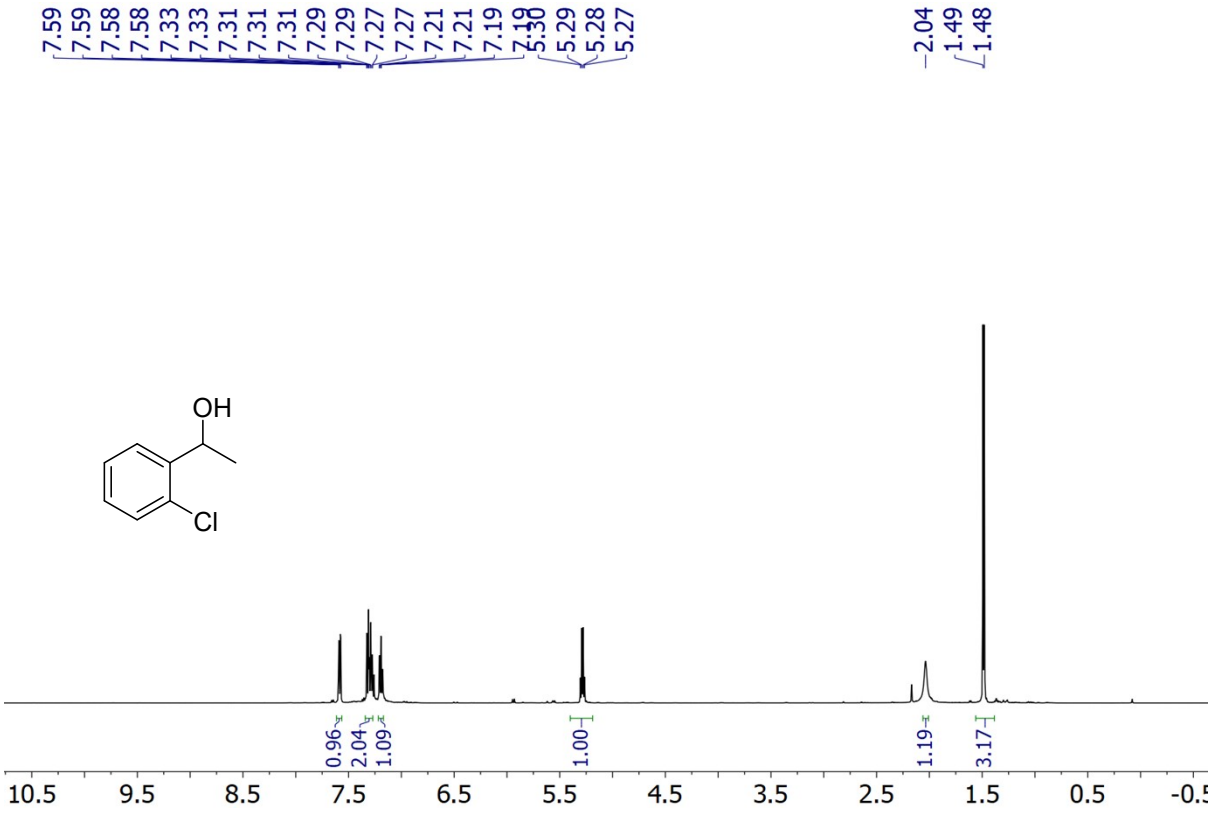

Figure S70. ^{1}H NMR ($CDCl_3$, 500 MHz) spectrum of 1-(2-chlorophenyl)ethan-1-ol.

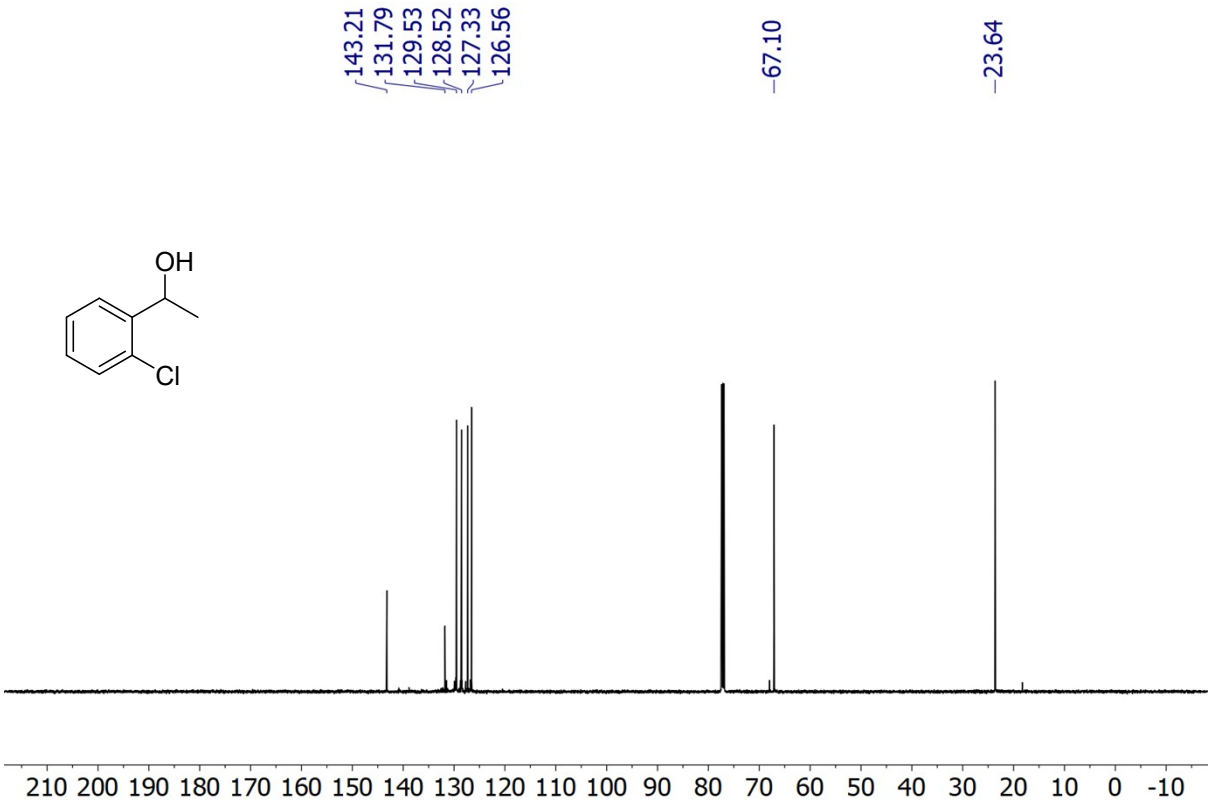

Figure S71. $^{13}C\{^{1}H\}$ NMR ($CDCl_3$, 125.75 MHz) spectrum of 1-(2-chlorophenyl)ethan-1-ol.

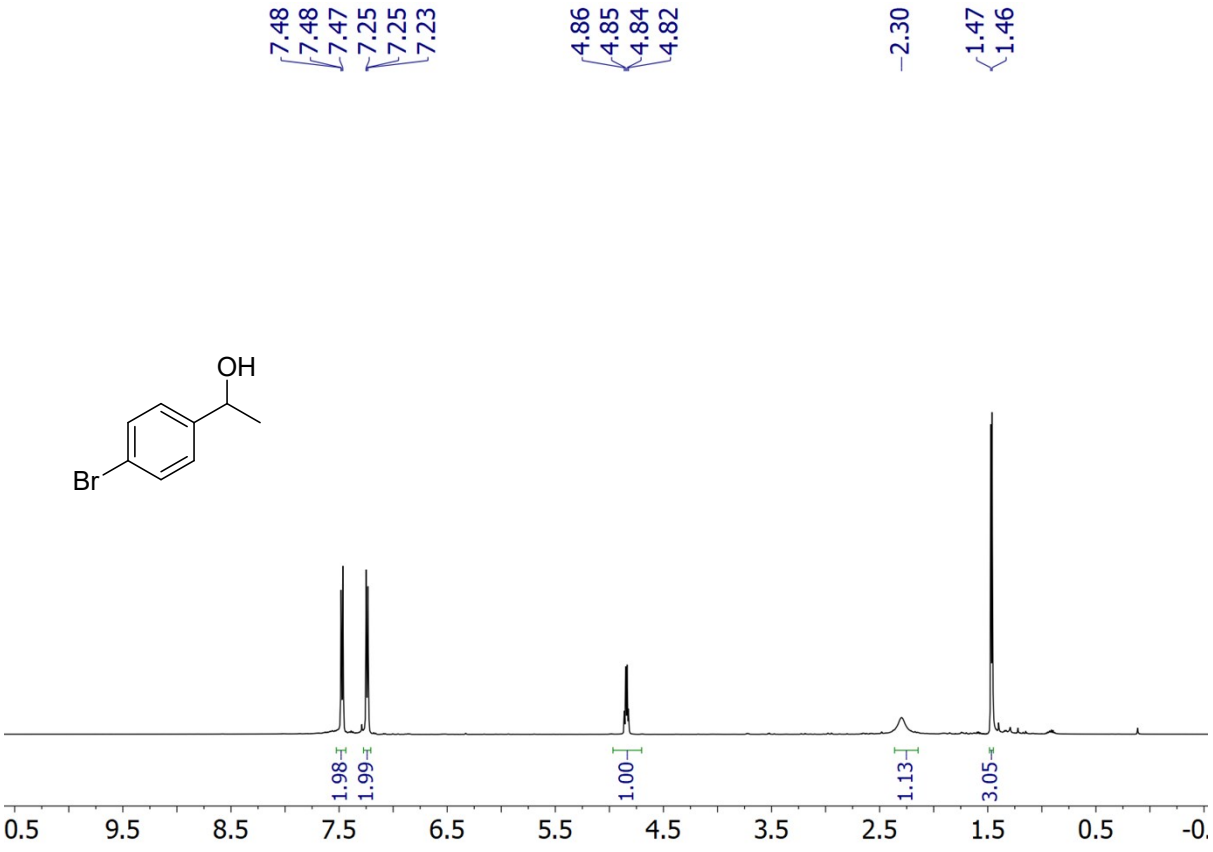

Figure S72. ^{1}H NMR ($CDCl_3$, 400 MHz) spectrum of 1-(4-bromophenyl)ethan-1-ol.

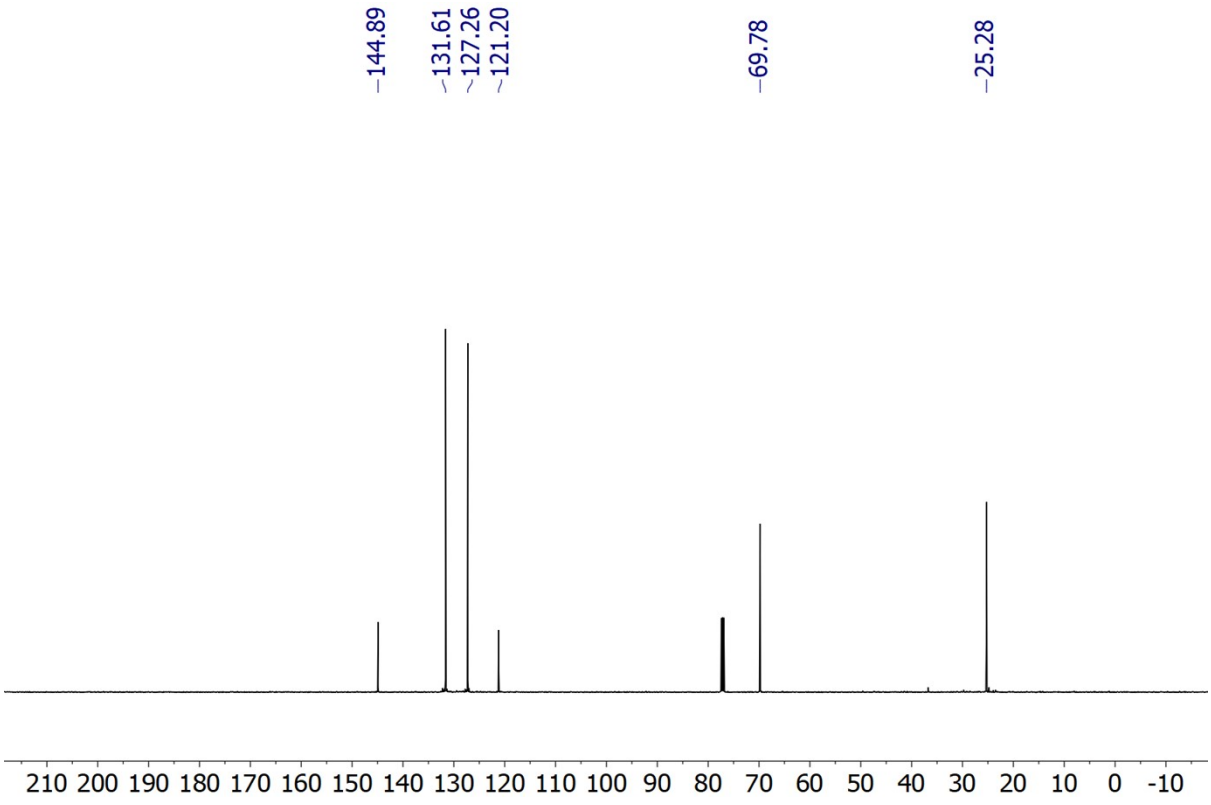

Figure S73. $^{13}C\{^{1}H\}$ NMR ($CDCl_3$, 125.75 MHz) spectrum of 1-(4-bromophenyl)ethan-1-ol.

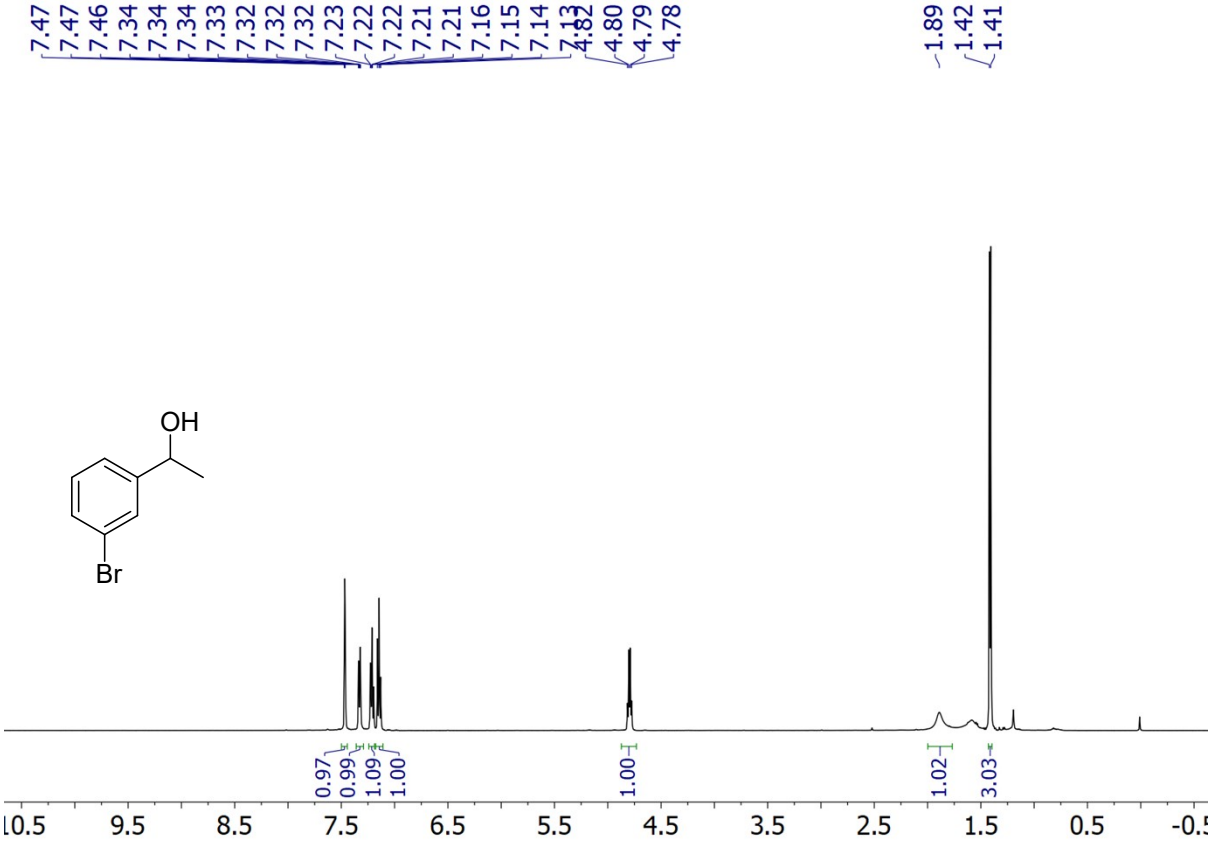

Figure S74. ^{1}H NMR ($CDCl_3$, 500 MHz) spectrum of 1-(3-bromophenyl)ethan-1-ol.

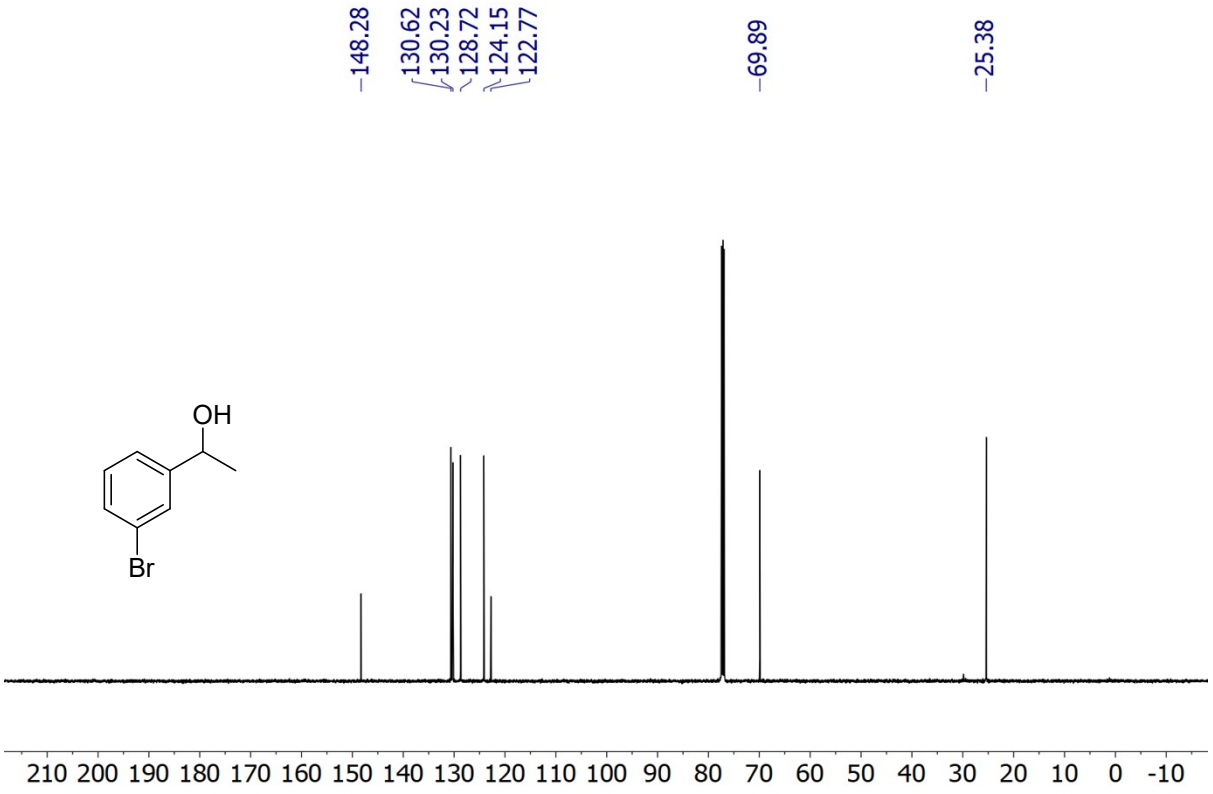

Figure S75. $^{13}C\{^{1}H\}$ NMR ($CDCl_3$, 125.75 MHz) spectrum of 1-(3-bromophenyl)ethan-1-ol.

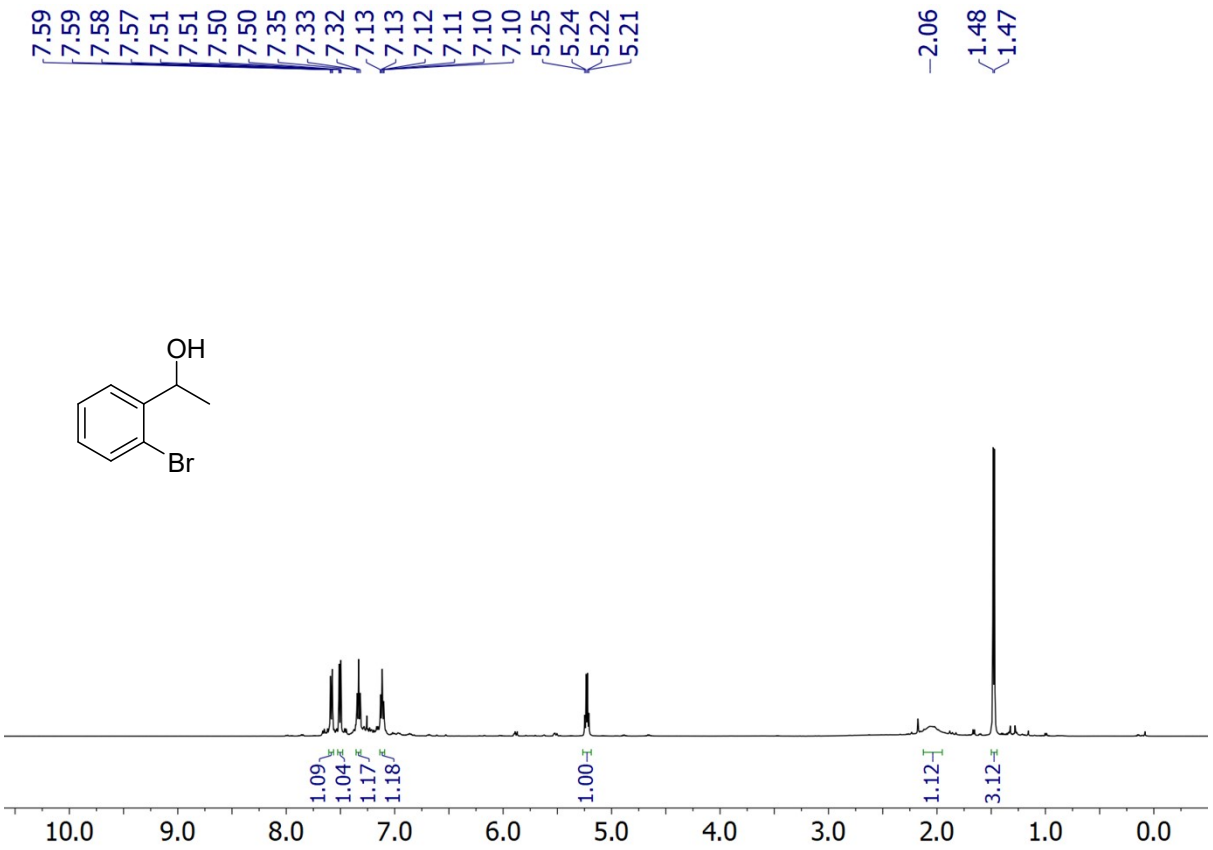

Figure S76. ^{1}H NMR ($CDCl_3$, 500 MHz) spectrum of 1-(2-bromophenyl)ethan-1-ol.

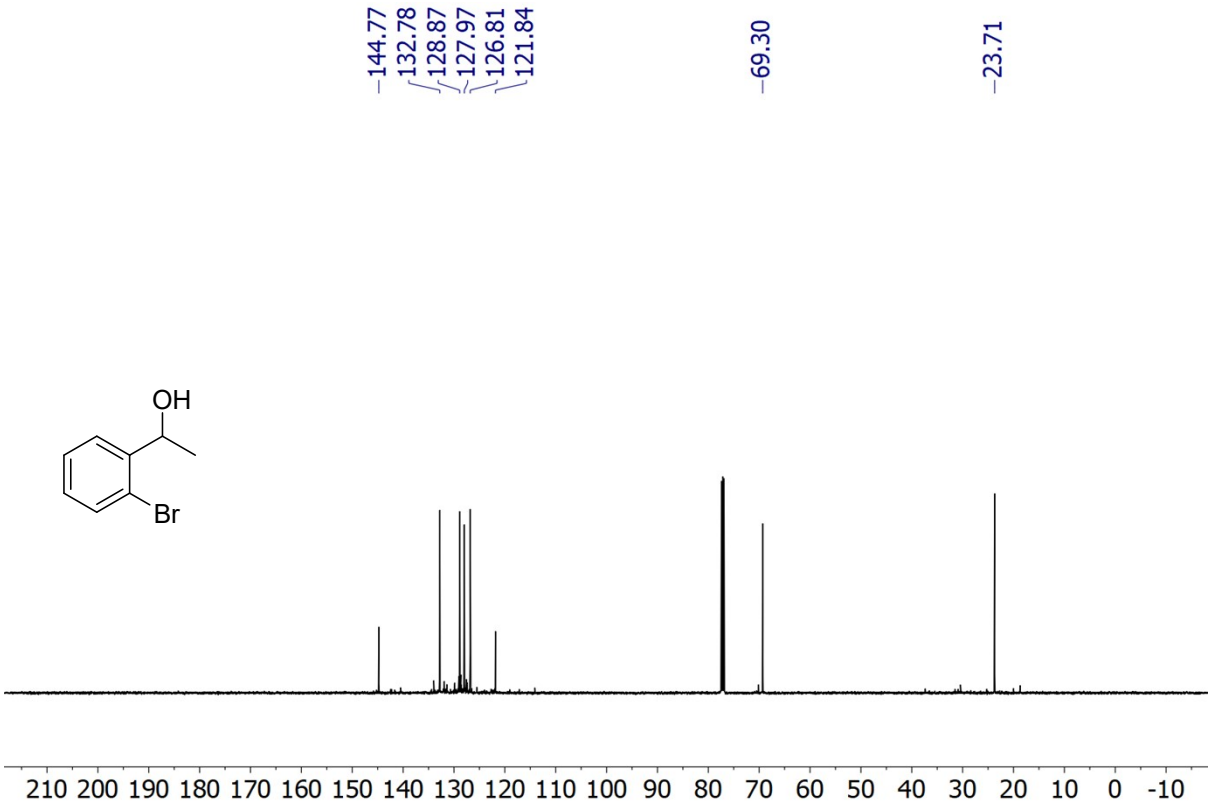

Figure S77. $^{13}C\{^{1}H\}$ NMR ($CDCl_3$, 125.75 MHz) spectrum of 1-(2-bromophenyl)ethan-1-ol.

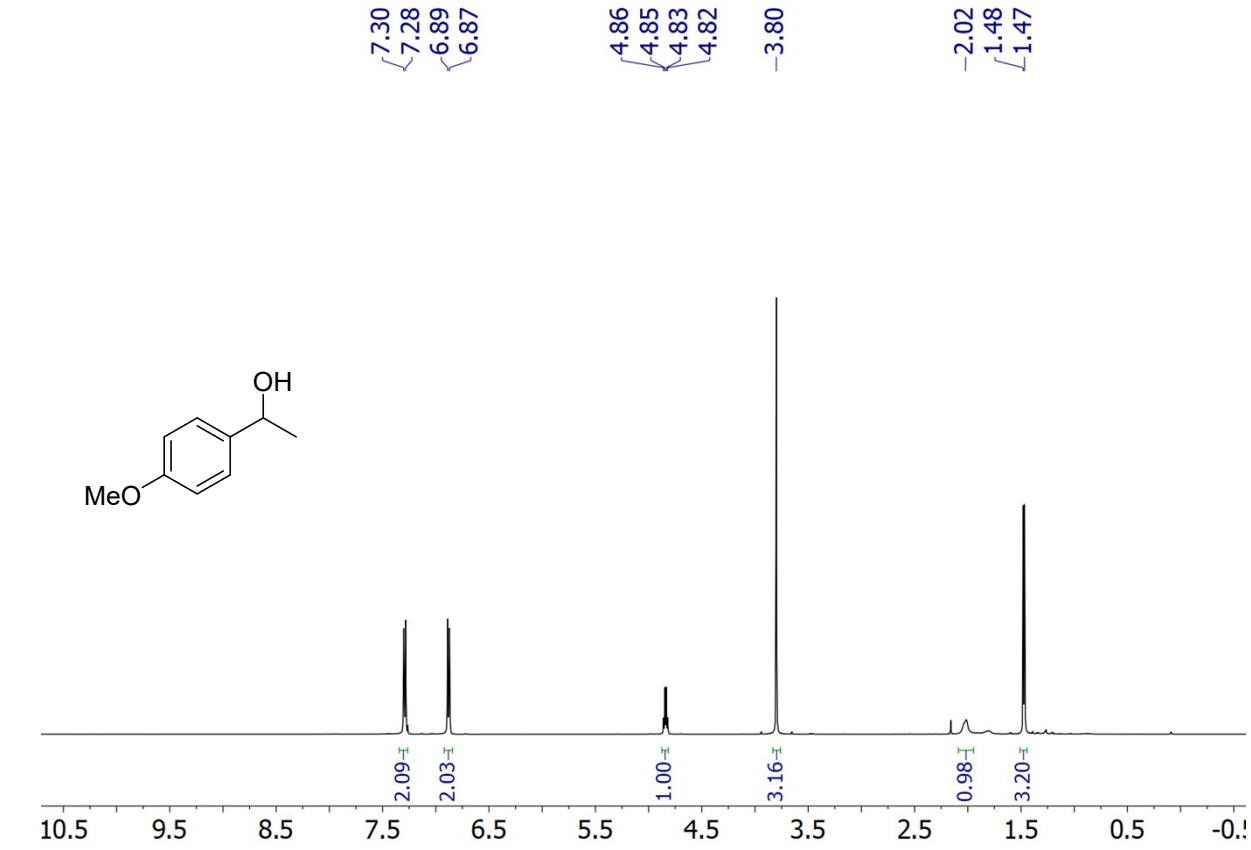

Figure S78. ^{1}H NMR ($CDCl_3$, 500 MHz) spectrum of 1-(4-methoxyphenyl)ethan-1-ol.

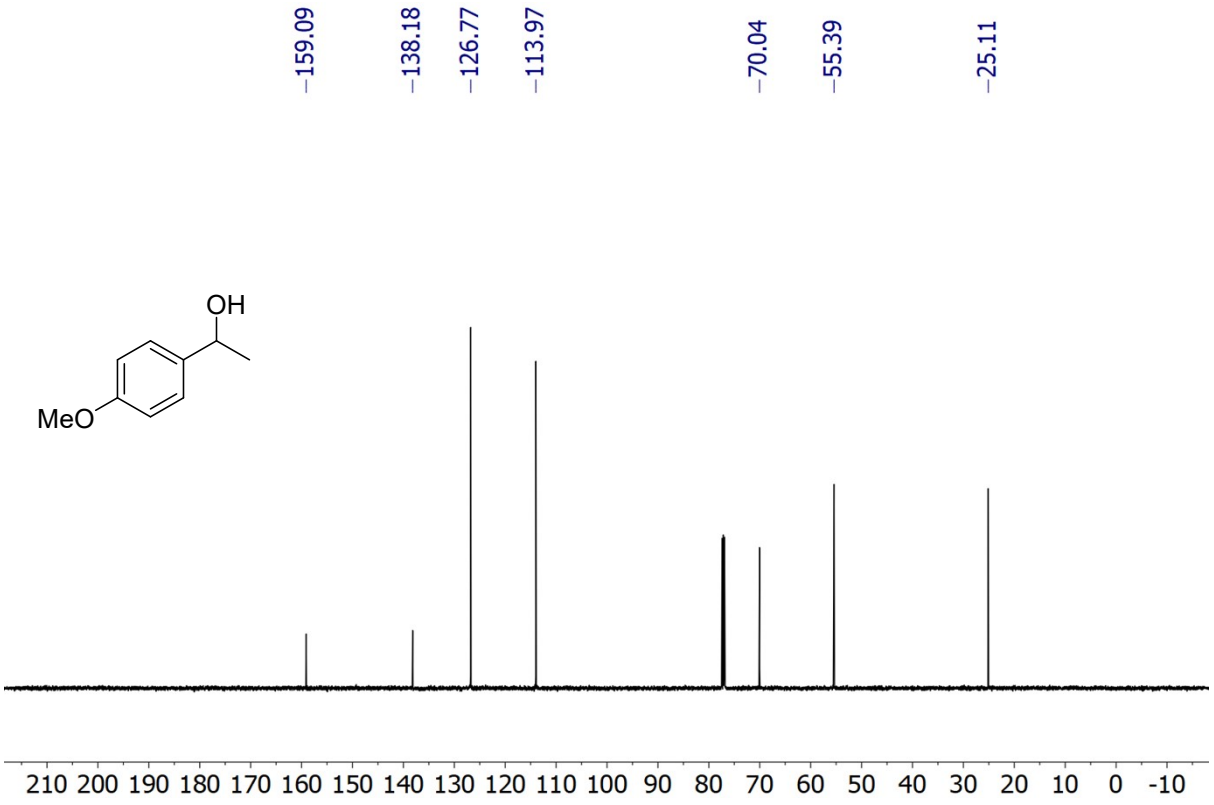

Figure S79. $^{13}C\{^{1}H\}$ NMR ($CDCl_3$, 125.75 MHz) spectrum of 1-(4-methoxyphenyl)ethan-1-ol.

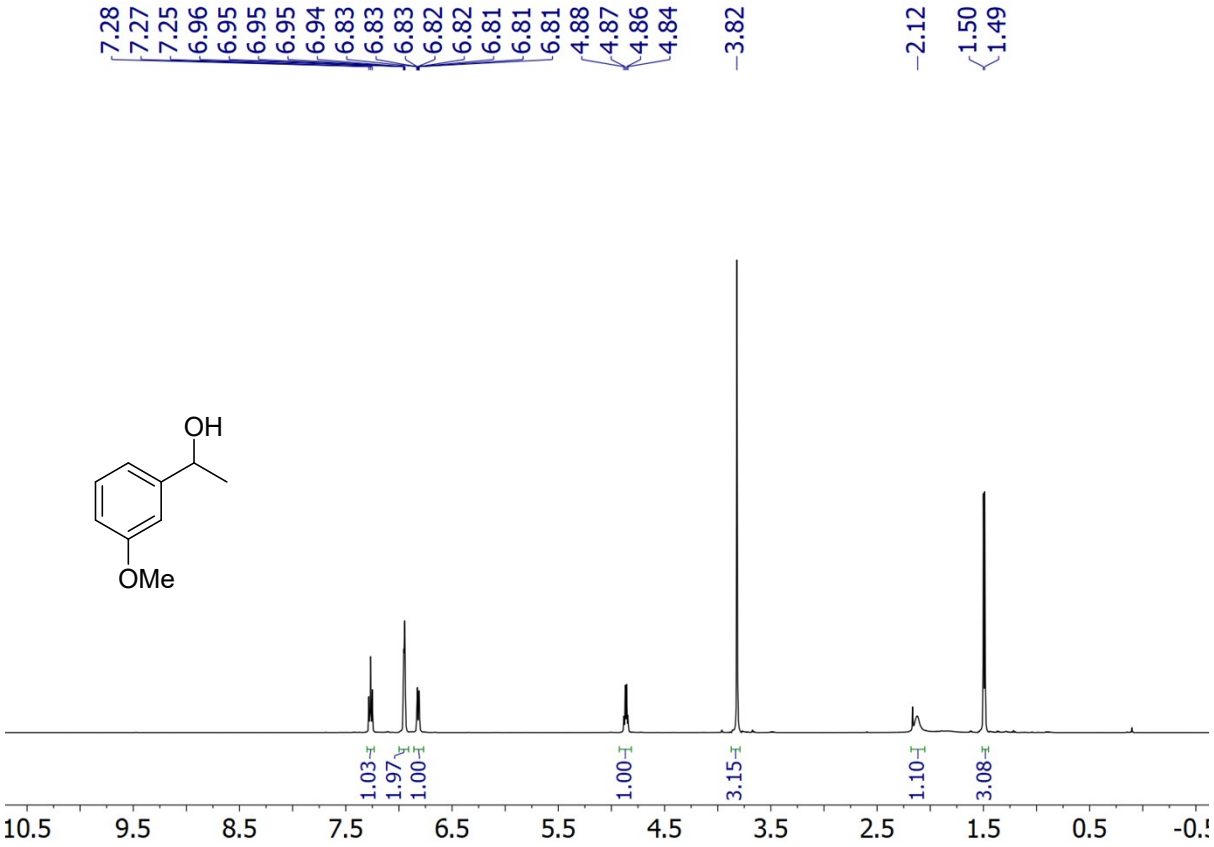

Figure S80. ^{1}H NMR ($CDCl_3$, 500 MHz) spectrum of 1-(3-methoxyphenyl)ethan-1-ol.

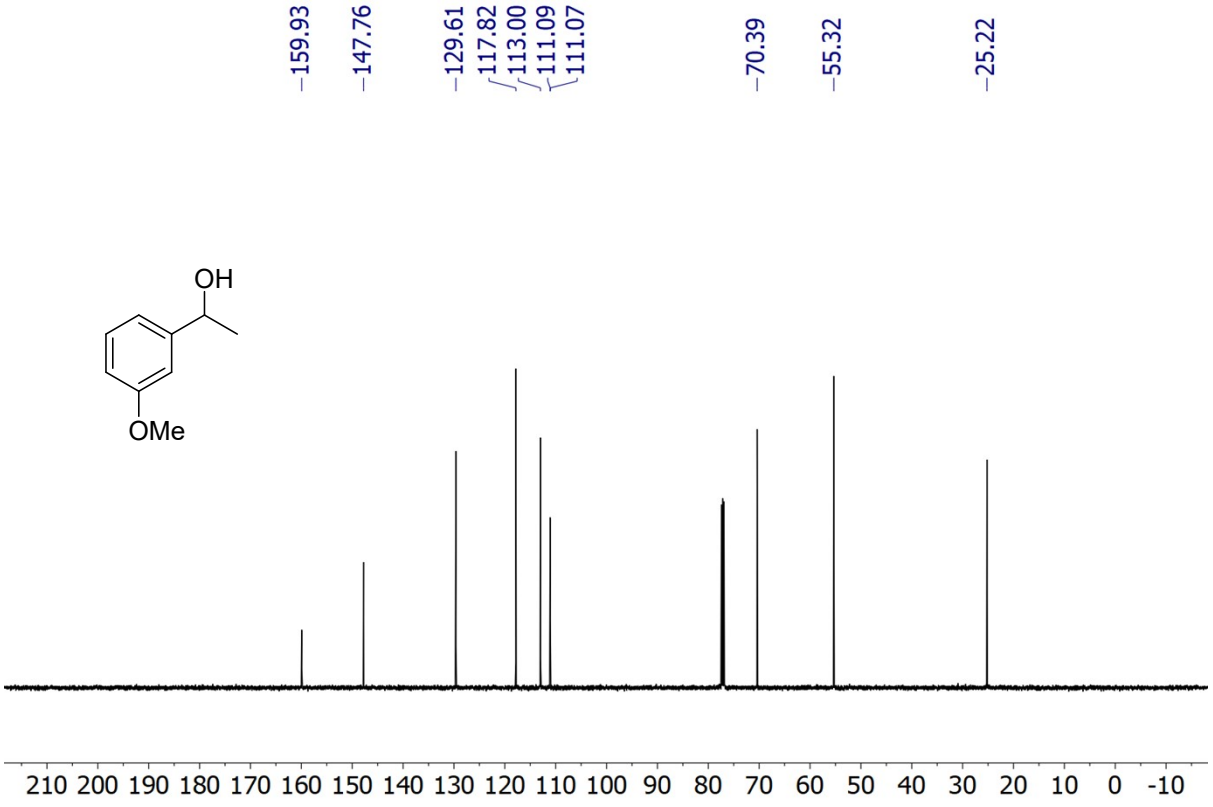

Figure S81. $^{13}C\{^{1}H\}$ NMR ($CDCl_3$, 125.75 MHz) spectrum of 1-(3-methoxyphenyl)ethan-1-ol.

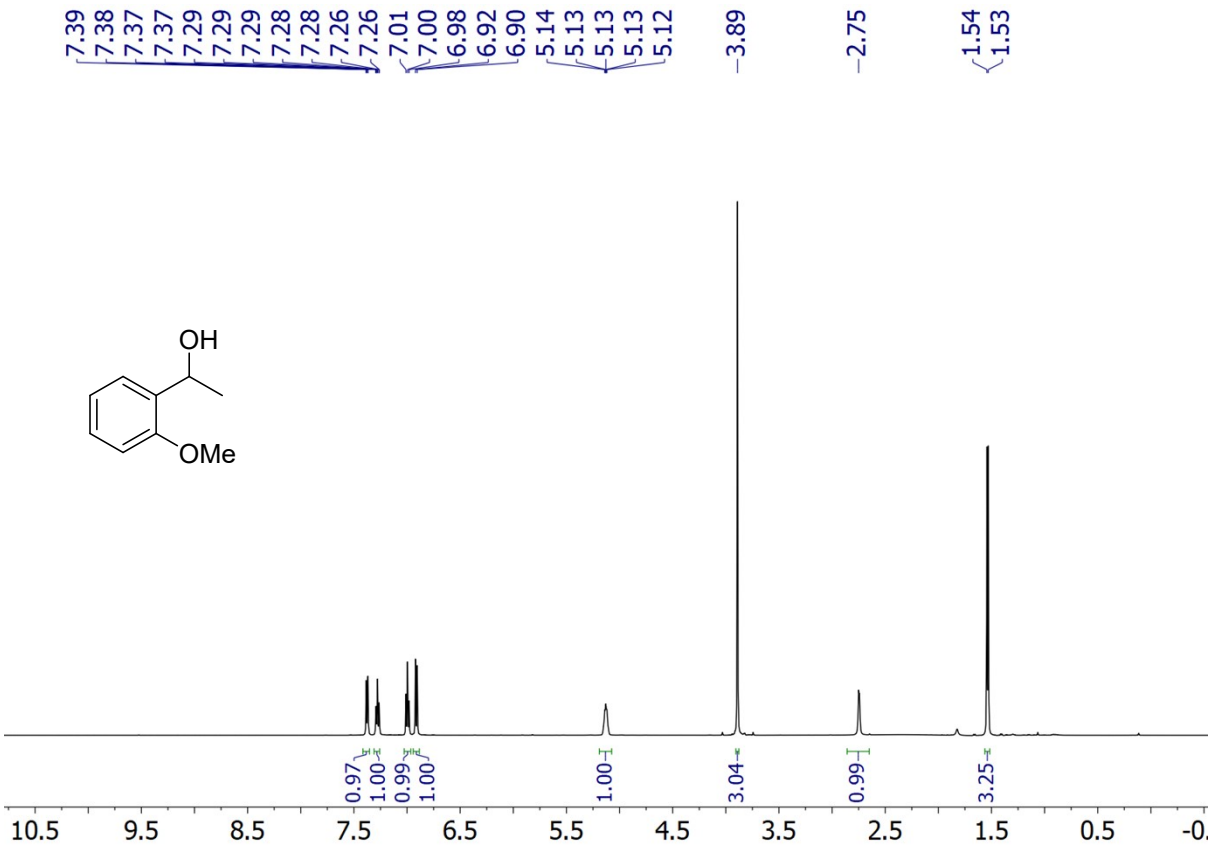

Figure S82. ^{1}H NMR ($CDCl_3$, 500 MHz) spectrum of 1-(2-methoxyphenyl)ethan-1-ol.

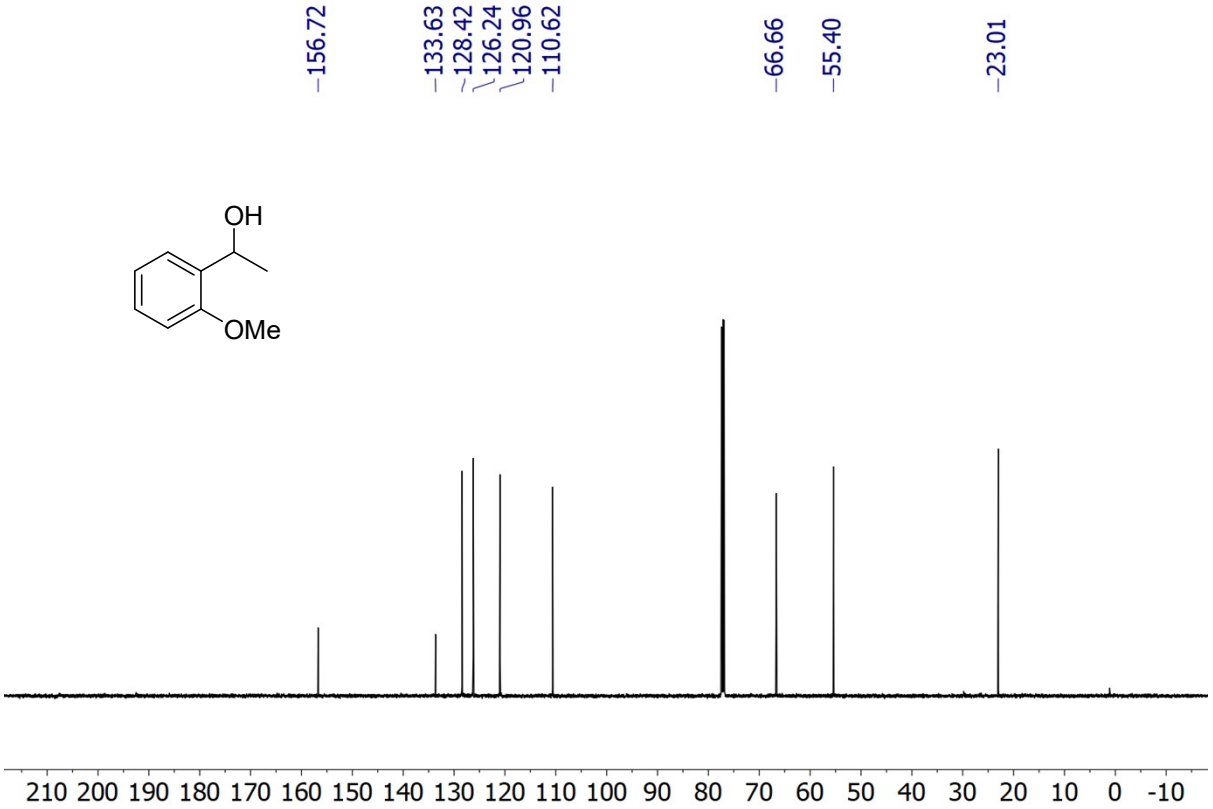

Figure S83. $^{13}C\{^{1}H\}$ NMR ($CDCl_3$, 125.75 MHz) spectrum of 1-(2-methoxyphenyl)ethan-1-ol.

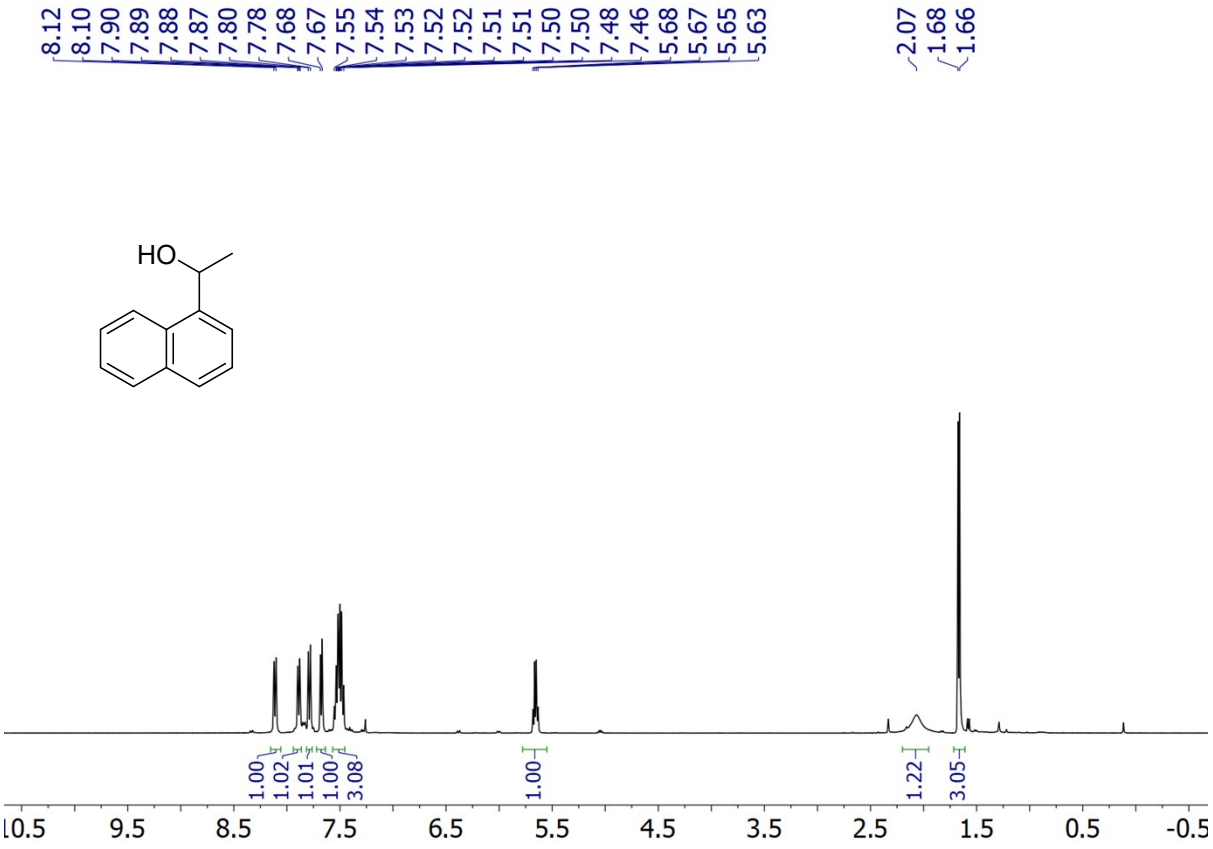

Figure S84. ^{1}H NMR ($CDCl_3$, 400 MHz) spectrum of 1-(napthalen-1-yl)ethan-1-ol.

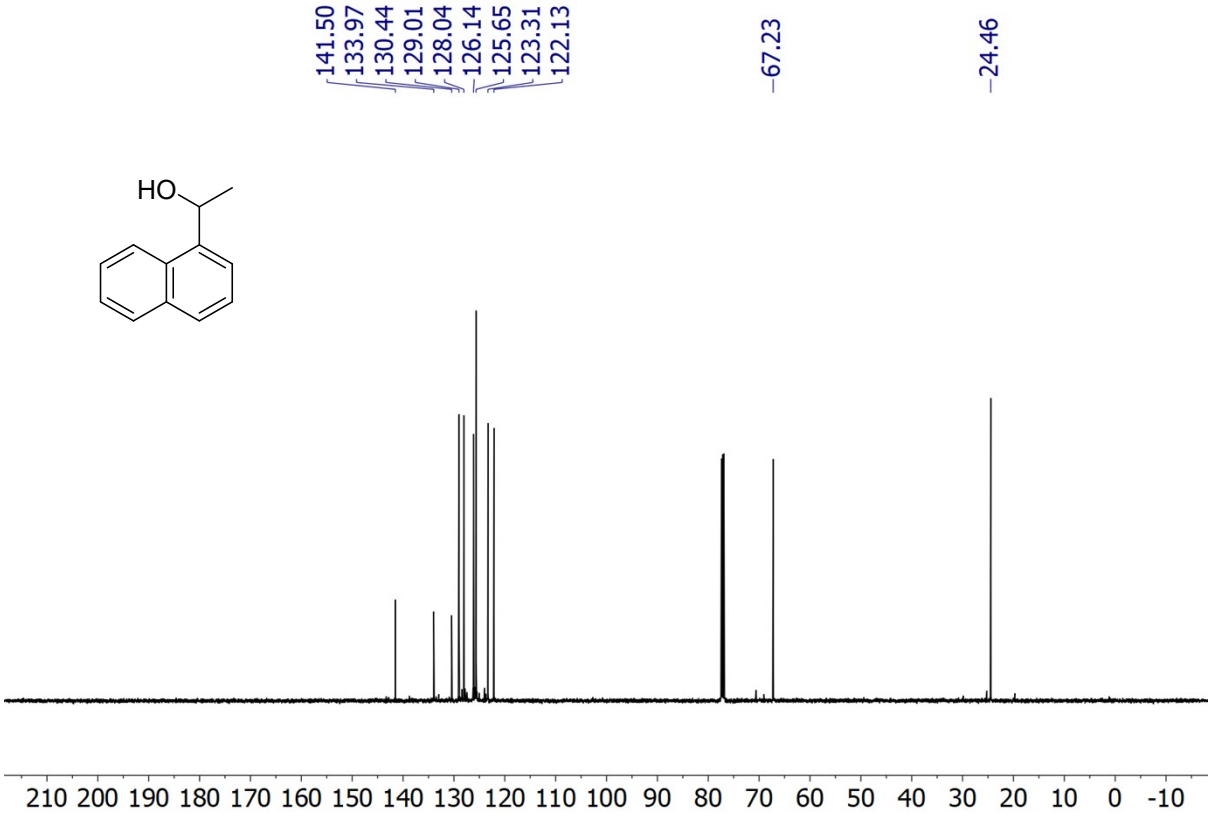

Figure S85. $^{13}C\{^{1}H\}$ NMR ($CDCl_3$, 125.75 MHz) spectrum of 1-(napthalen-1-yl)ethan-1-ol.

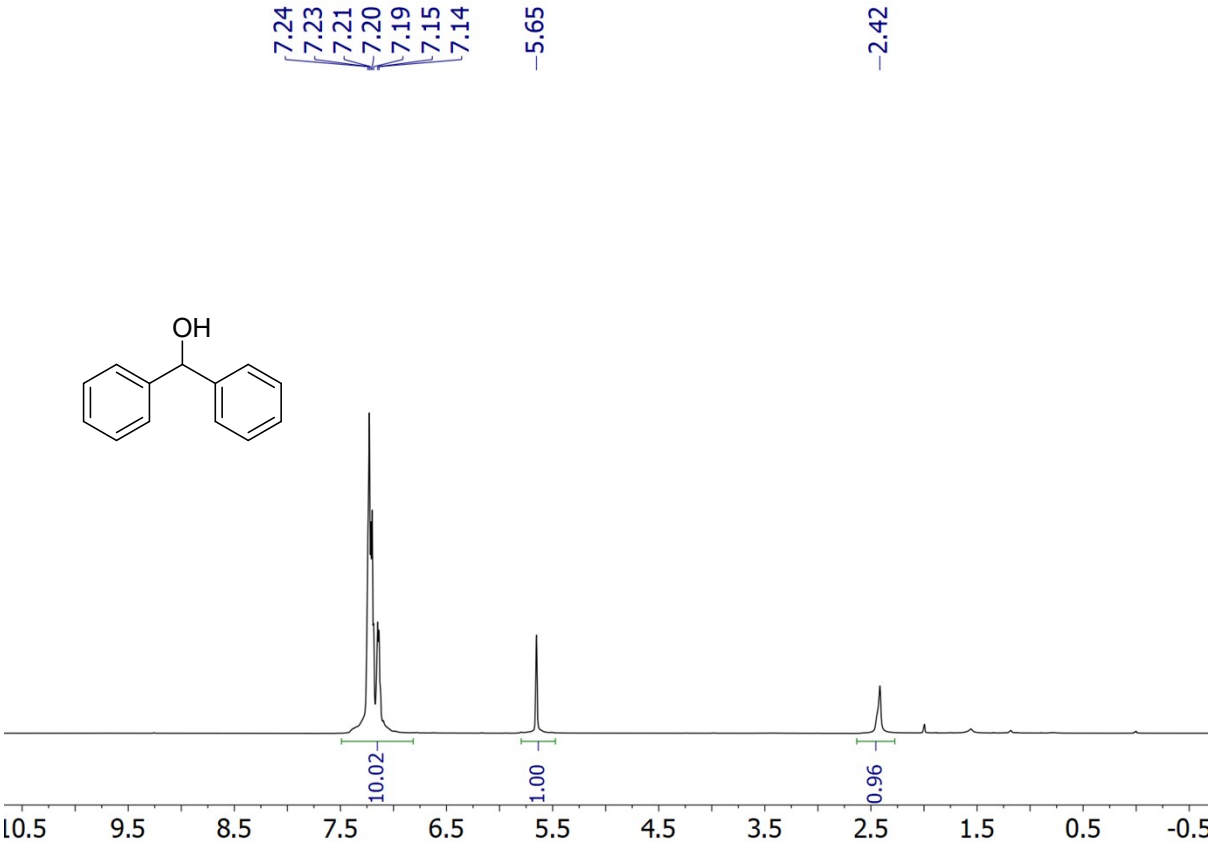

Figure S86. ^{1}H NMR ($CDCl_3$, 500 MHz) spectrum of diphenylmethanol.

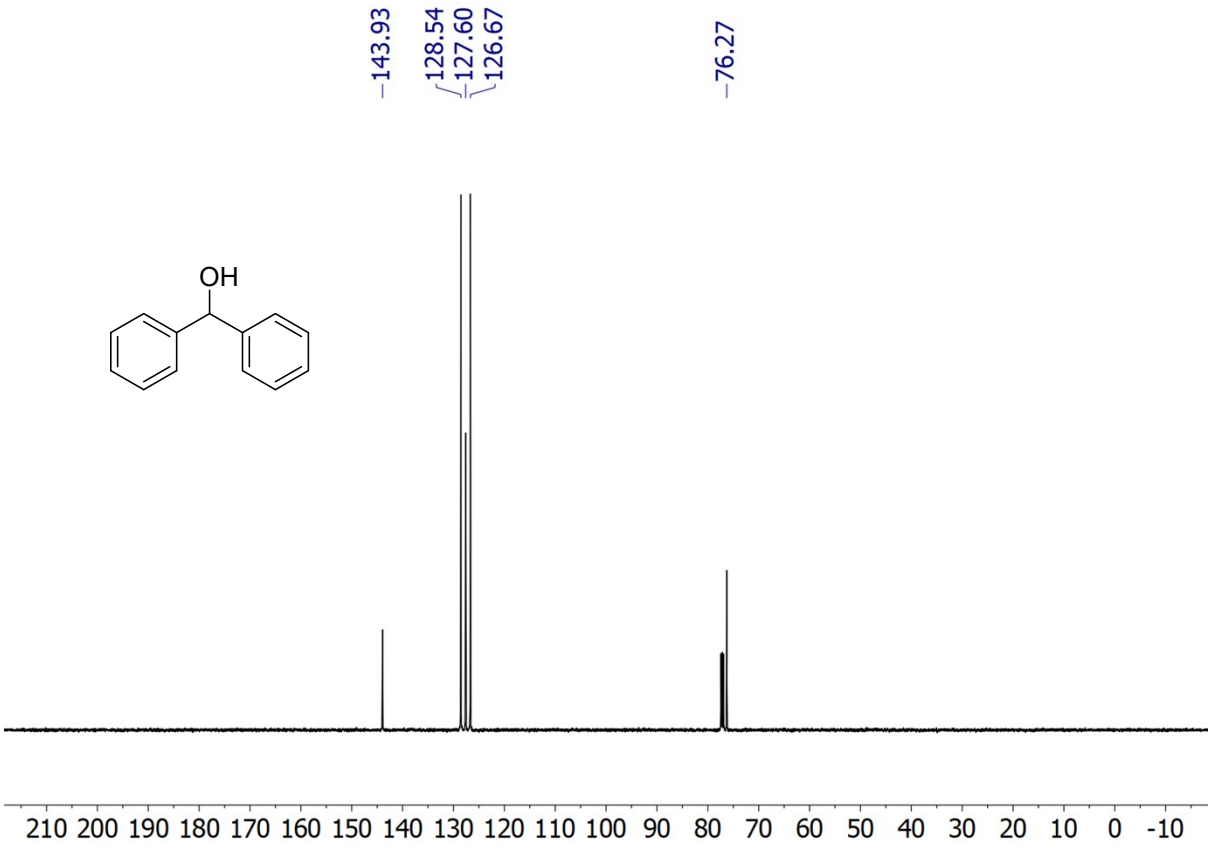

Figure S87. $^{13}C\{^{1}H\}$ NMR ($CDCl_3$, 125.75 MHz) spectrum of diphenylmethanol**.**

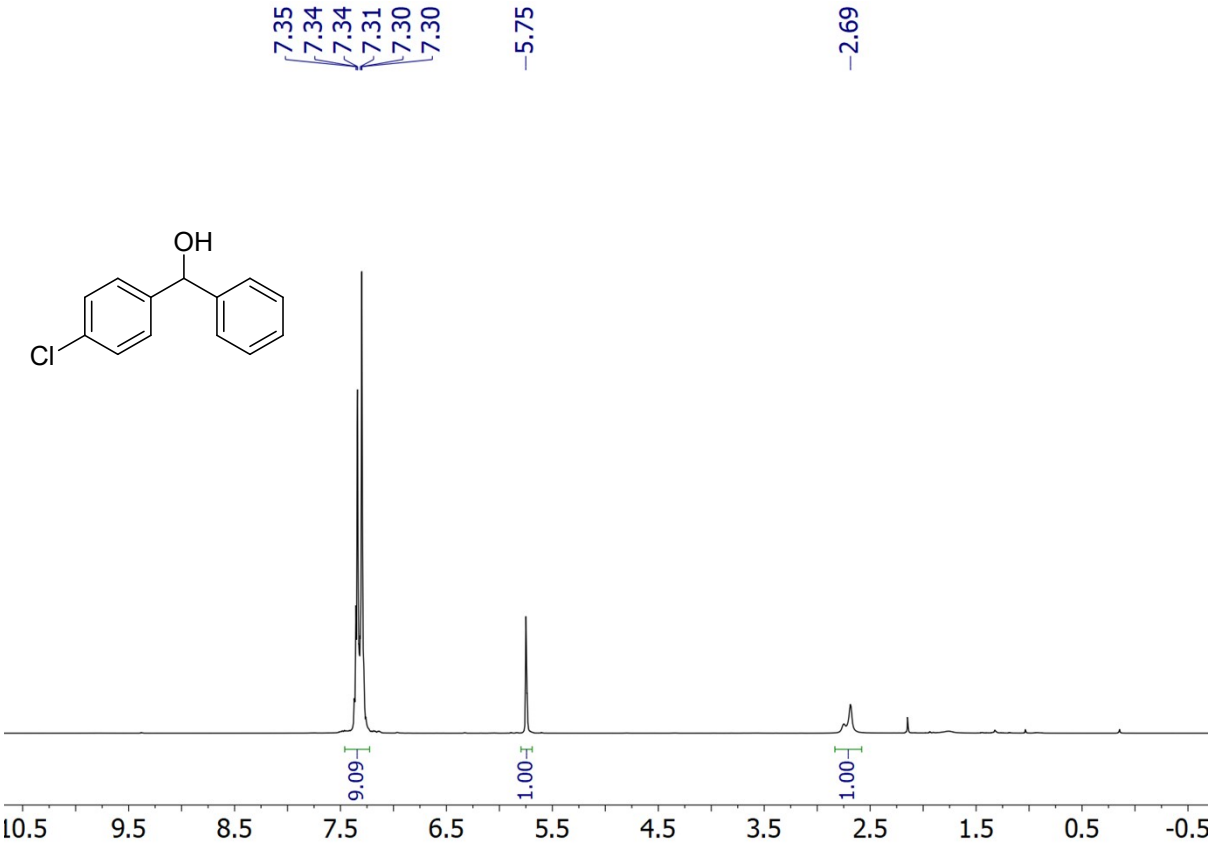

Figure S88. ^{1}H NMR ($CDCl_3$, 500 MHz) spectrum of (4-chlorophenyl)(phenyl)methanol.

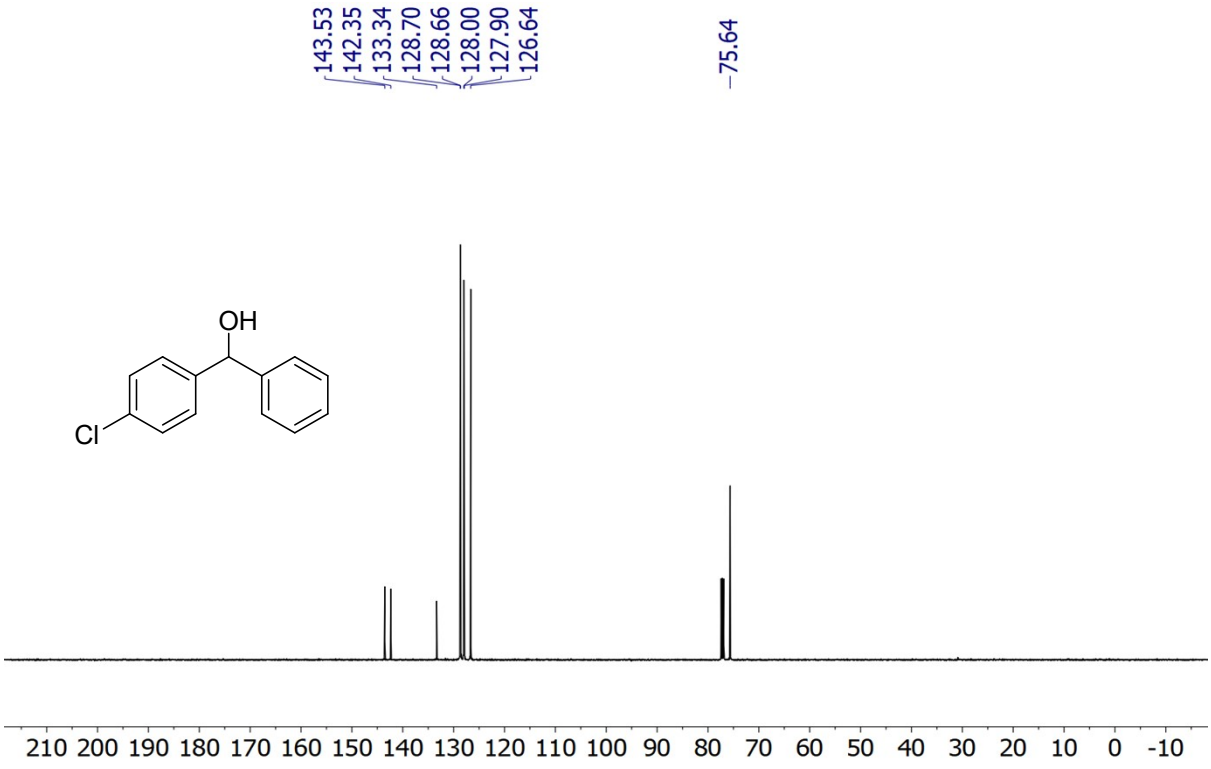

Figure S89. $^{13}C\{^{1}H\}$ NMR ($CDCl_3$, 125.75 MHz) spectrum of (4-chlorophenyl)(phenyl)methanol.

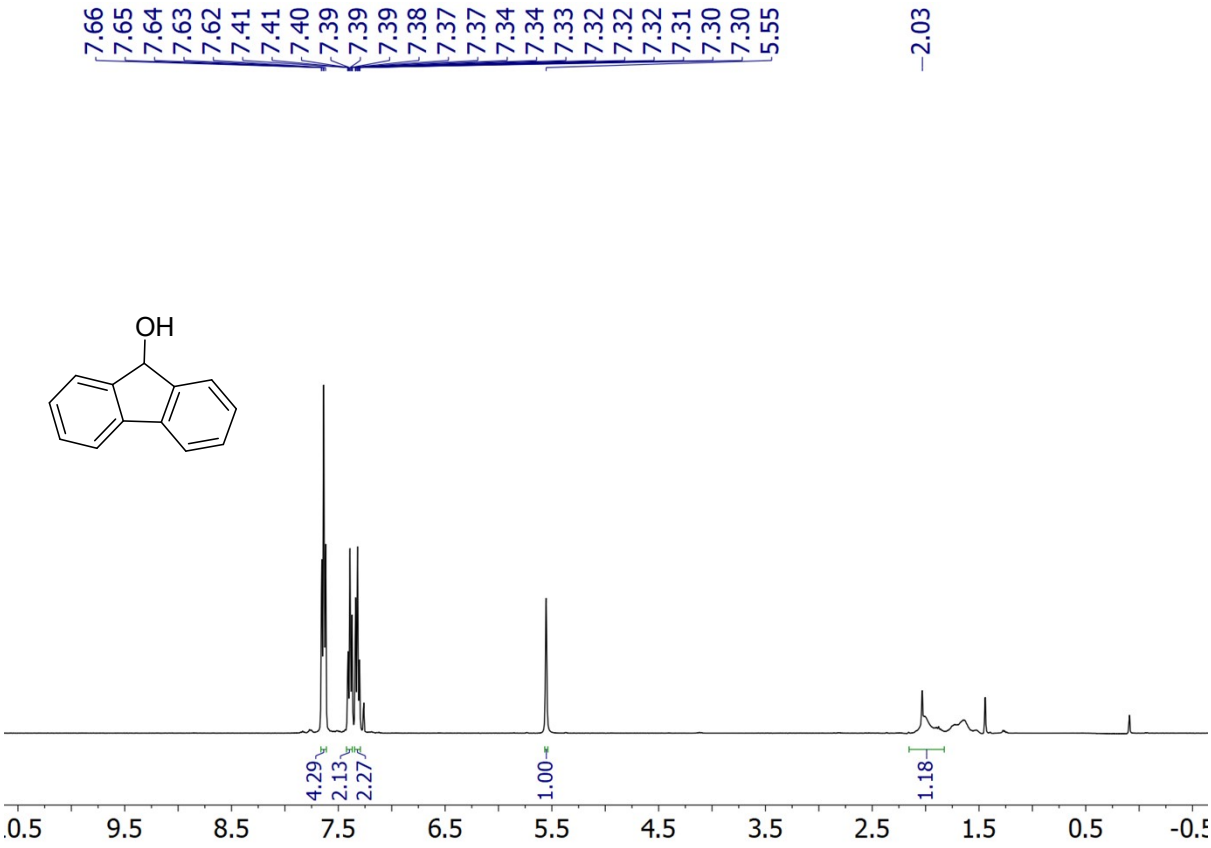

Figure S90. ^{1}H NMR ($CDCl_3$, 400 MHz) spectrum of 9H-fluoren-9-ol.

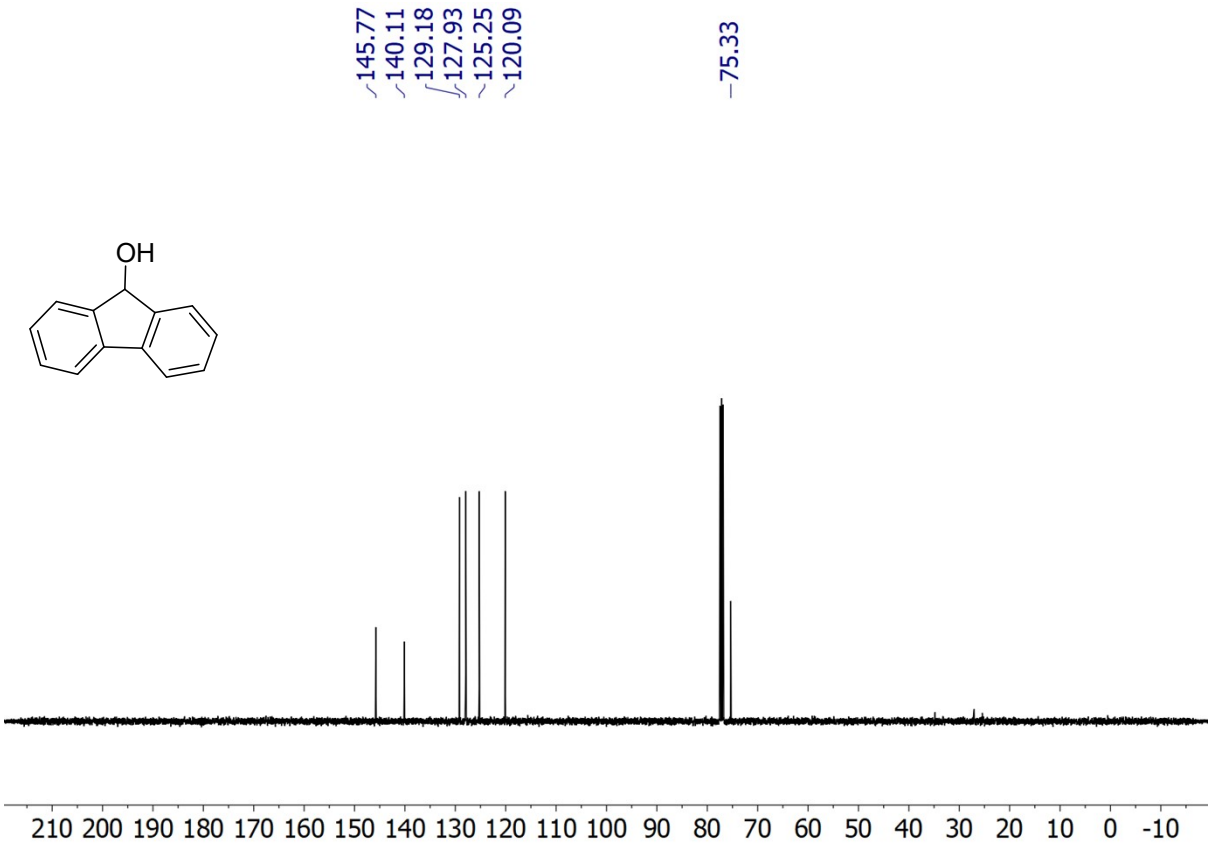

Figure S91. $^{13}C\{^{1}H\}$ NMR ($CDCl_3$, 100.6 MHz) spectrum of 9H-fluoren-9-ol.

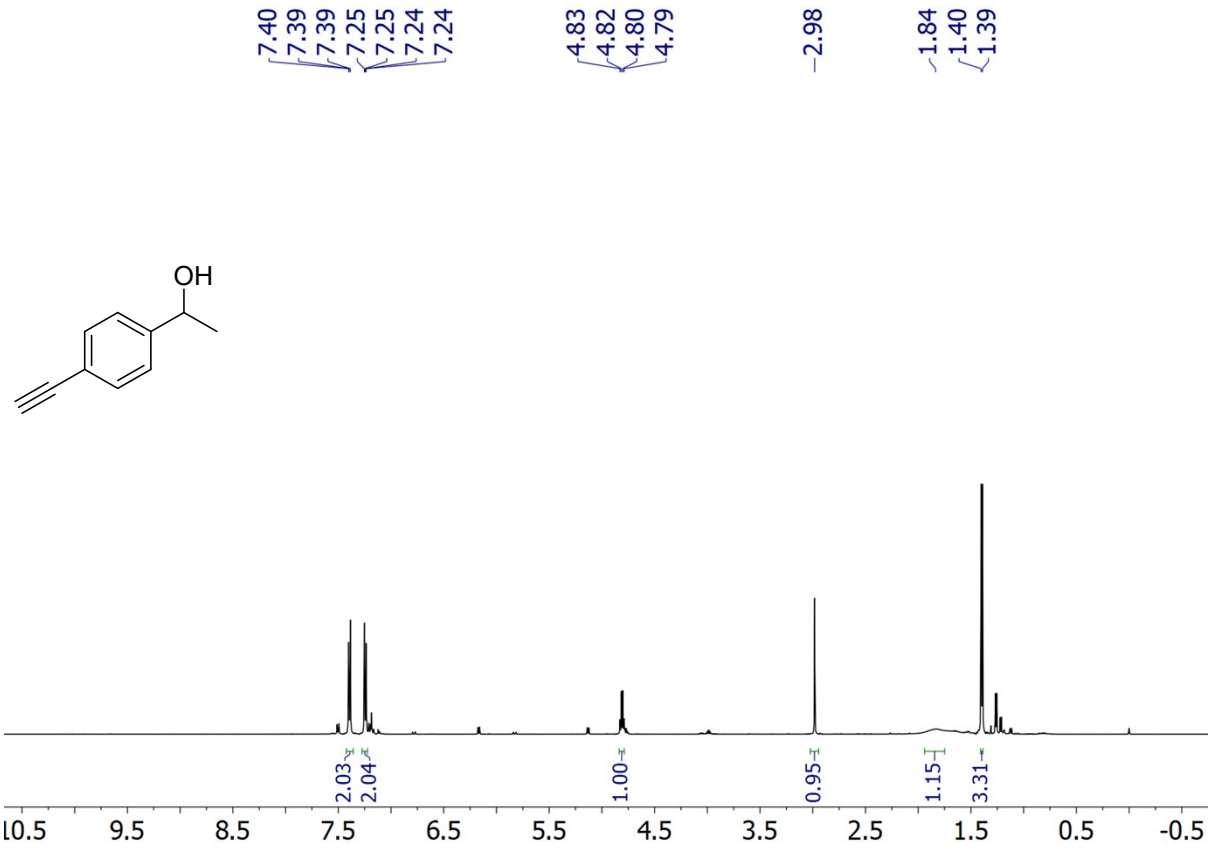

Figure S92. ^{1}H NMR ($CDCl_3$, 500 MHz) spectrum of 1-(4-ethynylphenyl)ethan-1-ol.

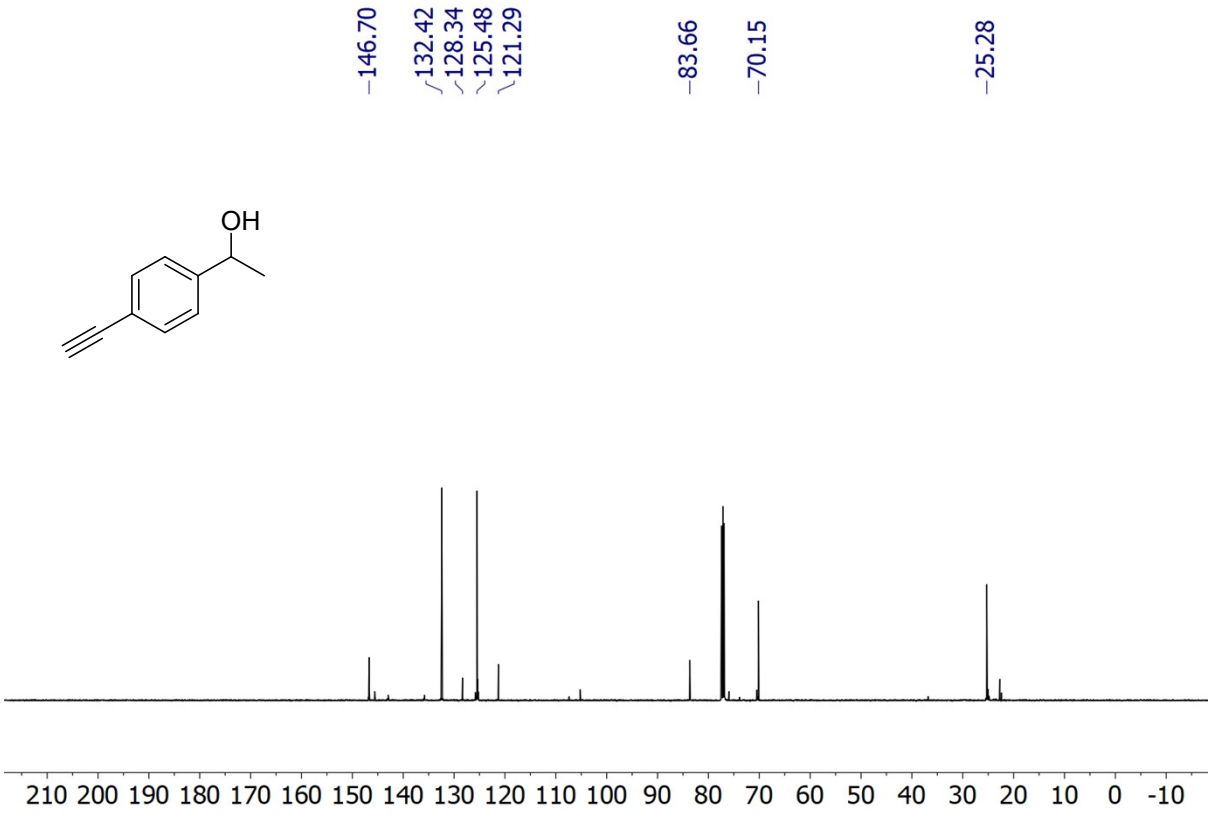

Figure S93. $^{13}C\{^{1}H\}$ NMR ($CDCl_3$, 125.75 MHz) spectrum of 1-(4-ethynylphenyl)ethan-1-ol.

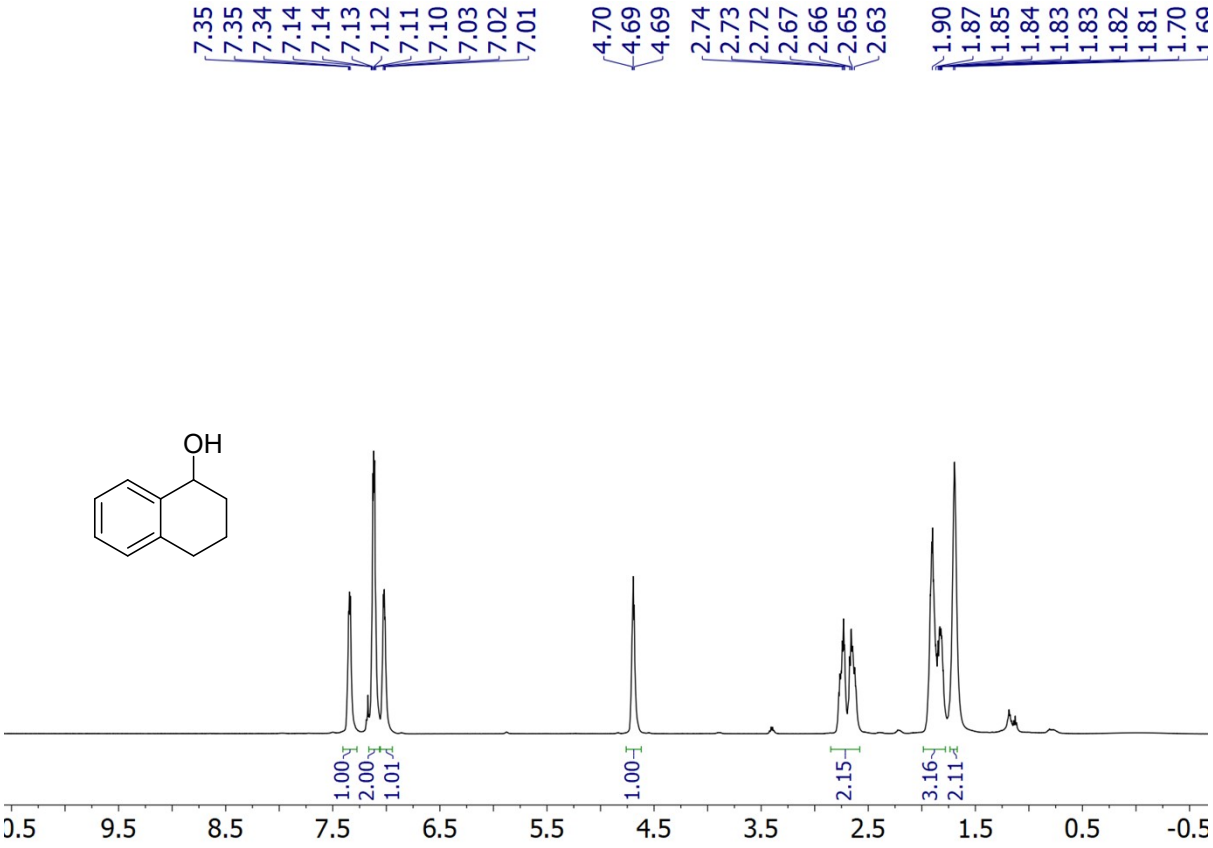

Figure S94. ^{1}H NMR ($CDCl_3$, 500 MHz) spectrum of 1,2,3,4-tetrahydronaphthalen-1-ol.

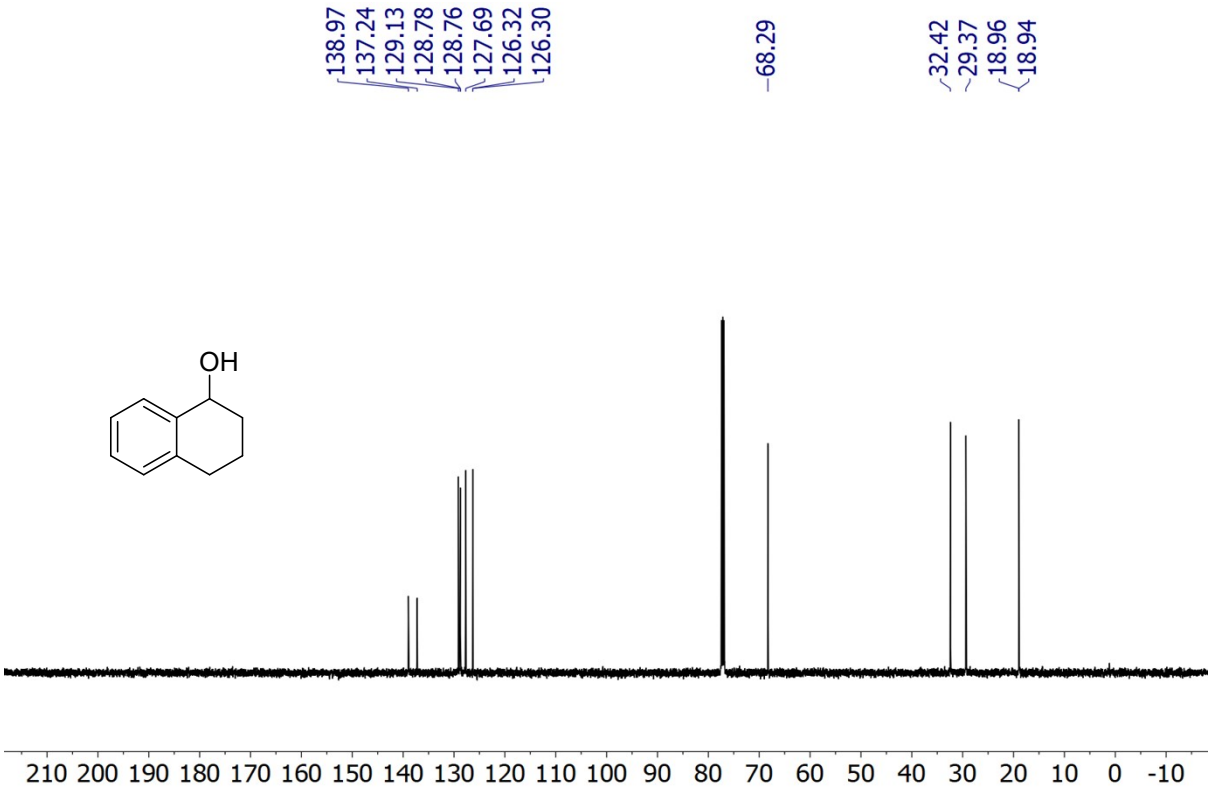

Figure S95. $^{13}C\{^{1}H\}$ NMR ($CDCl_3$, 125.75 MHz) spectrum of 1,2,3,4-tetrahydronaphthalen-1-ol.

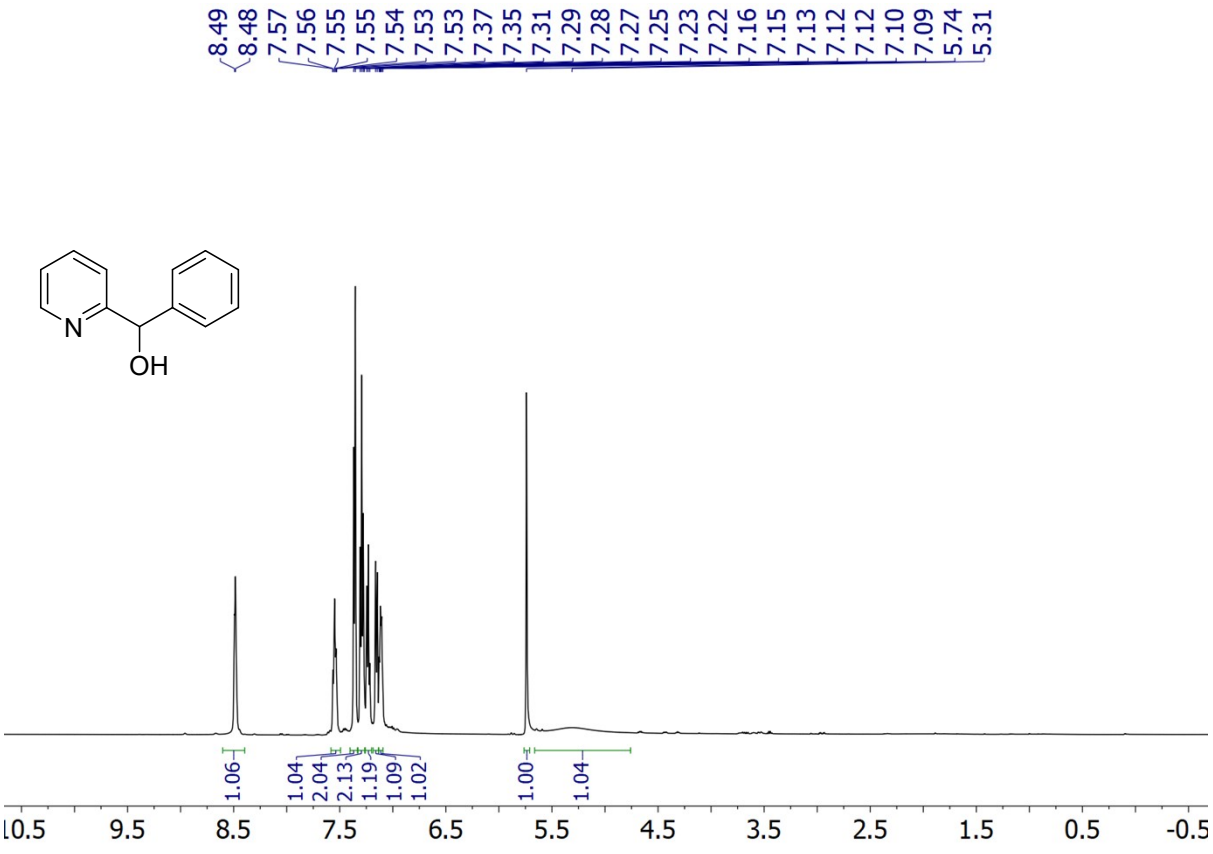

Figure S96. ^{1}H NMR ($CDCl_3$, 500 MHz) spectrum of phenyl(pyridin-2-yl)methanol.

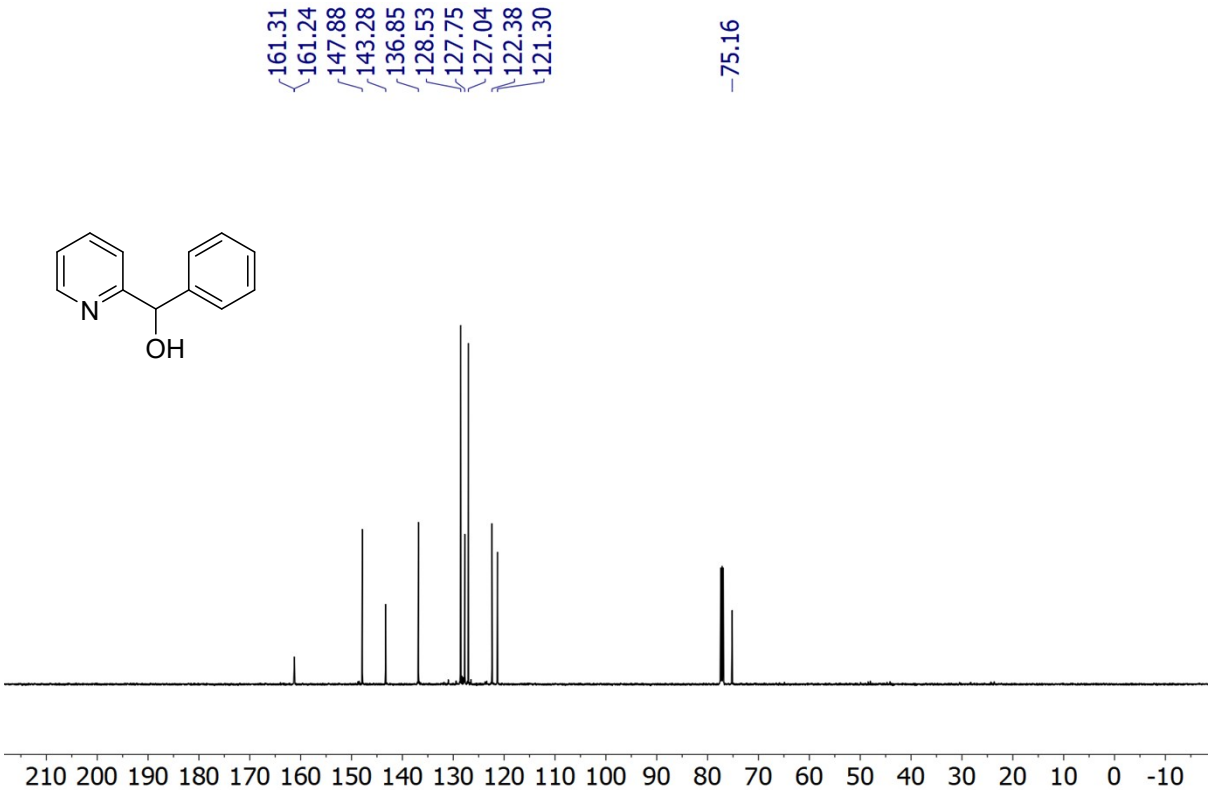

Figure S97. $^{13}C\{^{1}H\}$ NMR ($CDCl_3$, 125.75 MHz) spectrum of phenyl(pyridin-2-yl)methanol.

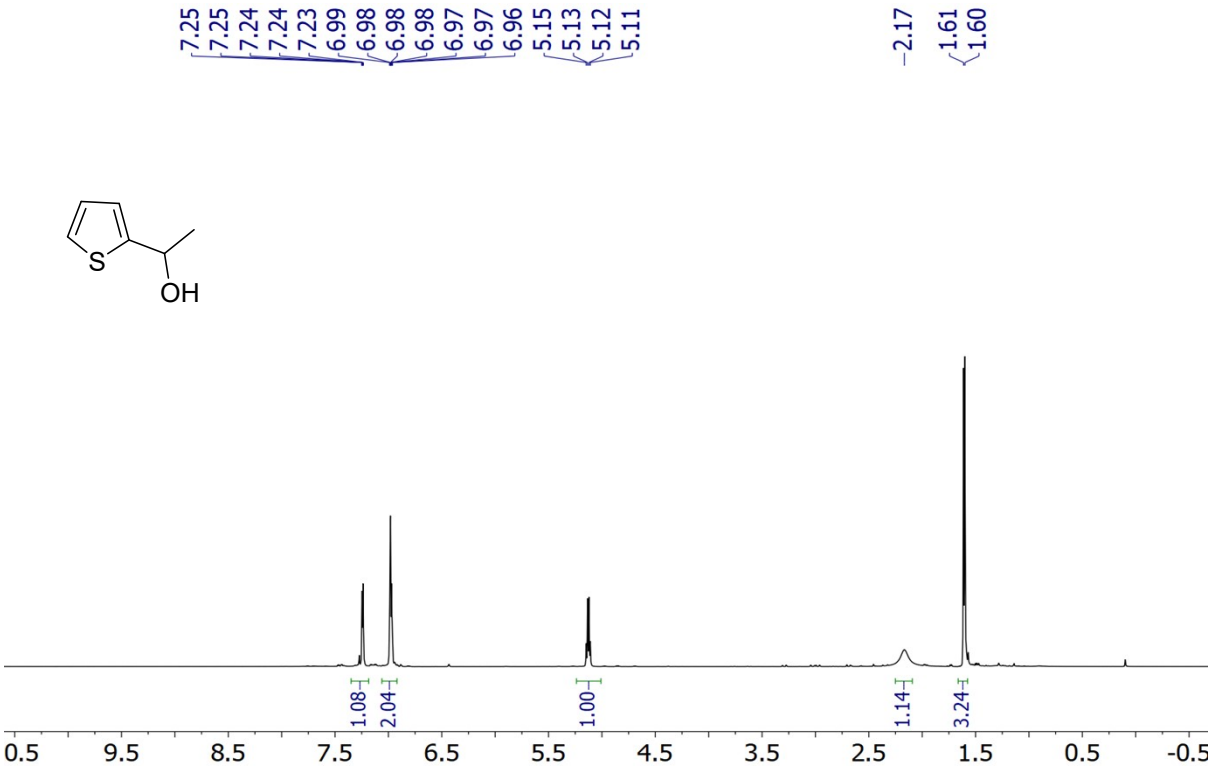

Figure S98. ^{1}H NMR ($CDCl_3$, 500 MHz) spectrum of 1-(thiophen-2-yl)ethan-1-ol.

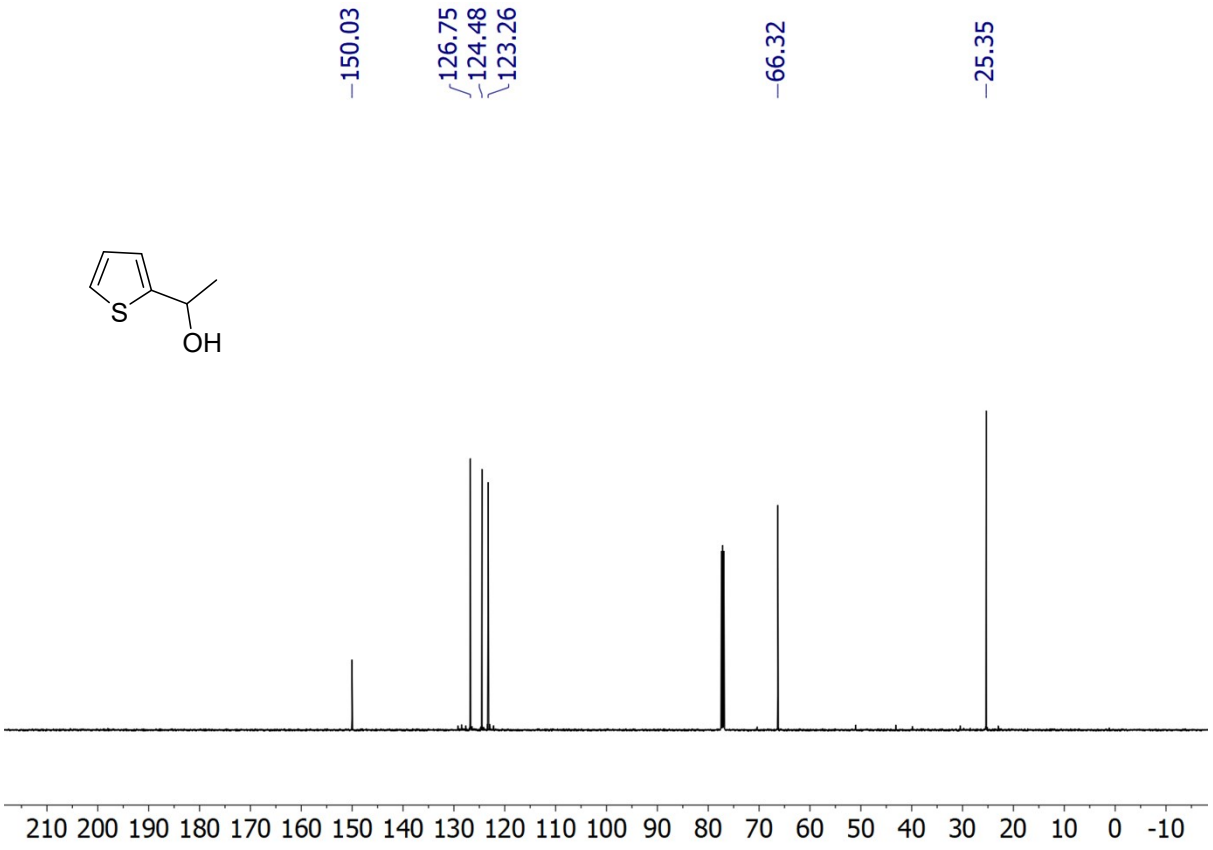

Figure S99. $^{13}C\{^{1}H\}$ NMR ($CDCl_3$, 125.75 MHz) spectrum of 1-(thiophen-2-yl)ethan-1-ol.

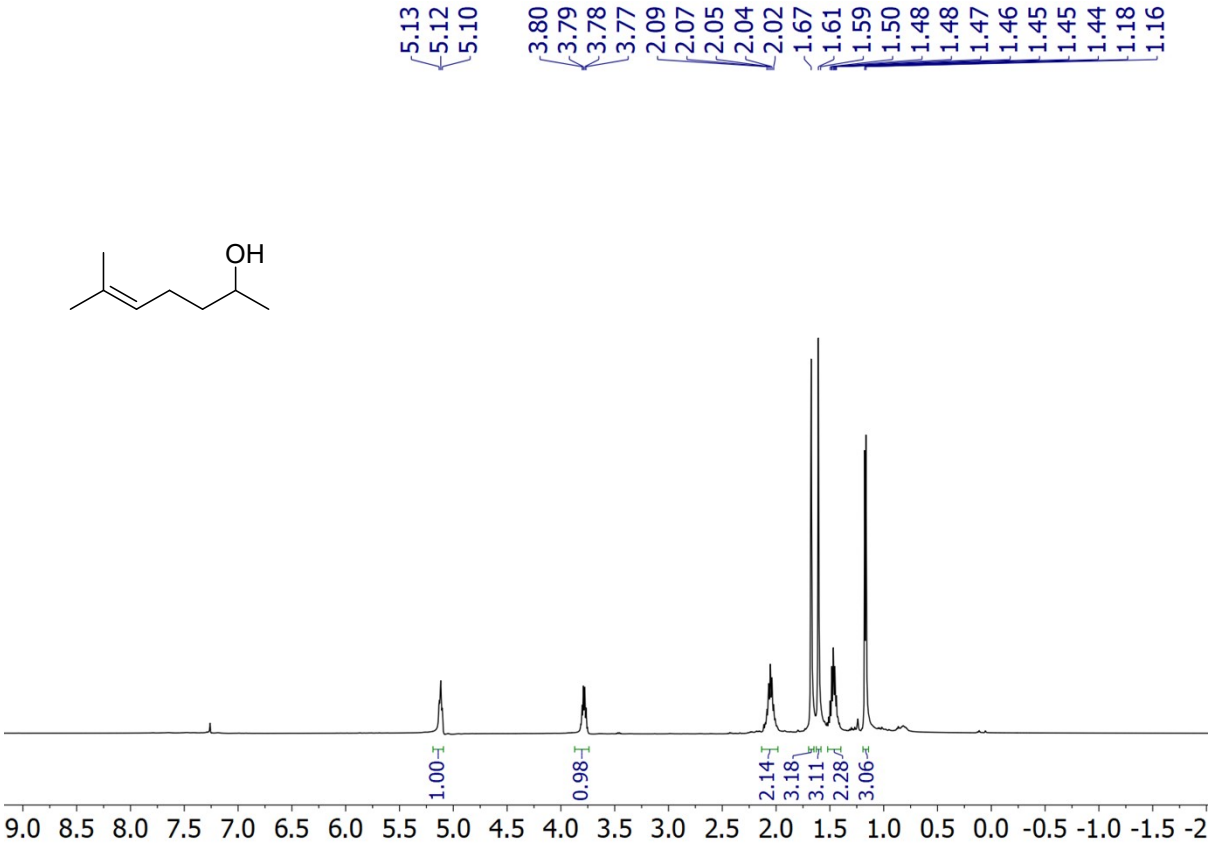

Figure S100. ^{1}H NMR ($CDCl_3$, 500 MHz) spectrum of 6-methylhept-5-en-2-ol.

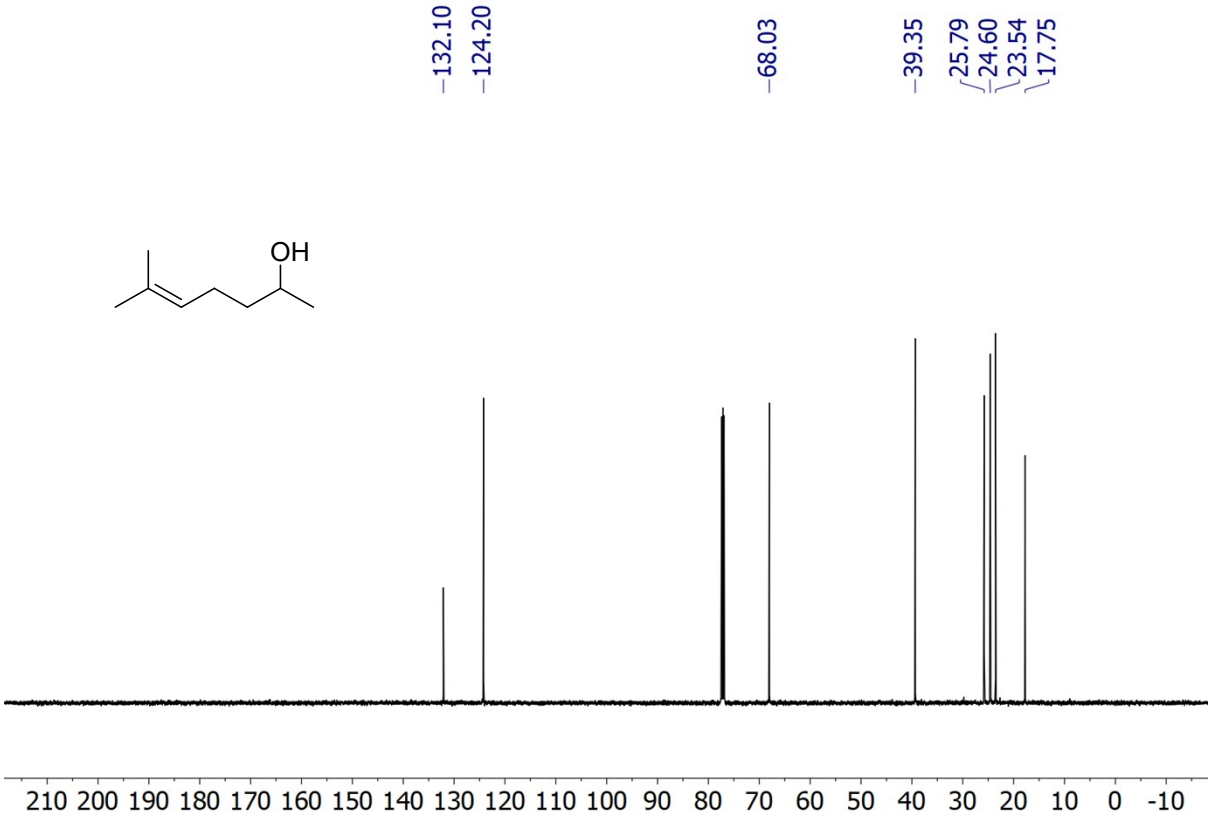

Figure S101. $^{13}C\{^{1}H\}$ NMR ($CDCl_3$, 125.75 MHz) spectrum of 6-methylhept-5-en-2-ol.

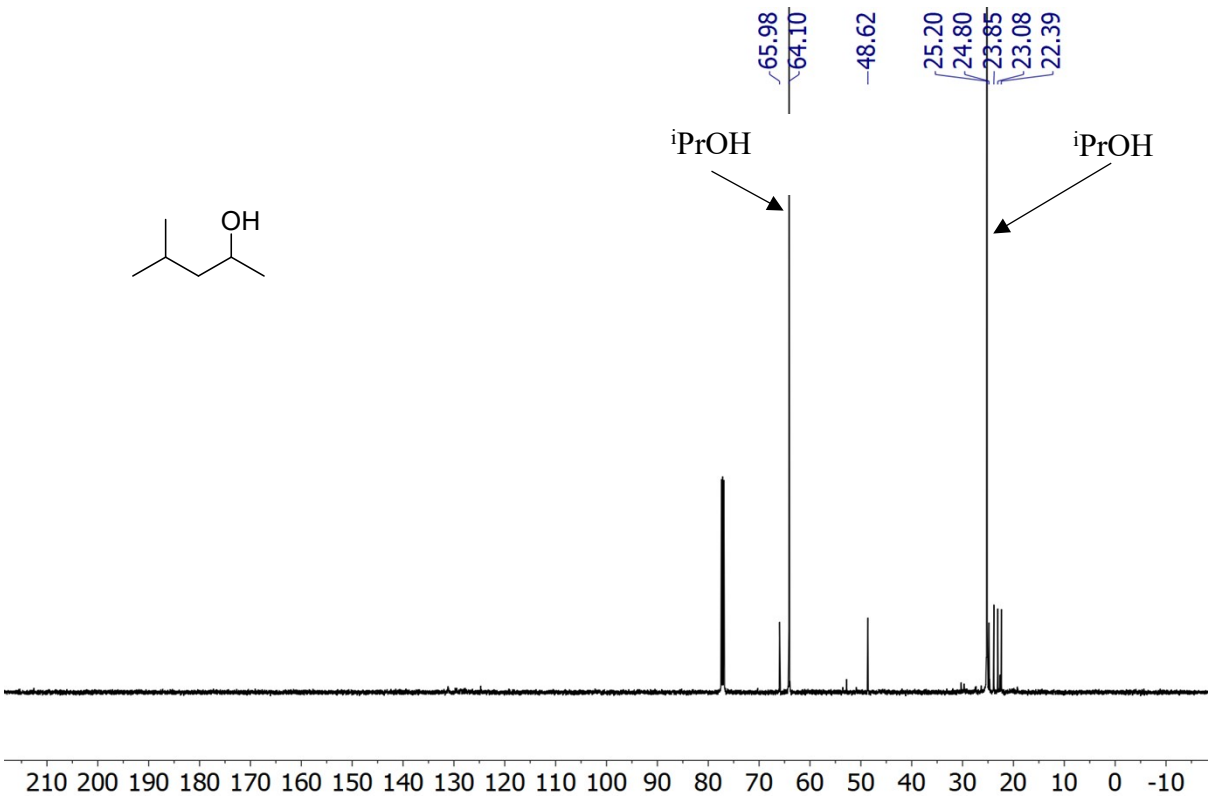

Figure S102. $^{13}C\{^{1}H\}$ NMR ($CDCl_3$, 500 MHz) spectrum of 4-methylpentan-2-ol.

X-ray structures and refinement data

The suitable single crystals of complexes **2a**, and **3a-c** were grown from the solvents mentioned in their respective experimental sections. Data collections were performed using a Bruker APEX-II or D8 Venture APEX3 CCD diffractometer with graphite monochromated Mo Kα radiation (λ = 0.71073 Å). The space group for every structure was obtained by XPREP program. The structures were solved by SHELXT[12] which successfully located most of the nonhydrogen atoms. Subsequently, least-squares refinements were carried out on F^2 using SHELXL Version 2018/3[13] to locate the remaining nonhydrogen atoms. Non-hydrogen atoms were refined with anisotropic displacement parameters. Hydrogen atoms attached to carbon atoms were fixed in calculated positions. The lattice benzene molecule in **3a** is disordered and was successfully modeled and refined using DELU, SIMU, SADI, and RIGU restraints. One of the ethyl groups in **3b** was found disordered and their coordinates were split and refined. The refinement data for all the structures are summarized in Table S4 and Table S5. Crystallographic data were deposited with the Cambridge Crystallographic Data Centre, CCDC, 12 Union Road, Cambridge CB21EZ, UK. These data can be obtained free of charge upon quoting the depository numbers CCDC 2297463-2297467 from web interface (at http://www.ccdc.cam.ac.uk).

Table S4 Crystallographic data for complexes **2a**, **3a**, and **3b**.

	2a	**3a**·C_6H_6	**3b**
Empirical formula	$C_{47}H_{40}Cl_2N_2NiP_2$	$C_{53}H_{44}N_2NiP_2$	$C_{39}H_{38}N_2NiP_2$
Formula weight	824.36	829.55	655.36
Wavelength (Å)	0.71073	0.71073	0.71073
Temperature (K)	296(2)	296(2)	296(2)
Crystal system	Monoclinic	Triclinic	Triclinic
Space group	$P2_1/n$	$P\bar{1}$	$P\bar{1}$
a/Å	15.4431(7)	12.2996(13)	13.178(2)
b/Å	15.2942(6)	13.4141(14)	16.184(2)
c/Å	17.7753(7)	14.7999(17)	17.888(3)
α/degree	90	107.311(7)	68.459(6)
β/degree	104.2620(10)	108.334(7)	78.918(7)
γ/degree	90	99.319(7)	70.131(6)
Volume (Å^3)	4068.9(3)	2123.1(4)	3327.4(9)
Z	4	2	4
D_{calcd}, g cm^{-3}	1.346	1.298	1.308
μ/mm^{-1}	0.732	0.571	0.709
F(000)	1712	868	1376
θ range (degree)	1.904 to 27.087	2.785 to 25.00	2.693 to 27.273
Limiting indices	-19<=h<=19, -19<=k<=19, -22<=l<=22	-14<=h<=14, -15<=k<=14, -12<=l<=17	-11<=h<=16, -17<=k<=20, -22<=l<=22
Total/ unique no. of reflns.	83247 / 8944	16798 / 7436	34375 / 14719
R_{int}	0.0897	0.0899	0.0311
Data / restr./ params.	8944 / 0 / 495	7436 / 98 / 578	14719 / 0 / 816
GOF (F^2)	1.019	1.011	1.015
R1, *wR2*	0.0405, 0.0881	0.0714, 0.1196	0.0392, 0.0960
R indices (all data) *R1*, *wR2*	0.0647, 0.0989	0.1616, 0.1613	0.0629, 0.1140
Largest different peak and hole (e Å^{-3})	0.385 and -0.327	0.393 and -0.637	0.503 and -0.313

Table S5 Crystallographic data for complexes **3c**, and **4**.

	(3c)$_2$·THF	**4**·(toluene)$_4$
Empirical formula	$C_{84}H_{84}N_4Ni_2OP_4$	$C_{138}H_{136}N_4Ni_2P_4$
Formula weight	1406.85	2091.80
Wavelength (Å)	0.71073	0.71073
Temperature (K)	143(2)	296(2)
Crystal system	Monoclinic	Monoclinic
Space group	$I_{2/a}$	$P2_1/n$
a/Å	24.594(5)	12.8416(15)
b/Å	9.933(2)	35.708(4)
c/Å	28.552(6)	13.5064(15)
α/degree	90	90
β/degree	94.190(6)	115.652(4)
γ/degree	90	90
Volume (Å^3)	6956(3)	5582.9(11)
Z	4	2
D_{calcd}, g cm^{-3}	1.343	1.244
μ/mm^{-1}	0.685	0.449
F(000)	2960	2216
θ range (degree)	2.172 to 27.094	2.156 to 28.318
Limiting indices	-31<=h<=31, -12<=k<=12, -36<=l<=36	-17<=h<=17, -46<=k<=47, -17<=l<=18
Total/ unique no. of reflns.	171729 / 7659	76740 / 13848
R_{int}	0.0482	0.1574
Data / restr./ params.	7659 / 0 / 429	13848 / 24 / 675
GOF (F^2)	1.040	1.007
R1, *wR2*	0.0302, 0.0767	0.0636, 0.1321
R indices (all data) *R1*, *wR2*	0.0351, 0.0802	0.1851, 0.1893
Largest different peak and hole (e Å^{-3})	0.768 and -0.758	0.460 and -0.332

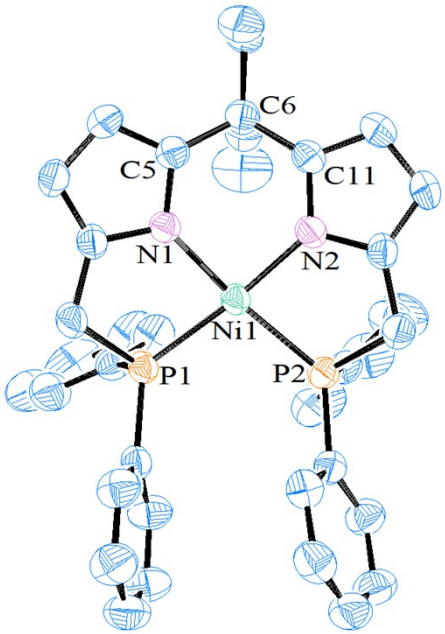

Figure S103. The X-ray structure of complex **3b** (50% displacement ellipsoids). One of the molecules in the asymmetric unit is given. The disordered ethyl group and all hydrogen atoms are omitted for clarity. Selected bond distances (Å) and bond angles (°): Ni1-N1 1.8767(18), Ni1-N2 1.8832(18), P1-Ni1 2.1636(7), P2-Ni1 2.1669(7), N1-Ni1-N2 91.59(8), N1-Ni1-P2 174.13(6), N2-Ni1-P2 83.12(6), N1-Ni1-P1 82.99(6), N2-Ni1-P1 174.56(6), P1-Ni1-P2 102.27(3), C5-C6-C11 112.5(2).

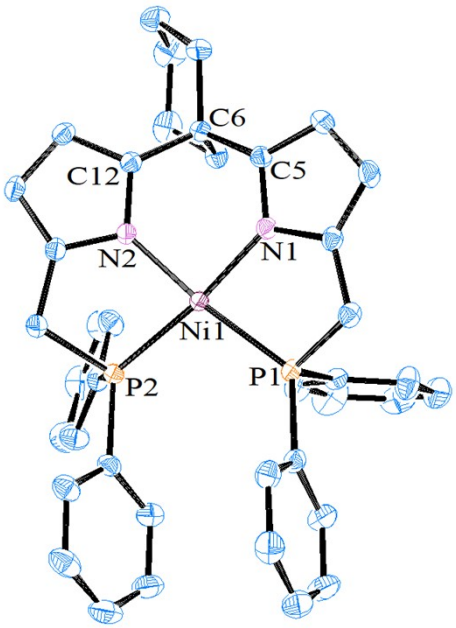

Figure S104. The X-ray structure of complex **3c** (50% displacement ellipsoids). The lattice THF and hydrogen atoms are omitted for clarity. Selected bond distances (Å) and bond angles (°): Ni1-N1 1.8861(13), Ni1-N2, 1.8852(13), P1-Ni1 2.1807(6), P2-Ni1 2.1650(6), N1-Ni1-N2 90.66(6), N1-Ni1-P2 173.16(4), N2-Ni1-P2 82.51(4), N1-Ni1-P1 83.07(4), N2-Ni1-P1 173.63(4), P1-Ni1-P2 103.77(1), C5-C6-C12 110.4(1). Symmetry transformations used to generate equivalent atoms: –x + 1/2, y, –z + 1.

References

1. D. Wittenberg and H. Gilman, *J. Org. Chem.*, 1958, **23**, 1063–1065
2. L. G. L. Ward and J. R Pipal, *Inorg. Synth.* 2007, 154– 164.
3. G. Mani, T. Guchhait, R. Kumar and S. Kumar, *Org. Lett.*, 2010, **12**, 3910–3913
4. S. Kumar, G. Mani, S. Mondal and P. K. Chattaraj, *Inorg. Chem.*, 2012, **51**, 12527.
6. A. Maity, A. Sil and S. K. Patra, *Eur. J. Inorg. Chem.*, 2018, **2018**, 4063–4073.
7. A. Kumar, R. Gupta and G. Mani, *Organometallics* 2023, **42**, 732–744.
8. K. Ganguli, S. Shee, D. Panja and S. Kundu, *Dalton Trans.*, 2019, **48**, 7358–7366.
9. M. Perez, S. Elangovan, A. Spannenberg, K. Junge and M. Beller, *ChemSusChem*, 2017, **10**, 83–86.
10. Q. Xuan, C. Zhao and Q. Song, *Org. Biomol. Chem.*, 2017, **15**, 5140.
11. A.V. Narsaiah, P. Narsimha and G. Navitha, Int. J. Appl. Biol. Pharm. Tech., 2010, **1**, 736-740.
12. E. Maerten, F. Agbossou-Niedercorn, Y. Castanet and A. Mortreux, *Tetrahedron*, 2008, **64**, 8700.
13. G. M. Sheldrick, *Acta Cryst. Sect. A: Found. Crystallogr.*, 2015, ***71***, 3.
14. G. M. Sheldrick, *Acta Cryst. Sect. C: Struct. Chem.,* 2015, ***71***, 3.